Properties of glutamate uptake in glial cells

Brian James Billups

A thesis submitted for the degree of
Doctor of Philosophy
in the
University of London

Department of Physiology
University College London

November 1996

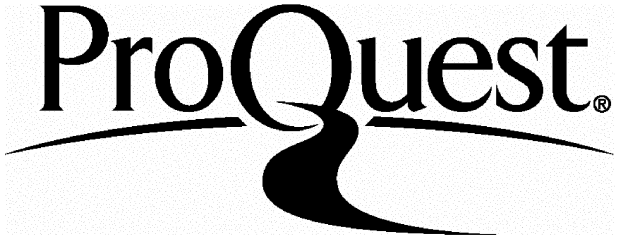

Abstract

Glutamate uptake carriers are ultimately responsible for terminating the synaptic action of glutamate by sequestering it into neurons and glia. Glutamate transport is accompanied by the co-transport of two sodium ions and the counter-transport of one potassium and one hydroxide ion, so it is electrogenic, carrying net positive charge inwards with each glutamate anion. The ionic changes occurring in pathological conditions like brain ischaemia cause glutamate uptake carriers to run backwards, pumping glutamate out of cells. Since glutamate uptake involves the movement of a hydroxide ion, and rapid pH changes occur during brain ischaemia, the effects of changing internal and external pH on forward and reversed uptake were studied.

Forward and reversed glutamate transport were studied by whole-cell voltage-clamping glial cells (Müller cells) isolated from the salamander retina. Glutamate release by reversed uptake was also monitored using isolated rat cerebellar neurons as glutamate sensors.

Internal alkalinization promoted, and external alkalinization inhibited glutamate uptake, probably by altering the gradient for hydroxide counter-transport. External acidification inhibited uptake, by decreasing the carriers' sodium affinity. Glutamate release by reversed uptake was inhibited by external acidification. This may be neuroprotective during anoxia, since the rise in external glutamate concentration is neurotoxic.

Cloned mammalian glutamate uptake carriers are known to have an integral anion conductance. This was also shown to be the case for the salamander transporter, and the gating of this conductance was studied. It was activated by either forward or reversed glutamate uptake. Furthermore, cycling of the carrier was not an

absolute requirement for channel opening. When cycling was inhibited, binding of glutamate and sodium to the internal and external carrier surface was sufficient to activate the anion conductance. Anion flow through the conductance was shown not to be coupled to glutamate transport, while the movement of hydroxide on the transporter is coupled to glutamate transport.

Acknowledgments

I am deeply indebted to David Attwell for his excellent supervision; for always being there to provide advise, support, encouragement and help. Sincere thanks also go to Peter Mobbs for his assistance and guidance.

I would like to specially thank the people I have directly collaborated with over the past three years: Daniela Kamm, David Rossi and Mona Spiridon. I am also very grateful to the other members of the lab, past and present, for their advise, inspiration and friendship: Suzette Allcorn, Alessandra Amato, Viola Bonneβ, Marina Catsicas, Martine Hamann, Monique Sarantis and Michiko Takahashi.

Finally, I would like to thank all my other friends and family for their help and support .

This work was supported by a grant from the Medical Research Council.

Contents

List of Figures

List of Abbreviations

AMPA	α-amino-3-hydroxy-5-methyl-4-isoxazole propionate
ATP	adenosine triphosphate
BCECF	2',7'-bis-(carboxyethyl)-5 (6')-carboxyfluorescein
cAMP	cyclic adenosine monophosphate
cGMP	cyclic guanosine monophosphate
CNQX	6-cyano-7-nitro-quinoxaline-2,3-dione
D-APV	D-2-amino-5-phosphonovaleric acid
DCK	5,7-dichlorokynurenic acid
DMSO	dimethyl sulphoxide
DNQX	6,7-dinitro-quinoxaline-2,3-dione
EDTA	ethylenediaminetetraacetic acid
EGTA	ethyleneglycol-bis-(β-aminoethylether) *N,N'*-tetraacetic acid
EPSC	excitatory post-synaptic current
GABA	γ-amino-butyric acid
HEPES	*N*-2-hydroxyethylpiperazine-*N'*-ethanesulfonic acid
IP_3	inositol trisphosphate
L-AP4	L-2-amino-4-phosphonobutyrate
MES	2-(*N*-morpholino)ethanesulfonic acid
MK-801	dibenzocycloheptenеimine
NMDA	N-methyl-D-aspartate
NMDG	N-methyl-D-glucamine
PDC	L-*trans*-pyrrolidine-2,4-dicarboxylate
TAPS	*N*-tris(hydroxymethyl)-3-aminopropanesulfonic acid
trans-ACPD	*trans*-1-amino-cyclopentyl-1,3-dicarboxylate

CHAPTER 1

Introduction

Glutamate, as well as playing a role in the metabolism of cells, is an excitatory neurotransmitter in the central nervous system. This thesis describes experiments on the mechanism which terminates glutamate's synaptic action. Unlike for other neurotransmitters such as acetylcholine, there is no extracellular enzyme to degrade glutamate in the synaptic cleft. Removal of glutamate from the synapse is instead mediated by it being taken up into neighbouring cells by glutamate uptake carriers. Thus, glutamate uptake is crucial for normal synaptic communication, and modulation of glutamate uptake could have implications for the signal processing properties of the brain. In addition, as described below, glutamate uptake carriers play an important role in the pathological events of ischaemia. This introduction gives the background on glutamate's role in physiological and pathological events which is necessary to put the experiments of this PhD thesis in context.

1.1 Glutamate as a neurotransmitter

The majority of excitatory synapses in the central nervous system use glutamate as the neurotransmitter (reviewed by Monaghan *et al.*, 1989). Glutamate released from the presynaptic terminal can activate several different types of postsynaptic receptors, as well as presynaptic autoreceptors. The glutamate receptors can be broadly classified into two groups: ionotropic receptors which open ion channels, and metabotropic receptors which are coupled to G-proteins. The ionotropic receptors can be further sub-divided, based on the pharmacological agents which also activate them, into NMDA, AMPA and kainate

receptors. The following sections review briefly the properties of these receptors which are relevant to the experiments in this thesis.

1.1.1 NMDA receptors

The NMDA receptor channel is permeable to sodium, potassium and calcium (Mayer *et al.*, 1987). The channel is blocked in a voltage-dependent manner by external magnesium ions (Mayer *et al.*, 1984; Nowak *et al.*, 1984). At a normal negative membrane potential this block prevents significant ion fluxes through the channel. Depolarization, such as would be caused by concurrent activation of non-NMDA receptors, removes the magnesium block. The entry of calcium through the NMDA receptor may have implications for cell signalling and is thought to be important during long-term potentiation (reviewed by Collingridge and Bliss, 1995) and during the glutamate-mediated neurotoxicity which is known to occur in anoxia (Choi and Rothman, 1990). Activation of the NMDA receptor is also dependent on the receptor having bound external glycine at a site different to that which binds glutamate (Johnson and Ascher, 1987).

NMDA receptors are activated by glutamate, L-aspartate, NMDA and quisqualate. They are not activated by kainate, AMPA or *trans*-ACPD. NMDA receptor responses can be distinguished pharmacologically by selective antagonists. Competitive antagonists for glutamate binding include D-APV. Competitive antagonists for the glycine binding site include DCK (Kemp and Leeson, 1993). Non-competitive antagonists have also been described, such as the open channel blocker MK-801 (MacDonald and Nowak, 1990).

Currently five sub-units of the NMDA receptor have been cloned, NMDAR1 and NMDAR2A-D (reviewed by Hollmann and Heinemann, 1994). Although NMDAR1 units can form homomeric channels when expressed in oocytes, the presence of an NMDAR2 subunit greatly potentiates the response. *In*

vivo NMDA receptors are thought to be heteromeric pentamers containing both NMDAR1 and NMDAR2 sub-units. The exact sub-unit composition determines properties such as the deactivation kinetics and degree of magnesium block, as well as the glycine affinity of the receptor. *In vitro*, certain combinations of NMDA receptor subunits give rise to receptors which can be activated by glycine alone (Kutsuwada *et al.*, 1992; Meguro *et al.*, 1992), although this has never been demonstrated *in vivo*.

1.1.2 AMPA receptors

AMPA receptors are permeable to sodium, potassium, and (depending on the sub-unit composition) calcium (Hollmann *et al.*, 1991; Verdoorn *et al.*, 1991). The receptor currents exhibit a high degree of desensitization when subjected to a continuous high concentration of glutamate (Tang *et al.*, 1989). Agonists for the AMPA receptor include glutamate, quisqualate, AMPA and kainate. Competitive antagonists for AMPA receptors include CNQX and DNQX.

At present four sub-units of the AMPA receptor have been cloned: GluR1-4 (reviewed by Hollmann and Heinemann, 1994). Functional AMPA receptors can take the form of homomeric or heteromeric ion channels, possibly in a pentameric arrangement. Each sub-unit can exist in either of two splice variants, termed "flip" and "flop" (Sommer *et al.*, 1990). The functional characteristics of the receptor may be determined by the different splice variants, in addition to the sub-unit composition (Jonas and Sakmann, 1992). A significant calcium permeability to the receptor is only observed if the GluR2 sub-unit is absent. A glutamine residue present in GluR1, GluR3 and GluR4 is replaced by an arginine residue in GluR2, as a consequence of post-transcriptional RNA editing. The arginine residue at this site greatly reduces the channel's permeability to calcium.

1.1.3 Kainate receptors

Kainate receptors are permeable to sodium, potassium and (depending upon RNA editing) calcium. Agonists for kainate receptors include glutamate, kainate and quisqualate, and they are antagonised by CNQX. Two classes of kainate receptor sub-units can be distinguished by their affinity for kainate: high-affinity sub-units (KA1 and KA2) and low-affinity sub-units (GluR5, GluR6 and GluR7).

In Vitro, GluR5 and GluR6 can form homomeric receptors. Like for the AMPA receptors, calcium permeability of receptors can be affected by post-transcriptional RNA editing at the same glutamine site. GluR7 does not form homomeric receptors and is not subject to the same RNA editing. KA1 and KA2 sub-units do not form homomeric receptors, but KA2 sub-units can form heteromeric receptors in combination with GluR5 or GluR6 sub-units.

1.1.4 Metabotropic glutamate receptors

Metabotropic glutamate receptors activate G-proteins inside the cell. They can be classified into three groups (reviewed by Pin and Duvoisin, 1995): the mGluR1 and mGluR5 clones are group-I receptors, mGluR2 and mGluR3 clones are group-II receptors, and mGluRs 4, 6, 7 and 8 are group-III receptors. In addition to activation by glutamate, group-I receptors are activated by quisqualate and trans-ACPD, group-II receptors by trans-ACPD, and group-III receptors by L-AP4.

Group-I receptors couple to G-proteins which activate phospholipase C, producing IP_3 and releasing calcium from internal stores. Group-II and group-III receptors couple to G-proteins which usually inhibit adenylate cyclase, decreasing the intracellular concentration of cAMP. In the retina, the hypopolarizing response of on-bipolar cells to glutamate is mediated by a metabotropic receptor which

activates phosphodiesterase, reduces the cGMP concentration and thus closes ion channels (Nawy and Jahr, 1990). The metabotropic receptor in on-bipolar cells is thought to be mGluR6 (Nakajima *et al.*, 1993).

1.2 Glutamate Uptake

In this section I shall review the importance of glutamate uptake in the brain, the properties of glutamate uptake carriers, how they can be studied electrically and how they are predicted to run backwards during brain ischaemia.

1.2.1 The role of glutamate uptake in the brain

Glutamate uptake is ultimately responsible for the removal of glutamate from the synaptic cleft, and hence terminating synaptic transmission. Blocking glutamate uptake in rat cerebellar slices results in a prolongation of Purkinje cell EPSCs, implying a direct association between the rate of glutamate uptake and the shape of the synaptic current (Barbour *et al.*, 1994; Takahashi *et al.*, 1995). In the hippocampus, no such effect of glutamate uptake blockers is observed (Sarantis *et al.*, 1993), implying a less intimate relationship between glutamate uptake and the time course of synaptic transmission. Despite this lack of direct association in the hippocampus, glutamate uptake carriers will still be responsible for keeping the extracellular glutamate concentration low, i.e. will set up the diffusion gradient which allows glutamate to diffuse out of the synaptic cleft.

In addition to its role as a neurotransmitter, or perhaps because of it, glutamate is a major neurotoxic element in the brain (see section 1.3). Prolonged increases in extracellular glutamate concentration are neurotoxic (Choi *et al.*, 1987), so the removal of glutamate from the extracellular space by glutamate uptake carriers is of paramount importance for the normal functioning of the brain.

1.2.2 Cloning and localization of glutamate uptake carriers

To date, four distinct plasma membrane glutamate uptake carriers have been cloned. They belong to a discrete family of transporters, separate from the transporters of other neurotransmitters, such as GABA, glycine, noradrenaline, dopamine and serotonin (Amara and Kuhar, 1993; Kanai *et al.*, 1993). A neutral amino acid uptake carrier also belongs to the same family as the glutamate uptake carrier (Arriza *et al.*, 1993; Shafqat *et al.*, 1993).

Two of the cloned glutamate uptake carriers, GLAST (Storck *et al.*, 1992) and GLT-1 (Pines *et al.*, 1992), were isolated from rat brain, and are expressed in brain glia. GLT-1 is expressed widely in brain astrocytes, whereas expression of GLAST is localized to the Bergmann glia of the cerebellum. The EAAC1 carrier was cloned from rabbit small intestine (Kanai and Hediger, 1992), and is expressed in the small intestine, kidney, liver, heart and neurons throughout the brain. More recently, the human homologues of these transporters have been cloned (Arriza *et al.*, 1994). EAAT1, 2 and 3 are homologous to GLAST (96% sequence identity), GLT-1 (95% sequence identity) and EAAC1 (92% sequence identity) respectively. In addition, another human carrier was also cloned, EAAT4 (Fairman *et al.*, 1995), which has some novel properties (see section 1.2.5) and is expressed in the cerebellum.

Detailed studies of the subcellular localization of the glutamate uptake carriers in the cerebellum (Chaudhry *et al.*, 1995) have revealed that GLT-1 carriers are localized to the regions of astrocyte membrane which are adjacent to nerve terminals, axons and dendritic spines. Fewer carriers are expressed in the regions of membrane which are adjacent to other astrocytes, blood vessels, pia or dendritic shafts. This distribution of carriers is consistent with a role in maintaining the extracellular concentration of glutamate below neurotoxic levels.

Antibody staining for the EAAC1 carrier in the cerebellum showed that expression was localized mainly to the soma and dendritic spines of Purkinje cells

(Rothstein *et al.*, 1994). Neuronal glutamate uptake has been conventionally thought of as being in pre-synaptic terminals, but in Purkinje cells which receive glutamatergic input from climbing and parallel fibres, these carriers are a post-synaptic uptake mechanism. Glutamate uptake has been recorded electrically in these postsynaptic cells (Takahashi *et al.*, 1996), suggesting a role for postsynaptic uptake in terminating synaptic transmission.

Using molecular biological techniques to prevent the expression of different glutamate uptake carriers in the rat brain, Rothstein *et al.* (1996) have shown that preventing expression of the glial carriers, GLT-1 and GLAST, results in a general rise in extracellular glutamate concentration which results in cell death. Preventing the expression of the neuronal carrier, EAAC1, does not produce cell death, but does cause epilepsy. This result suggests that the role of the glial transporters is to keep the extracellular glutamate from rising to a neurotoxic level, whereas the neuronal transporters play a more specific role in synaptic transmission.

Immunoreactivity studies in the rat retina have shown that GLAST is present in Müller cells, astrocytes and pigment epithelium cells only (Derouiche and Rauen, 1995). GLT-1 was found to be present in astrocytes, cones and bipolar cell, but not in Müller cells (Rauen and Kanner, 1994). The experiments in this thesis were performed on Müller cells from the salamander retina. In salamander Müller cells two distinct uptake carriers are found. One is homologous to GLAST and the other homologous to a GLT-1 carrier subtype (Scott Eliasof - personal communication).

1.2.3 Stoichiometry of glutamate uptake

Early studies of glutamate uptake were based on measuring the uptake of radiolabelled glutamate or aspartate. The dependence of uptake on the concentrations of various intra- and extracellular ions was determined. All studies

of glutamate uptake show a first order Michaelis-Menten dependence of uptake on the external glutamate concentration, indicating that one glutamate ion is transported per carrier cycle. External sodium ions are required to drive the uptake of glutamate (Hertz, 1979; Erecinska, 1987). Glutamate stimulates the uptake of radiolabelled sodium, demonstrating that the sodium ions are transported. Flux measurements suggest that two sodium ions are transported per glutamate ion (Baetge *et al.*, 1979; Stallcup *et al.*, 1979). Similarly, the uptake of D-aspartate into synaptosomes requires the binding of two sodium ions to the carrier (Erecinska *et al.*, 1983). Internal potassium activates the accumulation of glutamate (Kanner and Sharon, 1978; Burckhardt *et al.*, 1980; Nelson *et al.*, 1983), suggesting that a potassium ion is transported out. An alkalinization of the external medium is also observed (Erecinska *et al.*, 1983) and glutamate uptake is stimulated by the pH difference (interior alkaline) across the cell membrane (Nelson *et al.*, 1983), suggesting the transport of a pH-changing ion.

The ionic dependence of glutamate uptake was investigated further by studying the electrical currents produced using whole-cell voltage-clamping. This technique confirmed a first-order Michaelis-Menten dependence on external glutamate concentration with a K_M of 22μM in salamander Müller cells (Brew and Attwell, 1987). There is a sigmoid dependence of the glutamate uptake current on external sodium concentration, consistent with two sodium ions being required for transport (Barbour *et al.*, 1991). The glutamate uptake current shows a first-order Michaelis-Menten dependence on the internal potassium ion concentration (Barbour *et al.*, 1988), indicating that one internal potassium ion is required for transport. Direct measurements of potassium efflux using potassium-sensitive microelectrodes have shown that potassium is transported, rather than just being an intracellular modulator of glutamate uptake (Amato *et al.*, 1994). Analysis of the intra- and extracellular pH changes stimulated by glutamate uptake was used to suggest that one hydroxide ion is counter-transported (Bouvier *et al.*, 1992).

However, interpretation of some of the results of Bouvier *et al.* (1992) have been brought into question by the discovery of an anion conductance in the glutamate uptake carrier (see section 1.3.5). It is thus currently unknown if the glutamate uptake carrier counter-transports one hydroxide ion, or co-transports a proton with each glutamate ion. The stoichiometry of glutamate uptake therefore appears to be either that two sodium ions are co-transported and one hydroxide and one potassium ion are counter-transported with each glutamate ion (figure 1.1A), or a proton and two sodium ions are co-transported and a potassium ion is counter-transported (figure 1.1B).

Experiments on cloned glutamate uptake carriers expressed in oocytes have produced results consistent with the stoichiometry outlined above. Uptake of glutamate by all four cloned transporters is highly dependent on external sodium (Kanai and Hediger, 1992; Pines *et al.*, 1992; Storck *et al.*, 1992; Fairman *et al.*, 1995). The uptake of glutamate by EAAC1 and GLT-1 was dependent on internal potassium (Kanai and Hediger, 1992; Pines *et al.*, 1992). For the EAAC1 clone, glutamate uptake has also been shown to transport two sodium ions inwards, one proton in or a hydroxide ion out, and one net positive charge inwards with each glutamate ion (Kanai *et al.*, 1995).

Recently Zerangue and Kavanaugh (1996) have suggested that the EAAT3 (EAAC1) carrier transports three sodium ions per glutamate ion, in direct contradiction to the results of Kanai *et al.* (1995) working on a homologous cloned carrier, and other investigations performed on native carriers (Baetge *et al.*, 1979; Stallcup *et al.*, 1979; Erecinska *et al.*, 1983). No mention of this discrepancy is made by Zerangue and Kavanaugh (1996), and hence no explanation offered. It seems that either the stoichiometry is variable and sensitive to different experimental conditions, or that either the techniques of Zerangue and Kavanaugh (1996) or of Baetge *et al.*, (1979), Stallcup *et al.*, (1979) and Erecinska *et al.*, (1983) produce erroneous results.

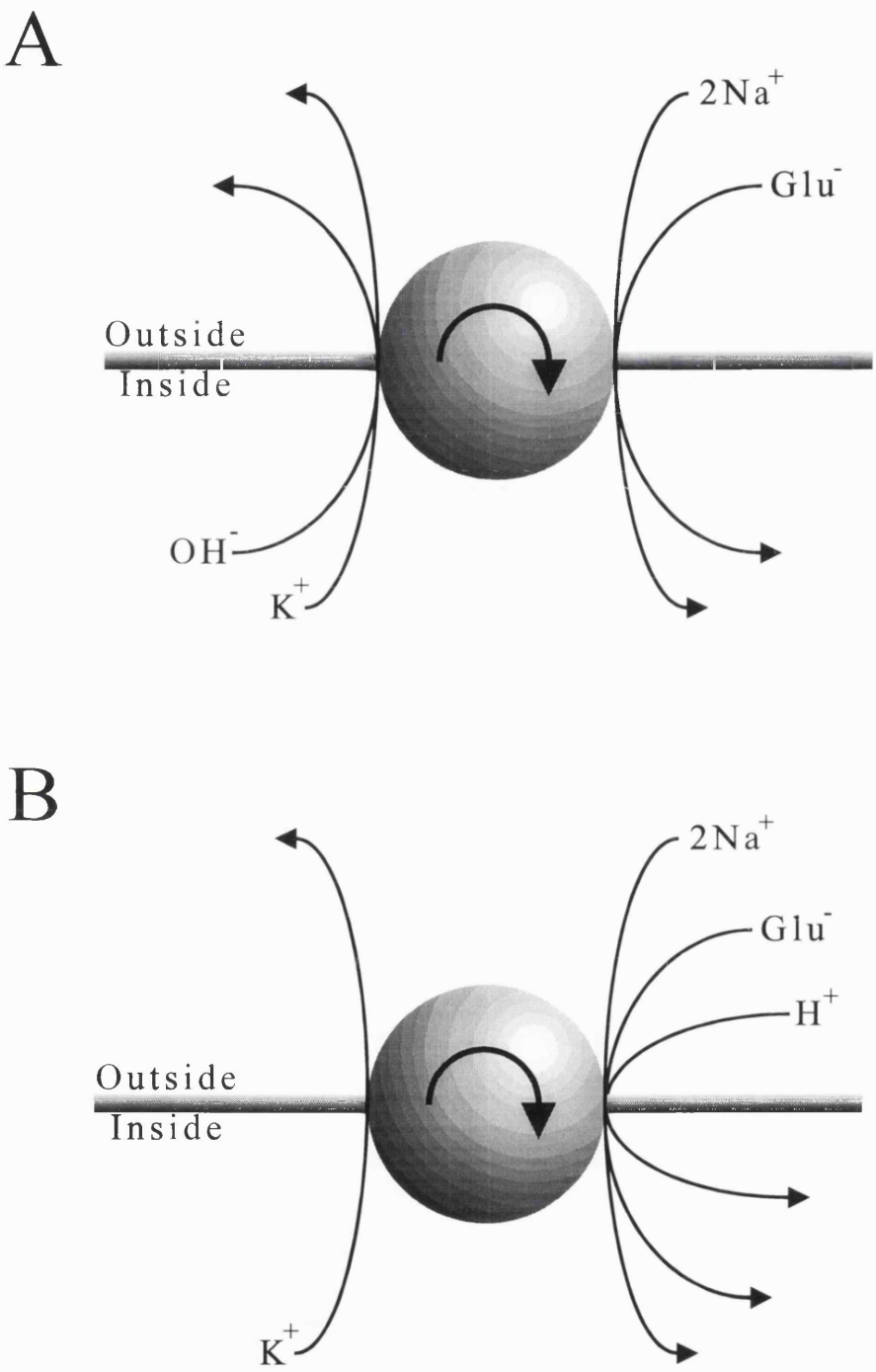

Figure 1.1 - Alternative stoichiometries of forward glutamate uptake

1.2.4 Electrical recording of glutamate uptake

The ionic stoichiometry of glutamate uptake outlined above (see figure 1.1) indicates that for each glutamate ion transported there will be movement of one net positive charge in the same direction. Glutamate uptake is thus an electrogenic process. This allows glutamate uptake to be studied as a membrane current by the whole-cell voltage-clamp technique (Hamill *et al.*, 1981). When salamander Müller cells are whole-cell voltage-clamped, an inward membrane current can be measured when glutamate is externally applied (Brew and Attwell, 1987). This current exhibits the pharmacology of glutamate uptake: it is activated by L-glutamate and L-aspartate, but it is not activated by other agonists of ionotropic or metabotropic glutamate receptors. The glutamate uptake agonist D-aspartate is exclusive for uptake and does not activate any glutamate receptors.

This electrical method of assessing glutamate uptake has the advantage over the radiotracing methods, in that the membrane voltage can be controlled. The rate of such an electrogenic process would be expected to be affected by the membrane voltage, and this was found to be the case for glutamate uptake. A positive membrane potential inhibits the current evoked by external glutamate, but does not cause it to reverse (Brew and Attwell, 1987), consistent with the activation of a transporter which transports net positive charge inwards when glutamate is applied to the outside of the cell.

1.2.5 Glutamate uptake gates an anion channel

The cloned glutamate uptake carrier EAAT4, when expressed in oocytes, mediates a glutamate-evoked membrane current which is carried mainly by chloride ions (Fairman *et al.*, 1995). This is attributed to an anion channel present in the glutamate uptake carrier, which is gated by the binding of external glutamate and sodium. Flux of anions through this channel is thermodynamically uncoupled to

the movement of glutamate, indicating that the chloride ion gradient does not help to power glutamate transport. Closer examination of the membrane current produced by the other three cloned human glutamate transporters, EAAT1-3, showed that chloride movement through an anion channel also contributes to their glutamate-evoked current (Wadiche *et al.*, 1995). However, the contribution of anion channel current to the total glutamate-evoked response is much smaller for these clones than for the EAAT4 clone.

The anion channel properties associated with EAAT4 are similar to those of what are now recognized to be glutamate uptake carriers in the presynaptic terminals of salamander retinal cones (Sarantis *et al.*, 1988; Eliasof and Werblin, 1993) and fish retinal bipolar cells (Grant and Dowling, 1995). These transporters posses an anion conductance which is activated by external glutamate and is critically dependent on external sodium ions. The glutamate uptake carrier in salamander Müller cells has also been shown to activate an anion conductance (Eliasof and Jahr, 1996). The properties and gating of this channel are examined in detail in chapter 5 of this thesis.

1.2.6 Reversed glutamate uptake

The glutamate uptake carrier accumulates glutamate inside cells against its concentration gradient; powered by the transmembrane gradients for sodium, potassium, pH and voltage. For the ionic stoichiometry outlined above, the equilibrium concentration of external glutamate (i.e. the lowest concentration that can be maintained by the carrier) can be calculated from the following equation (Attwell *et al.*, 1993):

$$[glu^-]_o = [glu^-]_i \cdot \left(\frac{[Na^+]_i}{[Na^+]_o}\right)^2 \cdot \left(\frac{[H^+]_i}{[H^+]_o}\right) \cdot \left(\frac{[K^+]_o}{[K^+]_i}\right) \cdot e^{(VF/RT)} \qquad [1.1]$$

If the external glutamate concentration is above this equilibrium concentration then glutamate will be pumped into cells. For the ionic concentrations normally

observed in mammalian brain, the equilibrium glutamate concentration is approximately 0.2μM (Attwell *et al.*, 1993), and glutamate will be taken up by cells.

If the transmembrane gradients for sodium, potassium, pH or voltage are disturbed, the equilibrium glutamate concentration may be increased. This will occur during pathological conditions such as brain anoxia (see section 1.3). The run-down of transmembrane gradients for sodium and potassium, and subsequent membrane depolarization would be expected to increase the equilibrium glutamate concentration in mammalian brain to 261μM (Attwell *et al.*, 1993). The equilibrium concentration is now above the external glutamate concentration, and glutamate will be pumped out of cells by the glutamate uptake carrier until the new equilibrium concentration is attained.

This reversed mode of glutamate uptake can be observed experimentally. Like forward uptake, reversed uptake is electrogenic, transporting one net positive charge outwards. In whole-cell voltage-clamped Müller cells this can be observed as an outward membrane current at depolarized membrane potentials, when the external potassium concentration is increased (Szatkowski *et al.*, 1990), providing that sodium and glutamate are present inside the cell.

Reversed glutamate uptake currents have also been observed in oocytes expressing the EAAC1 uptake carrier. With 98mM external potassium and no external sodium, outward membrane currents are observed when external glutamate is removed. These currents are enhanced by membrane depolarization, consistent with reversed glutamate uptake transporting a net positive charge outwards (Kanai *et al.*, 1995).

The stimulation of reversed glutamate uptake by the ionic conditions seen in brain anoxia or ischaemia is thought to underlie the observed rise in external glutamate concentration which triggers neuronal death (see section 1.3).

1.3 Glutamate neurotoxicity

Some of the experiments described in this thesis are on how glutamate transporters release glutamate in ischaemia or anoxia. Glutamate released in this way can trigger the death of neurons. The following section reviews the neurotoxic actions of glutamate.

1.3.1 External glutamate is neurotoxic

The neurotoxic properties of glutamate were first established by Olney and Sharpe (1969), who demonstrated that injection of glutamate into monkeys resulted in neuronal death. Five minutes' exposure of cultured neurons to external glutamate has been shown to trigger neuronal death with an ED_{50} of 50-100μM (Choi *et al.*, 1987). Normally the extracellular glutamate concentration in the brain is maintained at a low micromolar level by glutamate uptake carriers (Bouvier *et al.*, 1992). Pathological conditions such as brain anoxia or ischaemia, as would be caused for example by a stroke, perinatal asphyxia, cardiac arrest, carbon monoxide poisoning or drowning, may lead to an increase in the extracellular glutamate concentration to several hundred micromolar (Hagberg *et al.*, 1985).

The neurotoxicity of extracellular glutamate is thought to be mediated by excessive activation of glutamate-gated ion channels. Opening of sodium-permeable channels results in sodium influx, followed by an influx of chloride and water, resulting in rapid cell swelling which can cause early necrotic cell death. Removal of extracellular sodium and chloride prevent glutamate-induced cell swelling and death (Rothman, 1985; Olney *et al.*, 1986). More importantly, excessive activation of NMDA receptors and calcium-permeable AMPA receptors results in an influx of calcium which produces a delayed neuronal degeneration, that is inhibited by the removal of external calcium (Choi, 1987). Blocking NMDA receptors in culture (Choi, 1987; Hartley and Choi, 1989; Goldberg and Choi, 1993) and *in vivo* (Gill *et al.*, 1988) reduces the neuronal death observed in

ischaemia. Interestingly, NMDA receptor blockers are neuroprotective even when administered up to several hours after the ischaemic insult (Gill *et al.*, 1988; Hartley and Choi, 1989). This suggests that ischaemia results in a type of long-term potentiation of the NMDA receptor response, triggering a delayed neuronal death due to excessive calcium influx through potentiated NMDA receptors (reviewed by Szatkowski and Attwell, 1994).

1.3.2 Mechanism of glutamate release in ischaemia

Three main mechanisms have been proposed to underlie the glutamate release which triggers neuronal death in ischaemia: conventional calcium-dependent vesicular release (Drejer *et al.*, 1985), a swelling-activated anion transport mechanism (Kimelberg *et al.*, 1990), or reversal of the glutamate uptake carrier (Szatkowski *et al.*, 1990; Attwell *et al.*, 1993). Glutamate release during ischaemia has been shown to be largely calcium-independent after the first few minutes of ischaemia (Ikeda *et al.*, 1989; Lobner and Lipton, 1990; Katayama *et al.*, 1991), and the reduced ATP concentrations occurring in ischaemia inhibit exocytosis (Kauppinen *et al.*, 1988). In favour of the reversed uptake hypothesis is the observation that much of the glutamate release is inhibited by preloading with glutamate uptake blockers (Longuemare and Swanson, 1995).

1.3.3 Ionic changes in ischaemia stimulate reversed uptake

A summary of the ionic changes occurring in ischaemia is shown in figure 1.2. These changes can be split into two phases (reviewed by Siesjo, 1990). During the first phase, the reduced oxygen supply causes cells to respire anaerobically, producing lactate (Smith *et al.*, 1986). This results in an intra- and extracellular acidification of about 1 pH unit (Silver and Erecinska, 1992). (The importance of this pH change is dealt with in depth later in this thesis). Also during

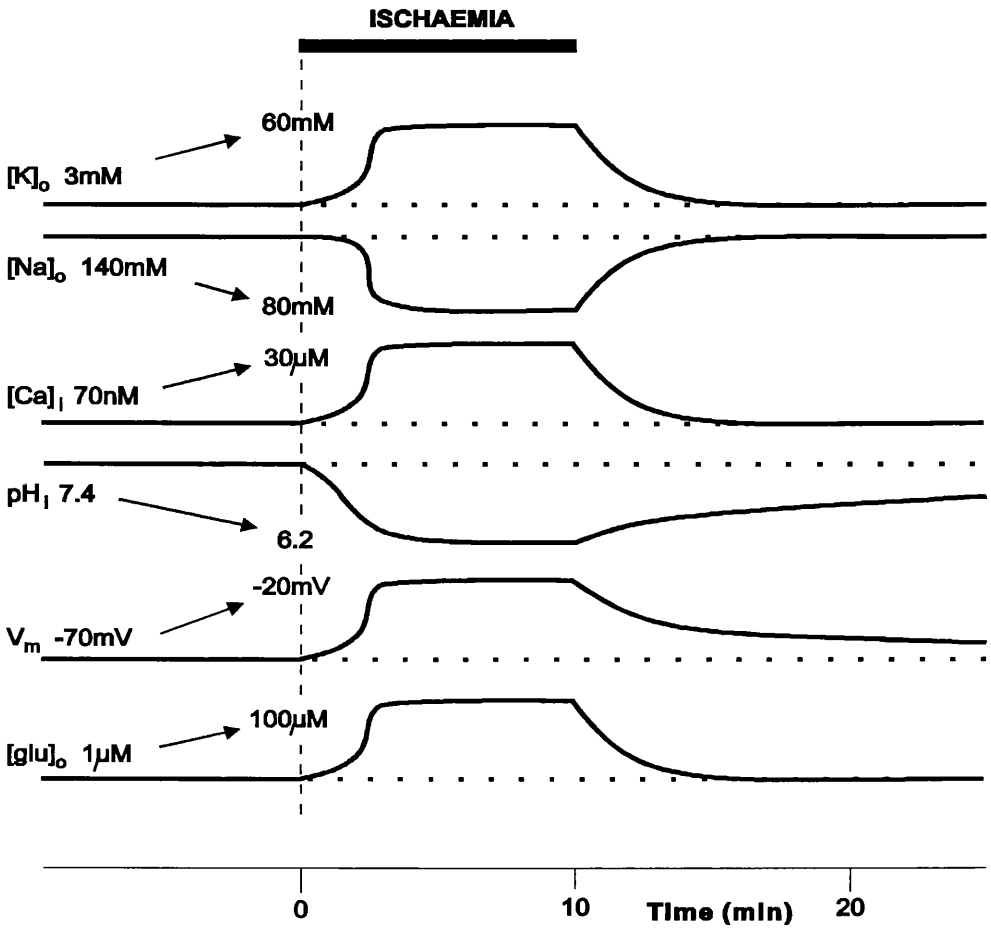

Figure 1.2 - Ionic changes in ischaemia

Diagram of the changes in ionic concentrations and membrane voltage before, during and after a 10 minute period of ischaemia (Reproduced from Szatkowski and Attwell, 1994). The extracellular pH also goes acid with a change of similar magnitude to the intracellular pH.

this initial phase there is a slow rise in external potassium concentration possibly due to an increase in potassium conductance resulting from a rise in internal calcium concentration (Silver and Erecinska, 1992).

After about a minute or two there is a sudden loss of transmembrane ion gradients. The reduced concentrations of ATP in the cell (Naruse *et al.*, 1984) leads to the Na^+/K^+ pump being inhibited. The external potassium concentration suddenly rises to about 60mM, causing membrane depolarization to approximately -20mV (Siesjo, 1990), the external sodium concentration falls by about 60mM, and there is a corresponding increase of intracellular sodium concentration and decrease of intracellular potassium concentration (but the intracellular changes are smaller than the extracellular changes because of the larger volume fraction). These changes in ion gradients will result in the glutamate uptake carriers starting to run backwards (as described in section 1.2.6) and raising the extracellular glutamate concentration. As calculated in section 1.2.6, the equilibrium (i.e. minimum maintainable) external glutamate concentration in the mammalian brain will be increased from 0.2μM to 261μM by an attack of ischaemia (Attwell *et al.*, 1993). The glutamate uptake carrier will therefore run in the reversed direction, pumping glutamate out of the cells until this new equilibrium value is obtained.

1.4 Structure of the retina

Experiments in this thesis were performed on Müller cells (glial cells) isolated from the salamander retina. In this section I will briefly discuss the structure of the vertebrate retina to give some indication of the location and role of its Müller cells.

The vertebrate retina consists of two synaptic layers (Dowling, 1987): the inner and outer plexiform layers, which separate three layers of cell bodies: the ganglion cell, inner nuclear and outer nuclear layers (figure 1.3). The

Figure 1.3 - Schematic diagram of the retina

A schematic diagram of the major cell types and their position in the vertebrate retina. The cell types shown are photoreceptor cells (PC), bipolar cells (BC), ganglion cells (GC), horizontal cells (HC), amacrine cells (AC) and Müller cells (MC). The cells are organized into three cellular layers: ganglion cell layer (GCL), inner nuclear layer (INL) and outer nuclear layer (ONL). There are two layers containing synaptic connections: the inner plexiform layer (IPL) and the outer plexiform layer (OPL). The axons of the ganglion cells form the fibre layer (FL), which combine to form the optic nerve. Müller cells are ideally placed to take up the glutamate released as a transmitter by the photoreceptor and bipolar cells.

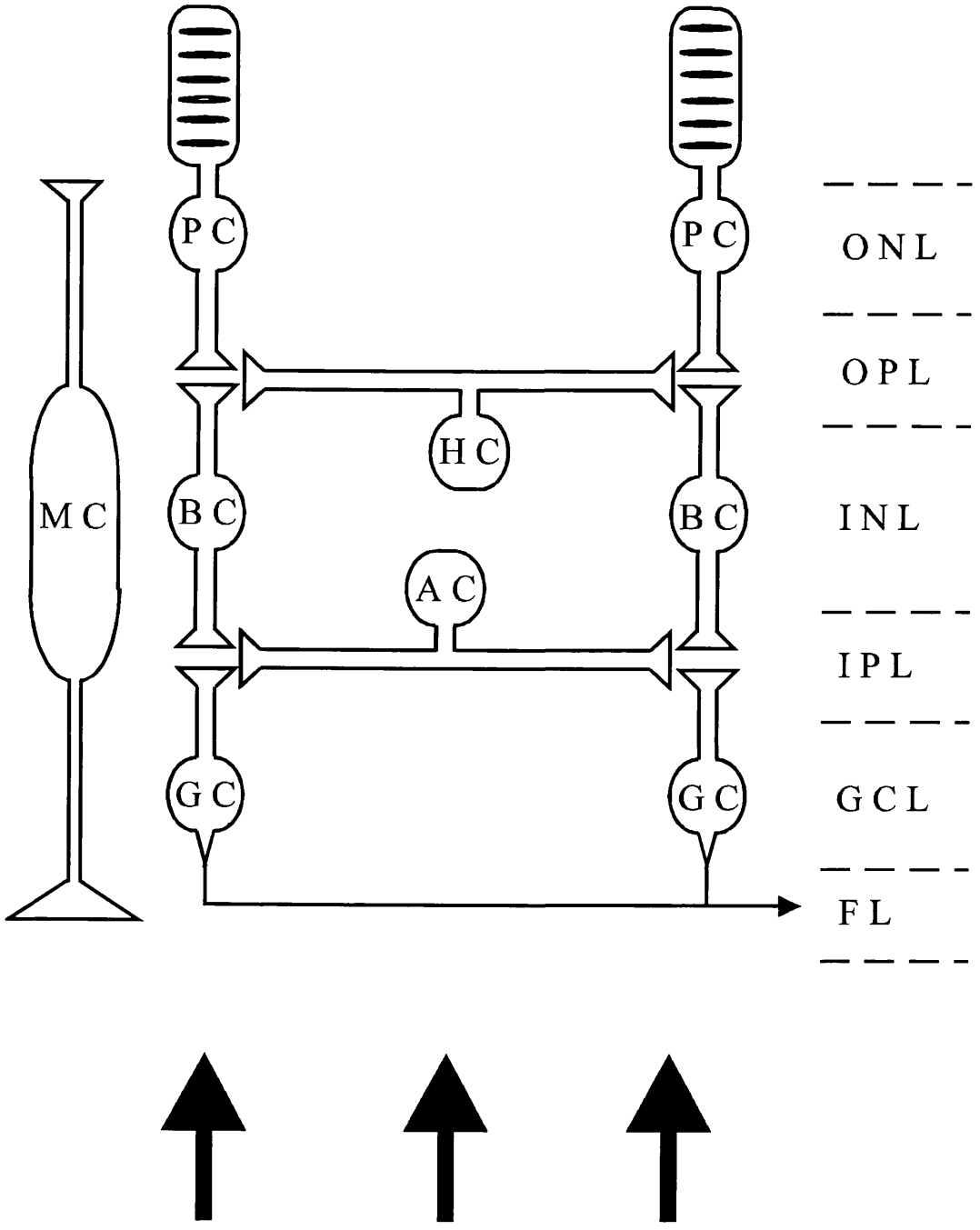
PC
PC
ONL
OPL
HC
MC
BC
BC
INL
AC
IPL
GC
GC
GCL
FL
LIGHT

photoreceptors of the outer nuclear layer contain a visual pigment which is located in the outer most segment. The retina is, in a sense, inverted, i.e. the outer nuclear layer is the most distal, and light must pass through all the other layers before reaching the photoreceptors.

Glutamate is the neurotransmitter released by the photoreceptors and bipolar cells. Glutamate release from the photoreceptors is maximal during darkness, and is inhibited by the detection of light. The distance across the retina is relatively short (approx. 200μm), so action potentials are not required to propagate a detectable electrical signal. The light stimulus is transduced into a graded membrane potential in the photoreceptor cells, which send output to bipolar cells. The bipolar cells project to the ganglion cells, which produce the final output from the retina. Their axons (the fibre layer) form the optic nerve, encoding the visual signal as action potentials. In addition to this vertical pathway from photoreceptors to ganglion cells, horizontal and amacrine cells mediate lateral interactions (notably lateral inhibition to enhance the detection of spatial gradients of light intensity) in the outer and inner plexiform layers respectively. Finally, interplexiform cells extend processes in both the inner and outer plexiform layers, and mediate feedback from the inner to the outer retina.

Müller cells are glial cells which span the entire width of the retina, extending vertically from the outer nuclear layer to the vitreous fluid. They are in intimate contact with the other cells and synapses. Their position, and abundance of glutamate uptake carriers (Brew and Attwell, 1987), makes them ideally placed to take-up the glutamate released by the photoreceptors and bipolar cells. The cell membrane contains a very large potassium conductance, 94% of which is situated in the endfoot apposed to the vitreous fluid (Newman, 1984; Brew *et al.*, 1986). Excess potassium produced by neuronal activity can be 'siphoned' away from the neuronal cells into the vitreous by this spatial distribution of glial cell potassium channels (Newman *et al.*, 1984). Changes in Müller cell membrane potential

caused by variations in the external potassium concentration are thought to underlie the generation of the 'b-wave' of the electroretinogram (Newman and Odette, 1984).

Müller cells may also play an important role in the recycling of neurotransmitters. The enzyme glutamine synthetase, which converts glutamate to glutamine, has been shown to be localized exclusively to Müller cells in the retina (Riepe and Norenburg, 1977; Linser and Moscona, 1979). Glutamine is thought to be released from glia and taken-up into neighbouring neurons, where it is used as a precursor for the synthesis of glutamate or GABA (van den Berg and Garfinkel, 1971).

CHAPTER 2

Methods

2.1 Müller cell preparation

Glutamate uptake was studied in isolated Müller cells from the retina of the aquatic phase tiger salamander (*Ambystoma tigrinum*). These cells were used because of their large size, abundancy of glutamate uptake carriers and lack of significant glutamate-gated ion conductances (Brew and Attwell, 1987). Müller cells have been shown to express non-NMDA glutamate receptors (Wakakura and Yamamoto, 1994; Peng *et al.*, 1995), but no non-NMDA receptor currents are observed when non-NMDA receptor analogues are continually perfused onto salamander or rabbit Müller cells (Brew and Attwell, 1987; Sarantis and Attwell, 1990).

Salamanders were killed by decapitation followed by immediate crushing of the brain. The eyes were removed and bisected slightly anterior to the ora serrata using a razor blade and ophthalmological scissors. The posterior eye-cup, containing the retina, was stored in a petri dish containing solution A (table 2.1) in a refrigerator (4°C) and used within 30 hours.

Cells were isolated by incubating approximately one quarter of the retina in 2ml of solution B (table 2.1), with 8.4 units of papain (from Sigma) added, at 32^{0}C for 20 minutes. The quarter-retina was then washed 4 times in 4ml of solution A (table 2.1), triturated with a fire polished Pasteur pipette and plated onto 13mm glass cover slips. Cells were allowed to settle on the cover slips for about 10 minutes before being used for an experiment, and remained viable for up to 4 hours. Müller cells could be easily identified by their large size and distinctive morphology (figure 2.1).

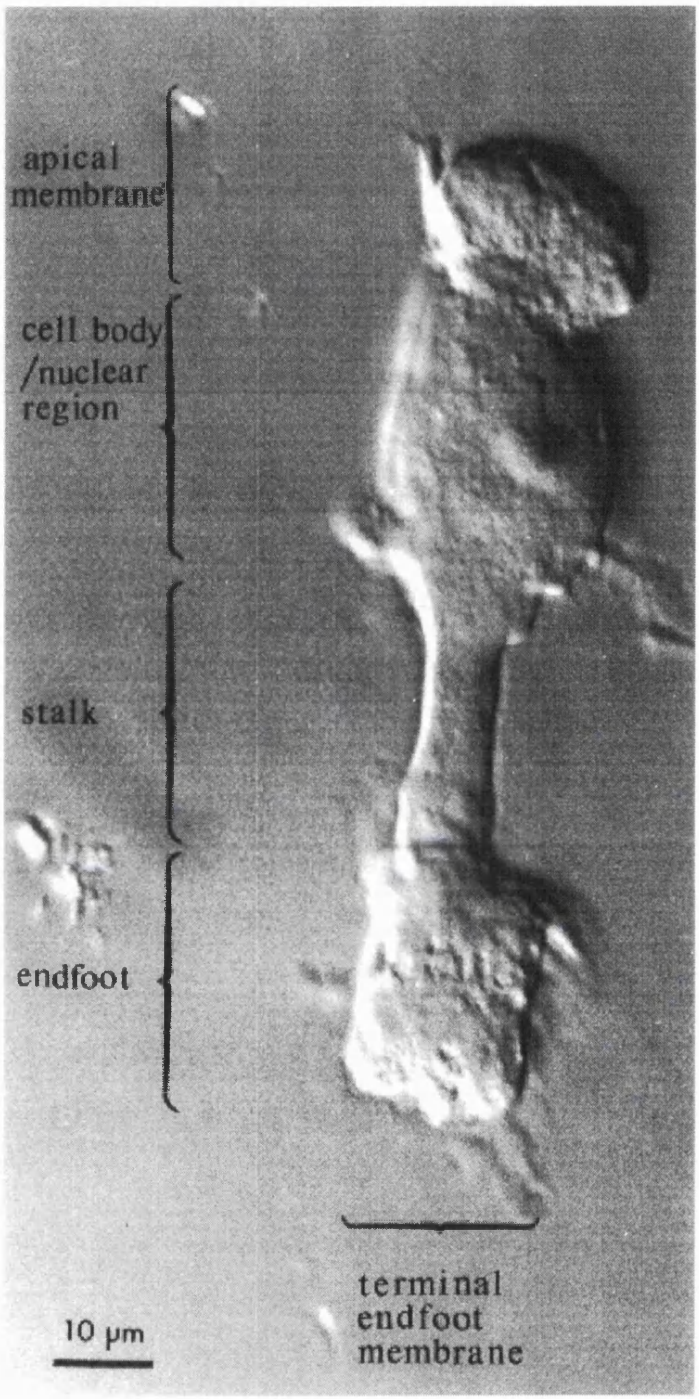

Figure 2.1 - Isolated Müller cell

The image shows a Müller cell isolated from the salamander retina

2.2 Purkinje cell preparation

Isolated rat cerebellar Purkinje cells were used as glutamate detectors to sense the glutamate released from Müller cells by reversed glutamate uptake (see chapter 4). 12 day old Sprague-Dawley rat pups were killed by dislocation of the cranial vertebrae follow by immediate decapitation. The brain was rapidly removed from the skull and placed in a petri dish containing ice-cold, oxygenated, solution C (table 2.1). The brain stem was removed and the cerebellum cut-off with a razor blade. The two side lobes of the cerebellum were removed, leaving the central portion (vermis) intact. This was cut into 200μm thick slices in the sagittal plane. Slices were stored at room temperature in oxygenated solution C (table 2.1) for up to 8 hours, prior to dissociation. Cells were isolated from the slices using the same dissociation procedure as described above for the salamander Müller cells, except that the tonicity of the incubating and washing solution was increased by the addition of 40mM NaCl, and the solution was bubbled with 100% O_2 during the incubation period. Isolated cells were plated onto 13mm glass cover slips and Purkinje cells could be identified by their large spherical appearance and remains of dendritic trees and axons (figure 2.2).

2.3 Perfusion system

Cover slips were placed on the bottom of a perspex and glass recording chamber, and stuck down with Vaseline. Solution was flowed into the chamber by a gravity feed system, from 50ml syringes via polythene tubing. The bath volume was kept constant by removing the liquid with a syringe needle connected to a vacuum pump. The solution flow rate was approximately 3ml/min.

Müller cells and Purkinje cells were lifted from the bottom of the recording chamber shortly after the whole-cell electrode was attached. They were positioned in front of the bath inlet tube, to facilitate fast solution changes.

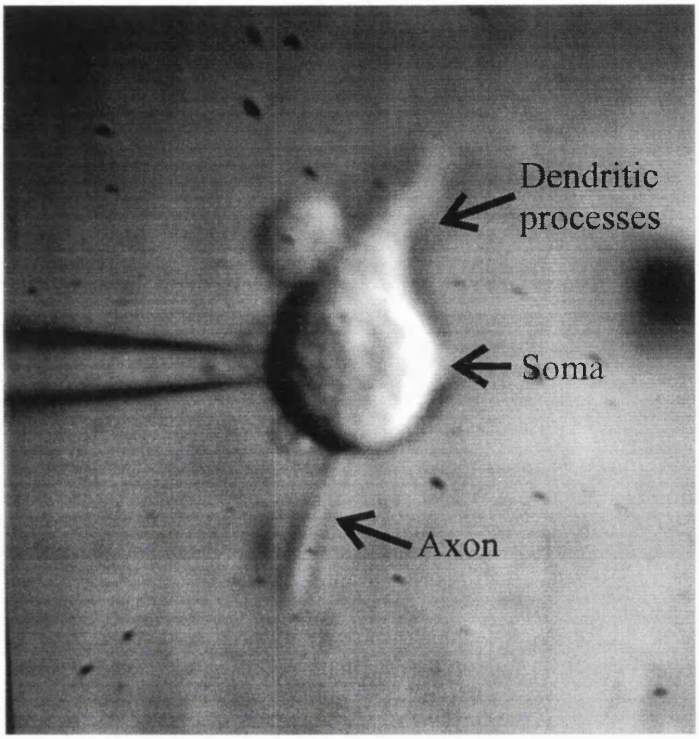

Figure 2.2 - Isolated Purkinje cell

The image shows a Purkinje cell isolated from the cerebellum of a 12 day old rat. The cell body and remains of its axon and dendritic processes are clearly visible. The cell body is approximately 18μm in diameter.

Solution flow was continuous throughout each experiment. All experiments were performed at room temperature (25°C).

2.4 Solutions

The compositions of the solutions used to prepare the cells are given in table 2.1. The solutions for each experiment are described in the figure legends. For experiments that were performed on Purkinje cells, the solutions in the perfusion syringes were usually buffered with HEPES and bubbled with 100% O_2. Solutions which were buffered with bicarbonate were bubbled with a mixture of CO_2 and O_2 (5%/95%).

6mM barium was include in the external solution to block the inward rectifying potassium channels present in the Müller cells (Newman, 1985; Brew and Attwell, 1987). The input resistance of the cell is increased from approximately 10MΩ to 200-500MΩ by the addition of barium. Barium does not affect the magnitude of the glutamate-evoked current (Barbour *et al.*, 1991).

Glutamate forms soluble complexes with divalent metal ions. For solutions containing 6mM Ba^{2+}, 3mM Ca^{2+} and 0.5mM Mg^{2+} (as used in all my experiments), this binding was calculated to reduce the free glutamate concentration by approximately 20% by Barbour *et al.* (1991). However, the calculations of Barbour *et al.* (1991) failed to take into account the pH dependence of the apparent stability constants for these interactions (Dawson *et al.*, 1986). When this factor is considered, less than 0.001% of the free glutamate will be bound to the divalent cations at pH 7.3.

Liquid junction potentials formed at the tip of the electrode were corrected for by the method of (Fenwick *et al.*, 1982). They were all within the range ±5mV.

Measurements of the effects of different conditions on the membrane

currents were always immediately preceded and followed by control measurements. For example, the effects of changing the external pH on the forward glutamate uptake current (figure 3.4) were assessed by applying glutamate to the cell at pH 7.3, changing to a solution of a different pH and applying glutamate, then applying glutamate again at pH 7.3. The relative magnitude of the glutamate evoked current at the altered pH is calculated by comparing the glutamate-evoked current at that pH to the average of the two control measurements.

2.5 Electrical recording from cells

Electrical currents in Müller cells and Purkinje cells were studied using whole-cell patch-clamping (Hamill *et al.*, 1981). Patch pipettes were pulled on a BBCH pipette puller (Mecanex, Geneva) from borosilicate glass capillaries (Clark Electromedical Instruments, GCT150TF10). The whole-cell series resistance of the electrodes was less than 5MΩ.

The electrodes were filled with internal solution and placed in a perspex holder connected to a micromanipulator. The electrode was lowered into the bath, and the junction potential set to zero. The reference electrode was usually a Ag/AgCl pellet, placed in the bath. For experiments which involved a change in extracellular chloride concentration, a 1M NaCl agar bridge was used to reduce changes in junction potential at the bath electrode to less than 0.4mV. The electrode was placed next to the cell while a slight positive pressure was applied to the electrode holder. A brief negative pressure was then applied to seal the electrode on to the cell. Typical seal resistances were in the range 1-5GΩ. A stronger negative pressure was applied to rupture the patch of cell membrane beneath the pipette tip, allowing the cell to be voltage clamped. The membrane current was monitored as the voltage drop across a 500MΩ resistor of a current-

to-voltage converter (EPC7 - List Medical).

Data were acquired on a chart recorder, on magnetic tape (RACAL store 4DS FM tape recorder), or on an IBM-compatible PC (using Pclamp). Analysis was performed by direct measurement of the chart record, by analysis of the magnetic tape on computer (PDP 11/73 via an analogue-to-digital converter), or by the Pclamp computer program.

2.6 Voltage-clamp quality

The non-spherical shape of the Müller cell could cause a lack of uniformity of the voltage-clamp. The degree of non-uniformity can be estimated by representing the Müller cell as a cylinder of length 100μm and average diameter 9μm (figure 2.3). Assuming that the cell is voltage-clamped at one end (actually the electrode was applied to the cell body), the cell can be treated as an electrical cable, terminating in a resistor to ground. With the inward rectifying potassium channels blocked by the addition of 6mM barium to the external solution (as was done in all my experiments), the membrane resistance can be considered uniform over the cell, and is approximately 200MΩ. Taking into account the resistance of the cylinder ends, the resistance per unit length of the cable (r_m) is thus 20.9kΩm; the internal resistance per unit length (r_i) is $3.14 \times 10^{10} \Omega m^{-1}$ (taking the resistivity of the cytoplasm to be 2Ωm); and the terminating resistance (R_{end}) is 9.3GΩ.

The steady-state voltage profile of a one-dimensional cable can be defined by the cable equation as

$$\frac{\lambda^2 d^2 V}{dx^2} - V = 0 \qquad [2.1]$$

where λ is the space constant, V is the voltage and x is the distance. The general solution to equation 2.1 is

$$V(x) = Ae^{x/\lambda} + Be^{-x/\lambda} \qquad [2.2]$$

where A and B are arbitrary constants determined by the boundary

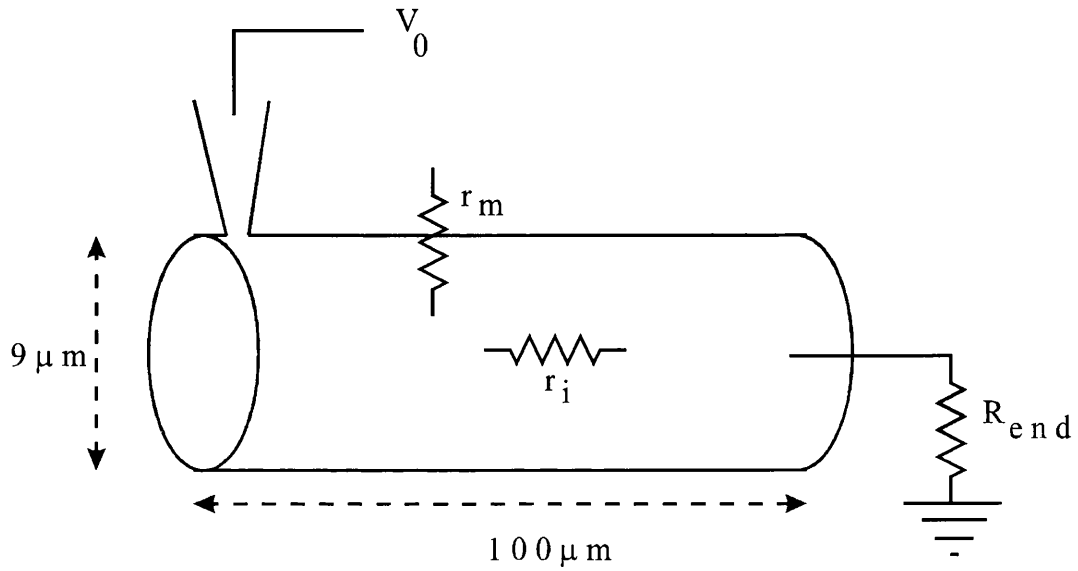

Figure 2.3 - Model of a voltage-clamped Müller cell

The voltage-clamped Müller cell can be represented as a cylinder of average diameter 9µm and length 100µm, with the electrode attached at one end.

conditions. Since at x=0, the voltage (V_0) is determined by the voltage clamp

$$V_0 = A + B \qquad [2.3]$$

The voltage at the other end of the cable (x=end) is determined by the resistor R_{end} and the axial current, i_a. Thus

$$i_a = \frac{(V)_{x=end}}{R_{end}} \qquad [2.4]$$

Now

$$i_a = -\frac{1}{r_i} \cdot \left(\frac{dV}{dx}\right)_{x=end} \qquad [2.5]$$

so from equations 2.4 and 2.5

$$\left(\frac{dV}{dx}\right)_{x=end} = \frac{-r_i (V)_{x=end}}{R_{end}} \qquad [2.6]$$

Substituting equation 2.2 and its derivative into equation 2.6 and simplifying gives

$$A = Be^{-2x/\lambda}\left(\frac{R_{end} - r_i\lambda}{R_{end} + r_i\lambda}\right) \qquad [2.7]$$

Using equations 2.3 and 2.7 to determine A and B, equation 2.2 becomes

$$V_{(x)} = V_0\left(\frac{K}{K+1}\right)e^{x/\lambda} + V_0\left(\frac{1}{K+1}\right)e^{-x/\lambda} \qquad [2.8]$$

where

$$K = e^{-2x/\lambda}\left(\frac{R_{end} - r_i\lambda}{R_{end} + r_i\lambda}\right) \qquad [2.9]$$

The space constant, λ, is equal to $\sqrt{(r_m/r_i)}$, i.e. 816μm for the values in the model above. The voltage at the end, a distance 100μm from the patch electrode can thus be calculated from equation 2.8 to be equal to $0.992V_0$. Thus the voltage drop along the cell is only 0.8% of the voltage applied to the electrode.

When glutamate is applied to the cell, a glutamate uptake current is evoked with a maximum value of the order of 400pA at -40mV, corresponding to a slope conductance of 10^{-8}S (Brew and Attwell, 1987). If this were evenly distributed across the cell, the values of r_m and R_{end} would be reduced to 6.96kΩm and 3.1GΩ respectively. Substituting these new values into equation 2.8 results in the conclusion that the voltage at the end 100μm away from the patch electrode is now

2.3% less than the voltage applied. The voltage-clamp uniformity is thus only slightly reduced by activating the glutamate uptake current.

2.7 Series resistance errors

The voltage drop across the resistance of the patch electrode may be significant if either the resistance is high or the whole-cell currents are large. The resistance of the patch pipette in my experiments was less then 5MΩ, and the whole cell currents were less than 0.5nA. The voltage drop (I x R) for this case would be 2.5mV. This is a negligible voltage error, and was not corrected for in the analysis of the results.

2.8 Analysis of cell capacitance

The whole-cell glutamate uptake current is expected to depend on the size of the cell since larger cells will presumably express a higher number of carriers. When comparing the magnitude of the currents between cells it is therefore desirable to normalize the currents by the cell capacitance. This manipulation reduces the cell-to-cell variation in the magnitude of the current (Barbour *et al.*, 1991).

The cell capacitance can be measured by analyzing the current response to a 10mV voltage pulse. The cell membrane can be considered as a resistor and capacitor in parallel, and the pipette resistance is in series with these two components (figure 2.4). The voltage step will evoke a current change, the time course of which is predicted to be

$$\Delta I(t) = \frac{\Delta V}{R_m + R_p}\left(1 + \frac{R_m e^{-t/\tau}}{R_p}\right) \qquad [2.10]$$

where ΔV is the change in membrane voltage, R_m is the membrane resistance, R_p is the pipette series resistance and τ is the time constant of the transient current

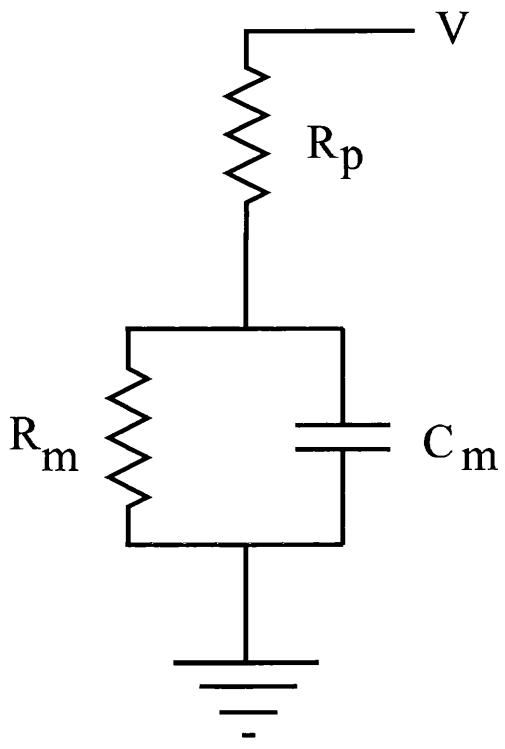

Figure 2.4 - Model of pipette and cell

The circuit diagram represents the whole-cell voltage-clamped cell. R_m and C_m represent the cell membrane resistance and capacitance respectively. R_p represents the pipette resistance.

(Tessier-Lavigne *et al.*, 1988).

At time=0 the capacitance is uncharged, so there is no voltage across it and all the applied voltage drops across the pipette resistance. The pipette resistance can thus be calculated from the voltage step and the current at time=0 as

$$R_p = \frac{\Delta V}{\Delta I_{t=0}} \qquad [2.11]$$

At time=∞, no current flows through the membrane capacitance. The membrane resistance can thus be calculated from the voltage step and the current at time=∞:

$$R_m + R_p = \frac{\Delta V}{\Delta I_{t=\infty}} \qquad [2.12]$$

Substituting Rp from equation 2.11 gives

$$R_m = \frac{\Delta V(I_{t=0} - I_{t=\infty})}{I_{t=0} \cdot I_{t=\infty}} \qquad [2.13]$$

τ was determined by fitting a single exponential to the capacitative transient current (figure 2.5), using the Pclamp computer program. The cell capacitance can then be calculated from (Tessier-Lavigne *et al.*, 1988)

$$C_m = \frac{\tau(R_m + R_p)}{R_m \cdot R_p} \qquad [2.14]$$

2.9 Fluorescence measurement of intracellular pH

Intracellular pH measurements were performed using the fluorescent pH-sensitive dye BCECF (Rink *et al.*, 1982). 100μM BCECF was added to the inside of the cell via the patch pipette. Cells were illuminated by a xenon light via a 490nm filter and neutral density (N.D.=2) filter. Emission from a chosen cell (restricted by a diaphragm) at 530nm was detected by a photomultiplier, amplified and recorded on a chart recorder and video tape. Over the pH range 6 to 8, the fluorescence of the dye at 530nm varies roughly linearly with pH (Rink *et al.*, 1982). Control experiments performed by exciting the dye at its isobestic point (440nm) determined that changes in fluorescence were solely due to changes in the

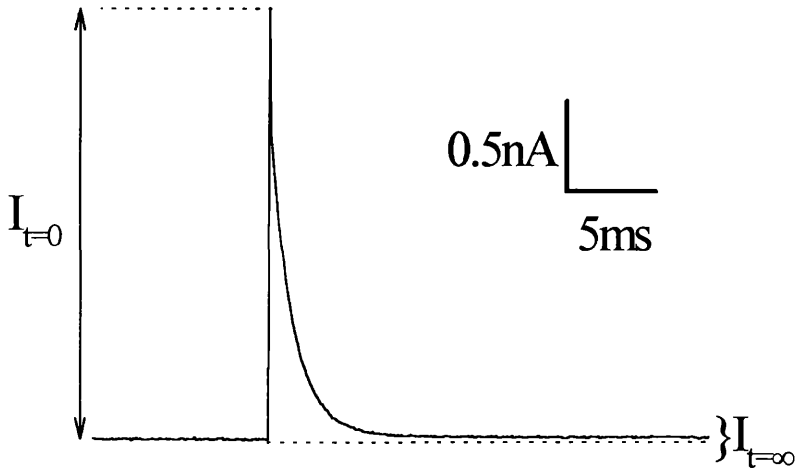

Figure 2.5 - Measurement of cell capacitance

The trace shows the current response to a 10mV voltage step in a whole-cell voltage-clamped Müller cell. For this cell $I_{t=0}$=2.3nA, $I_{t=\infty}$=15pA and τ (fitted with a single exponential using Pclamp) was 1.16ms. From equation 2.11, R_p=4.3MΩ; from equation 2.13, R_m=671MΩ and from equation 2.14, C_m=271pF.

intracellular pH. Calibration of the pH signal was achieved using the K^+-H^+ exchanger nigericin (Chaillet and Boron, 1985) in conjunction with external solutions of different pH.

2.10 Diffusion of substances from the patch pipette

The intracellular solution was controlled by dialyzing the inside of the cell with the solution in the patch pipette. The time taken for the cell's internal solution and the pipette solution to equilibrate can be calculated with the following equations

$$J = -D \cdot A \cdot \frac{dC}{dx} \qquad [2.15]$$

Where J is the diffusion flux from the electrode into the cell, D is the diffusion coefficient of the molecule, A is the area available for diffusion and C is the concentration of the molecule at point x. For the localized barrier at the end of the pipette,

$$J = \frac{D \cdot A \cdot \left(C_{pipette} - C_{cell}\right)}{w} \qquad [2.16]$$

where $C_{pipette}$ and C_{cell} are the concentrations of the molecule in the pipette and the cell, and w is the width of the barrier (i.e. the length of the narrow pipette tip). For a cell of volume V, the total amount of substance in the cell is $V.C_{cell}$. J tends to increase this amount, therefore:

$$J = \frac{d\left(V \cdot C_{cell}\right)}{dt} \qquad [2.17]$$

From equations 2.16 and 2.17:

$$\frac{V \cdot dC_{cell}}{dt} = \frac{D \cdot A\left(C_{pipette} - C_{cell}\right)}{w} \qquad [2.18]$$

The series resistance at the end of the pipette is:

$$R_p = \frac{\rho \cdot w}{A} \qquad [2.19]$$

where ρ is the resistivity of the pipette solution (approximately 0.8Ωm for 100mM

solutions). Rearranging this gives:

$$\frac{A}{w} = \frac{\rho}{R_p} \qquad [2.20]$$

From equations 2.18 and 2.20:

$$\frac{V \cdot dC_{cell}}{dt} = \frac{D.\rho.\left(C_{pipette} - C_{cell}\right)}{R_p} \qquad [2.21]$$

Since $C_{pipette}$ is constant,

$$\frac{V \cdot d\left(C_{cell} - C_{pipette}\right)}{dt} = -\left(\frac{D \cdot \rho}{R_p}\right) \cdot \left(C_{cell} - C_{pipette}\right) \qquad [2.22]$$

or

$$\frac{d\left(C_{cell} - C_{pipette}\right)}{dt} = -\frac{C_{cell} - C_{pipette}}{\tau} \qquad [2.23]$$

where

$$\tau = \frac{V \cdot R_P}{D \cdot \rho} \qquad [2.24]$$

Integrating equation 2.23 gives

$$\int \frac{dy}{y} = -\int \frac{dt}{\tau} \qquad [2.25]$$

where

$$y = C_{cell} - C_{pipette} \qquad [2.26]$$

or

$$\ln(y)_t - \ln(t)_{t=0} = -\frac{t}{\tau} \qquad [2.27]$$

Taking logs, rearranging and substituting y from equation 2.26 gives:

$$C_{cell(t)} - C_{pipette} = \left(C_{cell(t=0)} - C_{pipette}\right) \cdot e^{-t/\tau} \qquad [2.28]$$

If at time=0, C_{cell}=0, then:

$$C_{cell(t)} = C_{pipette} \cdot \left(1 - e^{-t/\tau}\right) \qquad [2.30]$$

Thus, the concentration in the cell rises to the final steady state concentration (the concentration in the pipette) with a time constant, τ, which is equal to $V.R_p/D.\rho$. For the KCl concentration inside a Müller cell to equilibrate with the concentration in the pipette solution, τ is estimated as 34s (taking V as $10^{-14}m^3$ estimated from

video images of the cell, ρ as 0.8Ωm, R_p as 5MΩ, and $D=1.844x10^{-9}m^2s^{-1}$ (at 100mM and 25^{0}C - Robinson and Stokes, 1959).

A low pipette resistance is thus required to ensure rapid control of the intracellular solution. High pipette resistances have been shown to be the cause of the erroneous result of Schwartz and Tachibana (1990), who suggested that removing internal potassium had little effect on aspartate uptake, whereas in fact uptake requires internal potassium (Szatkowski *et al.*, 1991). In my experiments pipette resistances of less than 5MΩ were used. In experiments where accurate control of the internal solution was required, such as for removal of internal potassium when evoking reversed glutamate uptake, five minutes was allowed between breaking the cell membrane and commencing recording.

Table 2.1

Solutions used in preparation of cells.

A=Wash ringer's

B=Dissociation solution

C=Hestrin's solution

All concentrations in mM

	A	B	C
KCl	2.5	3.7	2.5
NaCl	110.5	66	140
$MgCl_2$	0.5		2
$CaCl_2$	3		2.5
HEPES	5		10
Glucose	15	15	10
Na-pyruvate		1	
D,L-cysteine HCl		10	
$NaHCO_3$		25	
NaH_2PO_4		10	
pH with NaOH	7.3		7.6

CHAPTER 3

Effect of pH on forward glutamate uptake

3.1 Introduction

This chapter examines the effect of changing the intra- and extra-cellular pH on the glutamate uptake current. During brain anoxia or ischaemia, the intra- and extra-cellular pH become more acid by up to 1 pH unit (Mutch and Hansen, 1984; Silver and Erecinska, 1992). Since it is the rise in extracellular glutamate concentration which triggers neuronal death during anoxia (Choi and Rothman, 1990 and section 1.3), the effect of pH changes on the uptake carriers' ability to reduce the extracellular glutamate concentration is of interest. As the glutamate uptake carrier is known to transport a pH-changing ion (Bouvier *et al.*, 1992), changing the pH either inside or outside the cell could be expected to affect the rate of glutamate uptake by changing the concentration of one of the substrates the carrier requires to cycle. In addition pH changes might have a direct action on the glutamate uptake carrier, independent of changes in substrate concentration.

The pH range studied in these experiments was 5 to 9. The pK_a values of two amino acid side chains lie within this range. The side chain of histidine has a pK_a value of 6.04 and the side chain of cysteine has a pK_a value of 8.37 (Dawson *et al.*, 1986). The amino acid sequences of the mammalian homologues of the two salamander Müller cell carriers, GLAST (Storck *et al.*, 1992) and GLT-1 (Pines *et al.*, 1992) indicate that these proteins contain 4 and 11 histidine, and 3 and 8 cysteine residues respectively. Assuming these residues are conserved in the salamander proteins, these are possible sites of action by which the pH changes could affect the carriers.

Since each forward cycle of the glutamate uptake carrier results in the inward movement of net positive charge (section 1.2.4), forward glutamate uptake

was assessed by examining the inward current produced when glutamate was applied to the outside of voltage-clamped cells (Brew and Attwell, 1987).

3.2 Effect of pH on the glutamate molecule

The glutamate molecule (figure 3.1) has three ionizable groups, the alpha amino and carboxyl groups and the gamma carboxyl group of the side chain.

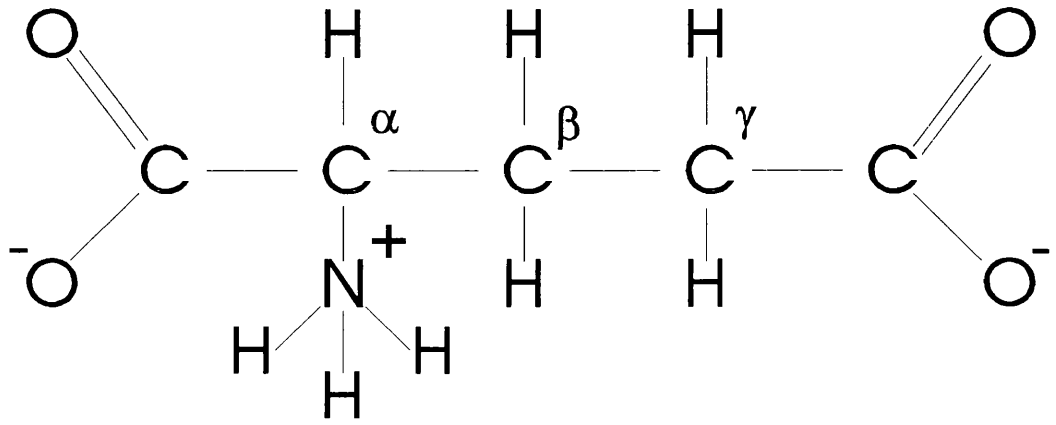

Figure 3.1 - Structure of fully ionized glutamate

These ionizable groups have pK values of 9.47, 2.10 and 4.07 respectively (Dawson *et al.*, 1986). It is assumed that the transported form of glutamate is that in which all the ionizable groups are in the charged form (i.e. Glu^{+---}), since 99% of the glutamate will be in this form at a physiological pH.

The proportion of each acid group which is in the charged form can be calculated by rearrangement of the Henderson-Hasselbach equation:

$$pH = pK + \log\frac{[A^-]}{[HA]} \qquad [3.1]$$

Therefore:

$$\frac{[HA]}{[HA]+[A^-]} = \frac{1}{1+10^{(pH-pK)}} \qquad [3.2]$$

The proportion of the basic groups in the ionized form can similarly be calculated as:

$$\frac{[A^-]}{[HA]+[A^-]} = \frac{1}{1+10^{(pK-pH)}} \qquad [3.3]$$

Multiplying equations 3.2 and 3.3 together for the three ionizable groups gives the proportion of glutamate in the transportable form:

$$\frac{[Glu^{+--}]}{[Glu]_{total}} = \frac{1}{(1+10^{(pH-9.47)})(1+10^{(2.10-pH)})(1+10^{(4.07-pH)})} \qquad [3.4]$$

This function is expressed graphically in figure 3.2. At pH 7.3, 99.3% of the total glutamate is in the fully ionized form. For pH 6.0 and pH 8.0 this has only fallen to 98.8% and 96.7% respectively. These resulting small changes in effective glutamate concentration will make no significant differences to the dose-response curves presented below.

3.3 Internal pH measurements

Manipulations of the cells' internal pH were performed by changing the pH of the solution in the whole-cell pipette, using a high concentration (≥60mM) of intracellular buffer (see figure 3.3 legend). To test that changing the pipette pH did indeed change the internal pH to the desired value, fluorescence measurements of the intracellular pH were made using the pH-sensitive dye BCECF (see section 2.9). Confirmation that changing the external pH did not affect the carrier indirectly by changing the internal pH was also obtained using this method. The fluorescence signal was calibrated using external solutions of different pH, in the presence of the H^+-K^+ exchanger nigericin (Chaillet and Boron, 1985). When nigericin is added to the external solution at the end of the experiment, the relationship between internal and external pH can be calculated from the equation (Chaillet and Boron, 1985):

$$\frac{[K^+]_i}{[K^+]_o} = \frac{[H^+]_i}{[H^+]_o} = \frac{10^{-pH_i}}{10^{-pH_o}} \qquad [3.5]$$

The internal potassium concentration for these experiments was 60mM, and the external concentration was 105mM. The theoretical internal pH is thus calculated

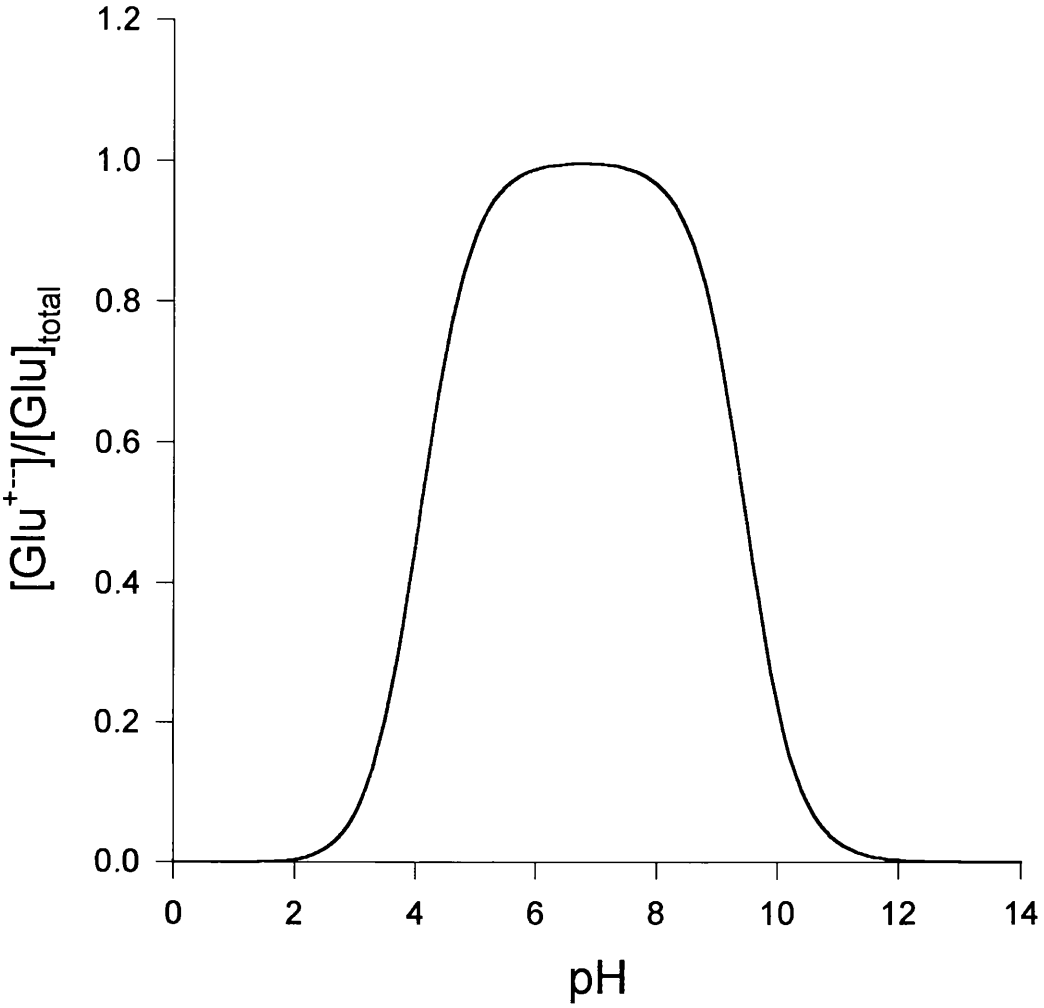

Figure 3.2 - The proportion of glutamate in the fully ionized form (Glu^{+--}) as a function of pH, calculated from equation 3.4.

Figure 3.3 - Fluorescence measurement of internal pH

Müller cells were whole-cell voltage-clamped, and held at -40mV. The internal pH was monitored fluorescently by adding BCECF to the pipette solution. The internal fluorescence signal and the external pH are plotted on the same scale. Only slight changes in the internal pH were observed when the external pH was changed from 7.35 to 5.95, to 8.05 and back to 7.35. The fluorescence signal was then calibrated using nigericin, indicated by the shaded bar at the bottom of the graph. The dashed line represents the theoretical internal pH, when the external pH was changed in the presence of nigericin. It is offset from the external pH due to the different potassium concentrations inside and outside the cell, as calculated in equation 3.6. The internal fluorescence trace has been positioned on the pH axis in such a way that the signal coincides closely with the theoretical value in the presence of nigericin.

Solutions - External solutions contained (in mM) KCl 5, NaCl 104.5, $CaCl_2$ 3, $MgCl_2$ 0.5, $BaCl_2$ 6, glucose 15 and buffer 5. The solutions were titrated to pH 7.35 (buffered with HEPES), 8.05 (TAPS) or 5.95 (MES) using NMDG. For calibration with nigericin, the external solution was the same except KCl 105, NaCl 0 and nigericin 0.001 (0.1%DMSO). The solutions were titrated to the desired pH with KOH.

Internal solutions contained (in mM) KCl 50, K_2EGTA 5, NaCl 5, Na_2ATP 5, $CaCl_2$ 1, $MgCl_2$ 7, BCECF 0.1 and buffer. The buffers used were: for internal pH=6.9 HEPES 77mM, for pH=7.7 66mM TAPS, and for pH=5.9 60mM MES. The solutions were titrated to the desired pH with 19, 30 and 36mM NMDG respectively.

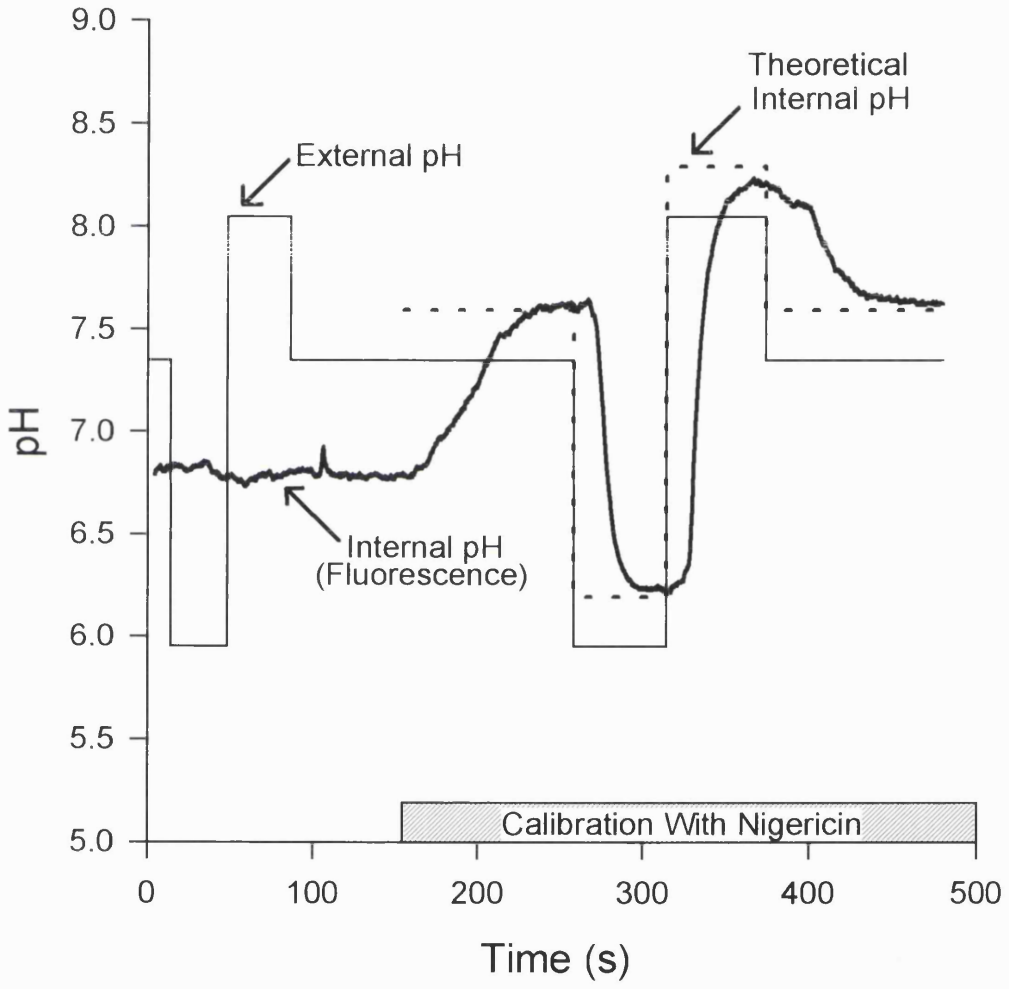
9.0
8.5
8.0
7.5
7.0
6.5
6.0
5.5
5.0
pH
Theoretical
Internal pH
External pH
Internal pH
(Fluorescence)
Calibration With Nigericin
0
100
200
300
400
500
Time (s)

as follows:

$$pH_i = -\log\left(\frac{[K^+]_i}{[K^+]_o}\right) + pH_o \qquad [3.6]$$
$$= 0.243 + pH_o$$

An example of changes in the fluorescence of intracellular BCECF when the external pH was changed, along with a calibration using nigericin, is shown in figure 3.3.

In normal external solution (no nigericin) changing the external pH from 7.35 to 8.05 resulted in an average change in internal pH of 0.07±0.03 pH units (mean±SEM of data from 6 cells). Changing the external pH from 7.35 to 5.95 resulted in an internal pH change of 0.05±0.01 pH units (mean±SEM of data from 5 cells). These small changes show that changes in the external pH will not have significant effects on the cells due to alterations of the internal pH.

When the cells were voltage-clamped with electrodes containing highly buffered solutions at pH 6.9, pH 7.7 or pH 5.9, the internal pH measured was within 0.13±0.07 pH units (mean±SEM of data from 12 cells) of the desired value. This is a relatively minor deviation from the desired value, so in the following figures pipette pH is plotted.

3.4 External pH-dependence of the maximal rate of forward uptake

First, the dependence of the inward current produced by forward glutamate uptake on external pH was investigated. The pH-dependence of the maximal uptake rate was tested by measuring the current produced by applying a near-saturating dose of glutamate (200μM) to the outside of the cells at different pH values (Fig. 3.4). The external pH was changed by using external solutions titrated to different pH values with NMDG. For acid external solutions ($pH_o < 6.7$), the buffer MES (pK_a =6.1) was used instead of the normal HEPES. For alkali solutions ($pH_o > 7.9$) TAPS (pK_a =8.4) was used.

Figure 3.4 - pH-dependence of the maximal rate of forward uptake

A. Typical membrane currents recorded in a whole-cell voltage-clamped Müller cell at different external pH values. The holding potential was -40mV. The black bar above each trace represents bath application of a near-saturating dose (200μM) of glutamate. The external pH is indicated by the column of numbers on the right.

B. The magnitude of the maximal glutamate uptake current, from experiments like in A, is plotted as a function of external pH. The currents are normalized by the size of the current observed at pH 7.3, and are shown as the mean±SEM of data from 6 cells. The data are fit with a line calculated from equation 3.7.

Solutions - External solutions contained (in mM) KCl 2.5, NaCl 104.5, $MgCl_2$ 0.5, $CaCl_2$ 3, $BaCl_2$ 6, glucose 15 and buffer 5. For solutions with pH < 6.7 the buffer used was MES, for pH 6.7 to 7.9 the buffer was HEPES, and for pH > 7.9 TAPS. The solutions were titrated to the appropriate pH using NMDG.

The internal solution contained (in mM) KCl 50, K_2EGTA 5, NaCl 5, Na_2ATP 5, $CaCl_2$ 1, $MgCl_2$ 7, HEPES 71. It was titrated to pH 7.0 with 25mM NMDG.

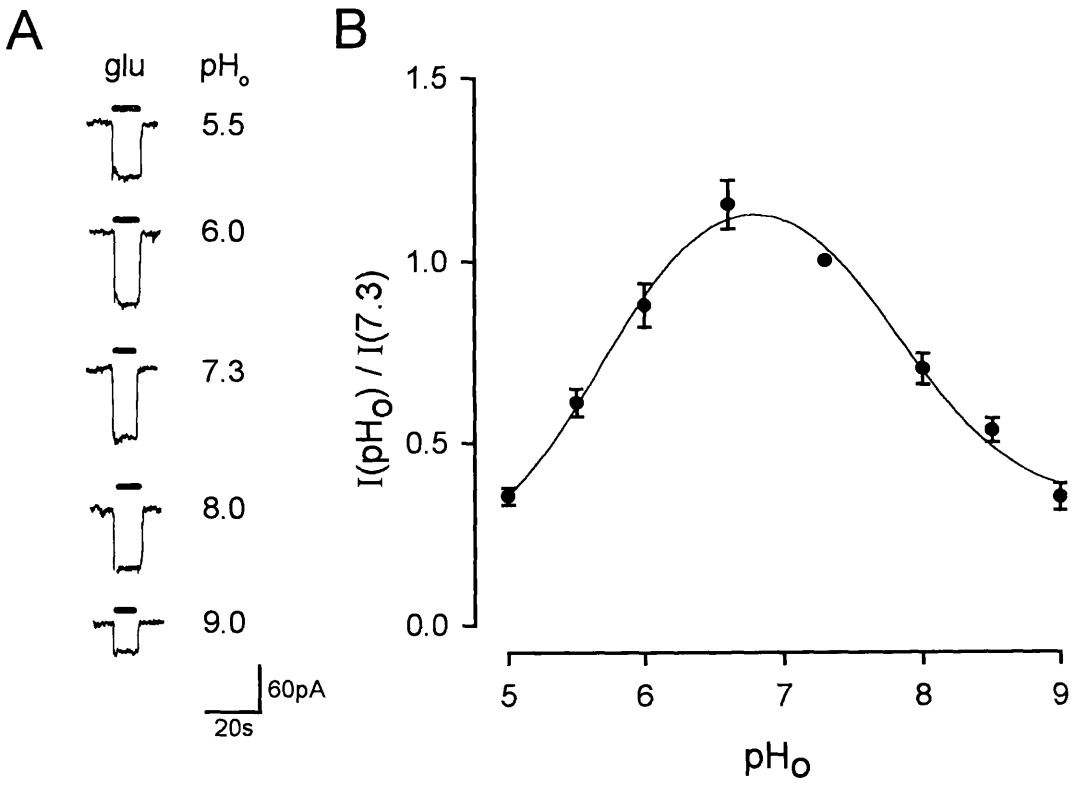
A
glu
pH$_o$
5.5
6.0
7.3
8.0
9.0
60pA
20s
B
I(pH$_O$) / I(7.3)
1.5
1.0
0.5
0.0
5
6
7
8
9
pH$_O$

Control experiments were performed to test if the different buffers used directly affected the glutamate uptake carrier. Solutions titrated to the same pH, but with different buffers were used. The pH was chosen to be mid-way between the pK_a of the two buffers concerned, so that the buffering powers of the two solutions were approximately equal. For external pH 6.8, buffered with either MES or HEPES, the maximal glutamate uptake currents were 96±10% and 93±8% (mean±SEM of data from 5 cells) respectively of the control current at pH 7.3. There is no significant difference between the currents recorded with these two buffers ($p=0.69$, paired t-test). For external pH 8.0, buffered with either TAPS or HEPES, the maximal glutamate uptake currents were 73±3% and 78±3% (mean±SEM of data from 5 cells) respectively of the control current at pH 7.3. This difference between the currents recorded with HEPES and TAPS is significant ($p=0.03$, paired t-test), but is a small enough change to be of little consequence. Thus, differences in uptake currents at different pH values (figure 3.4) presumably reflect the altered pH rather than the altered buffer species or concentration.

Since glutamate uptake is known to cause changes in the intracellular pH (Bouvier *et al.*, 1992), and the external pH change itself may influence the internal pH, an internal solution containing a high concentration of buffer (71mM HEPES) was used to minimize any effects of intracellular pH changes on the uptake current (see figure 3.3).

The data in figure 3.4 show that a maximum current was produced around pH 7, with an inhibition of uptake at both a higher and a lower pH. The inhibition at a high pH could be explained by the extra hydroxide present outside the cell preventing the unbinding of hydroxide transported out of the cell at the external surface of the carrier (see figure 1.1), thus preventing the carrier cycling. By the same argument, an acid external pH would have been expected to increase the rate of glutamate uptake. The inhibition actually observed at an acid pH might reflect

the extra protons titrating an area of the external surface of the carrier protein, distinct from the hydroxide binding site, as discussed later.

The data are fit with a line with the following equation:

$$I = I_{max}\left(\min_1 + \frac{(1-\min_1)}{1+10^{K_1-pH}}\right)\left(\min_2 + \frac{(1-\min_2)}{1+10^{pH-K_2}}\right) \qquad [3.7]$$

This represents a bell-shaped function, where I_{max} is the maximum value, min_1 and min_2 are the two minimum values at low and high pH respectively (expressed as fractions), and K_1 and K_2 are constants - the pH values for each side of the curve at which the curve is half way between its maximum and minimum values. Best fitting a line with this equation gives values for K_1 and K_2 of 5.71 and 7.8 respectively. These values are close to the pK values of the amino acid side chains of histidine (6.04) and cysteine (8.37), indicating that the reduction in transport at low and high pH could be due to changes in the ionization of these amino acid side chains.

3.5 External pH-dependence of the apparent affinity for external glutamate

The effect of external pH on the apparent affinity of the carrier for external glutamate was tested by performing complete dose-response curves for the glutamate-evoked current at different extracellular pH values. Figure 3.5A shows specimen data comparing the current produced by a near-saturating (200μM) and a non-saturating (30μM) dose of glutamate at a normal, an acid, and alkali pH. The smaller size of the current produced by the non-saturating dose, relative to that produced by the saturating dose, is an indication of a lower affinity of the carrier for external glutamate at higher external pH values.

The complete dose-response curves at the different pH values are shown in figure 3.5B. The data are best-fit with Michaelis-Menten functions, constrained to a V_{max} of 1, to determine the apparent K_M for glutamate. These observed K_M values were then adjusted to take into account the reduced concentration of

Figure 3.5 - External pH-dependence of the apparent affinity for external glutamate

A. Whole-cell voltage-clamped Müller cells were held at -40mV. Membrane currents produced by a near-saturating (200μM) and a non-saturating (30μM) dose of glutamate (indicated by the black bar above the current trace) are compared for external pH 5.0, 7.3 and 9.0.

B. Complete glutamate dose-response curves at different extracellular pH values. The currents at each pH are normalized to the maximum value at that pH. The observed K_M (in μM) is determined by best-fitting the data with a Michaelis-Menten equation. The real K_M (in μM) for each pH is calculated by taking into account the effects of pH on the proportion of glutamate in the transportable form (from equation 3.4). Data points are mean±SEM of data from 6 cells.

Solutions External solutions contained (in mM) KCl 2.5, NaCl 104.5, $MgCl_2$ 0.5, $CaCl_2$ 3.0, $BaCl_2$ 6, glucose 15 and buffer 5. For external pH 9.0 the buffer was TAPS, for pH 7.3 HEPES, and for pH 5.0 MES. Solutions were titrated to the appropriate pH with NaOH.

The internal solution contained (in mM) KCl 95, K_2EGTA 5, NaCl 5, Na_2ATP 5, $CaCl_2$ 1, $MgCl_2$ 7 and HEPES 5. It was titrated to pH 7.0 with KOH.

A

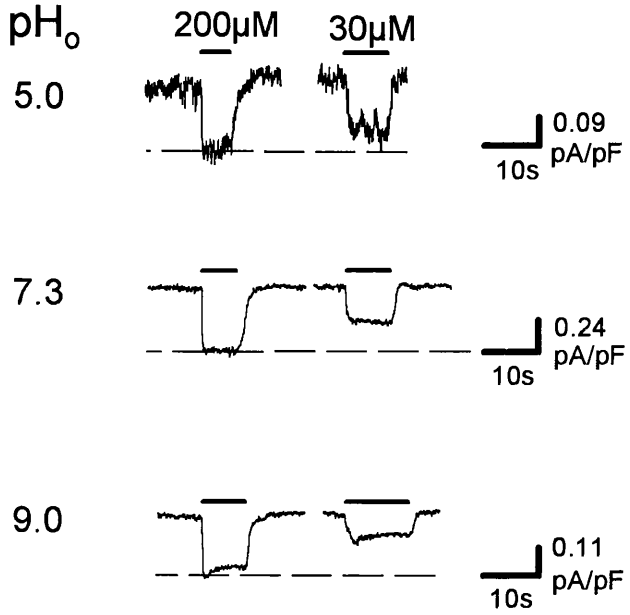
pH$_o$
200μM
30μM
5.0
0.09
pA/pF
10s
7.3
0.24
pA/pF
10s
9.0
0.11
pA/pF
10s

B

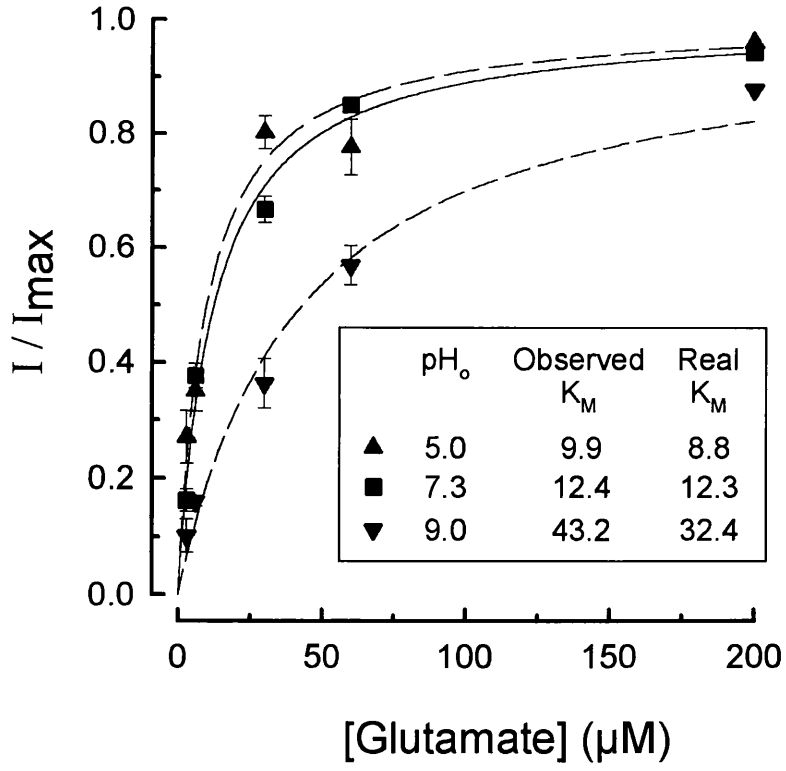
1.0
0.8
0.6
0.4
0.2
0.0
I / Imax
0
50
100
150
200
[Glutamate] (μM)
pH$_o$
Observed K$_M$
Real K$_M$
5.0
9.9
8.8
7.3
12.4
12.3
9.0
43.2
32.4

completely ionized glutamate at the different pH values (from equation 3.4).

The calculated K_M values show an increase with increasing extracellular pH, indicating that the apparent affinity of the carrier for glutamate is higher at an acid pH. The K_M is plotted as a function of external pH in figure 3.6A. The relationship between the affinity of the carrier for external glutamate, and the maximal rate of uptake, is shown in figure 3.6B

3.6 Effect of external pH on apparent sodium affinity

The affinity of the glutamate uptake carrier for external sodium ions was tested by applying a near-saturating dose of glutamate (200μM), at different external sodium concentrations. Sodium was replaced by choline. Since the uptake carrier is thought to transport two sodium ions per carrier cycle, the data were fit with the square of a Michaelis-Menten function (i.e. simplistically assuming independent rather than ordered binding) to determine the apparent affinity for sodium at different extracellular pH values. The sodium-dependency curves are plotted in figure 3.7

As the external pH was made more acid, the apparent affinity for sodium was decreased, with no significant change in the maximum current produced at saturating sodium concentrations. This suggests that the inhibition of glutamate uptake by an acid external pH, in figure 3.4, is due to protons and sodium ions competing for the same binding site on the external surface of the carrier. This site could involve a histidine residue, because of the pK value for the fit to the decrease at acid pH in figure 3.4.

3.7 Effect of internal pH on the maximal rate of forward glutamate uptake

The effect of changing the internal pH on the maximal rate of forward glutamate uptake was tested by whole-cell voltage-clamping the cells using pipette

Figure 3.6 - Relationship between external pH, K_M and V_{max}

A. The K_M for external glutamate (real K_M from figure 3.5) plotted as a function of external pH.

B. The carrier's V_{max} (from figure 3.4) plotted as a function of the K_M for external glutamate (from figure 3.5).

A

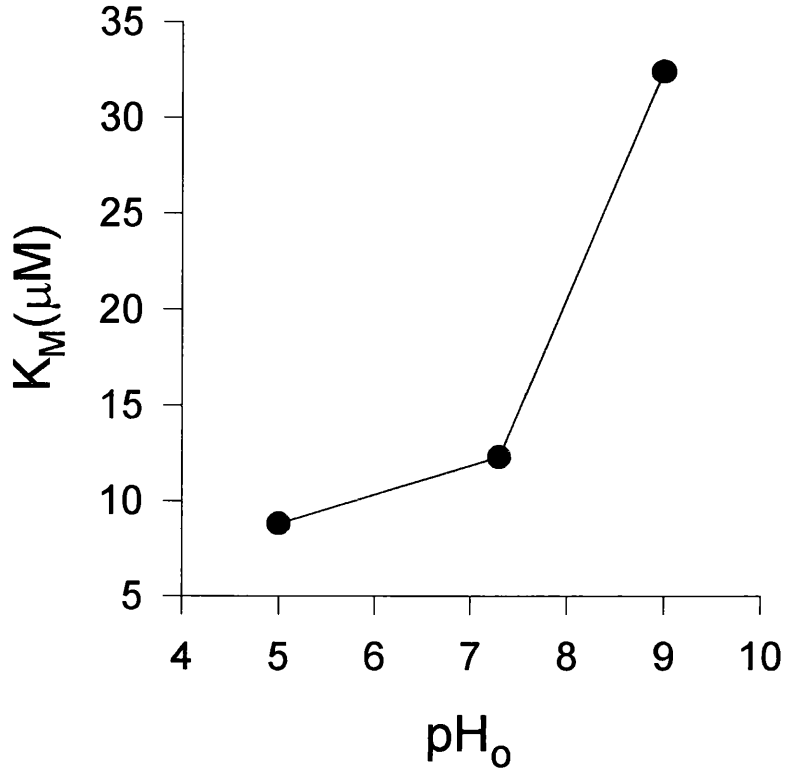
35
30
25
20
15
10
5
$K_M(\mu M)$
4
5
6
7
8
9
10
pH_o

B

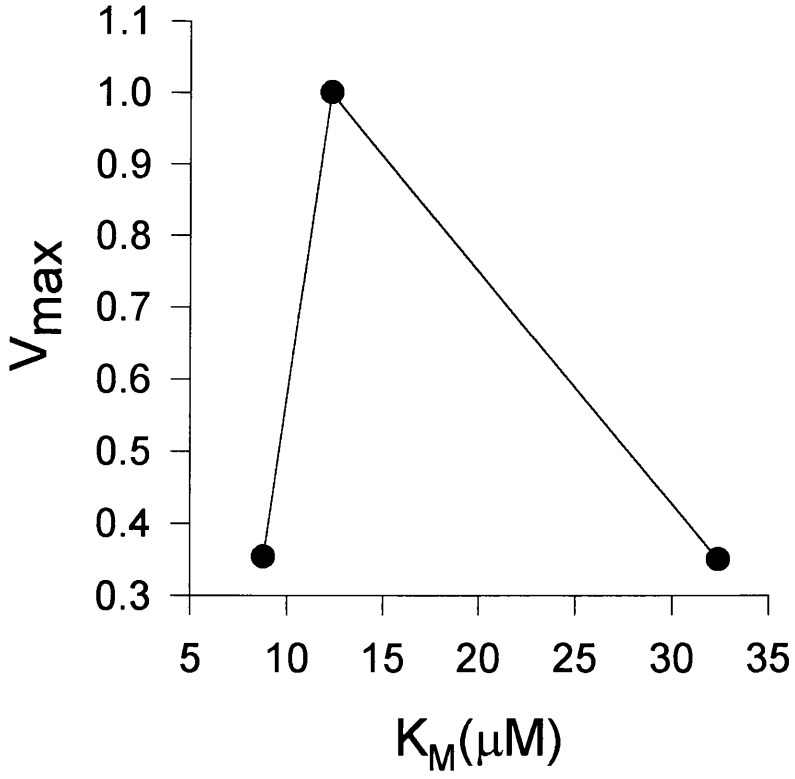
1.1
1.0
0.9
0.8
0.7
0.6
0.5
0.4
0.3
V_{max}
5
10
15
20
25
30
35
$K_M(\mu M)$

Figure 3.7 - The sodium-dependence of the maximal glutamate uptake current at different external pH values

Whole-cell voltage-clamped Müller cells were held at -40mV. The current evoked by 200μM glutamate is plotted as a function of external sodium concentration for external pH 7.3, 6.1 and 5.0. The currents are normalized to the value obtained with 110mM Na^+ at external pH 7.3. The data points are mean±SEM of the data from 5 cells. The data were fit with the square of a Michaelis-Menten function (inset), and the parameters of these fits are shown on the right. An acid pH decreased the sodium affinity with little effect on the maximum current at a saturating external sodium concentration.

Solutions External solutions contained (in mM) KCl 2.5, NaCl 110, $MgCl_2$ 0.5, $CaCl_2$ 3, $BaCl_2$ 6, glucose 15 and buffer 5. For external pH 7.3 the buffer used was HEPES, for pH 6.1 and 5.0 MES was used. The pH was adjusted to the desired value with NMDG. The sodium concentration was reduced by replacing NaCl with choline-Cl.

The internal solution contained (in mM) KCl 50, K_2EGTA 5, NaCl 5, Na_2ATP 5, $CaCl_2$ 1, $MgCl_2$ 7, HEPES 71. The pH was adjusted to 7.0 with 25mM NMDG.

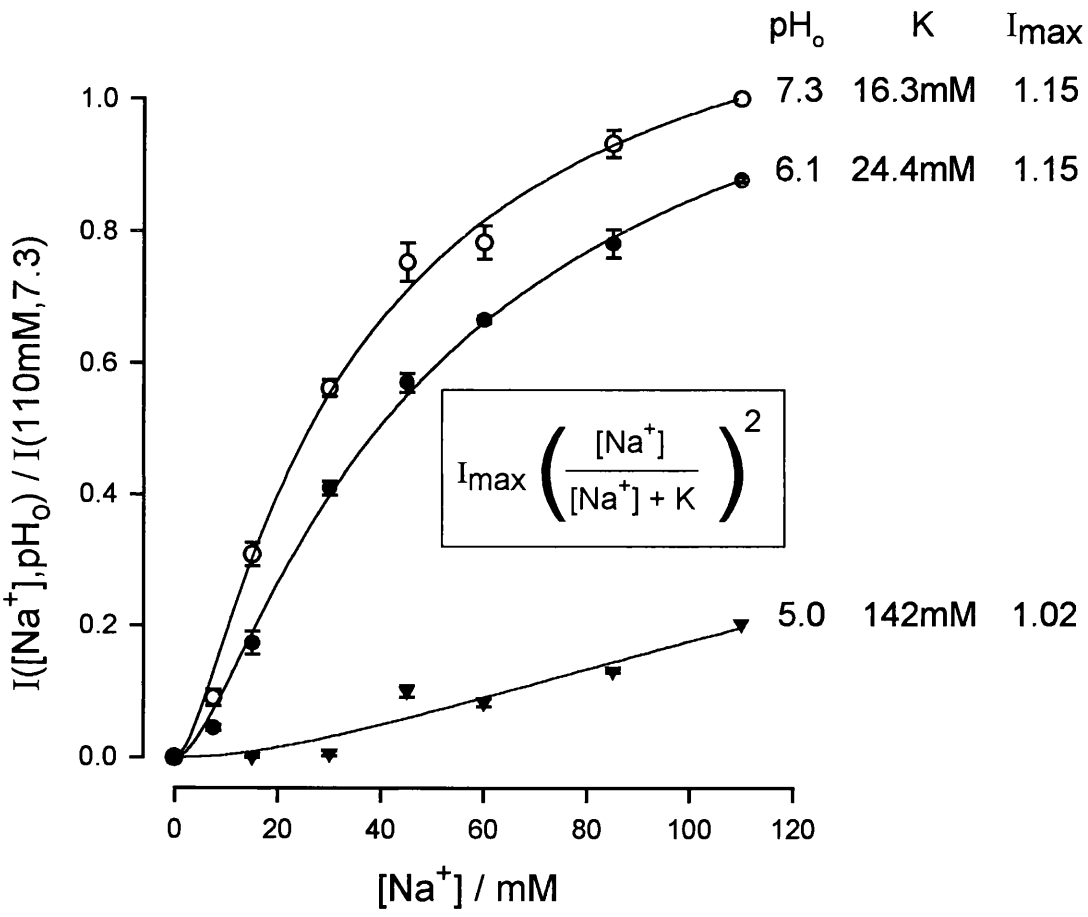
pH$_o$ K Imax
7.3 16.3mM 1.15
6.1 24.4mM 1.15
5.0 142mM 1.02
$I_{max}\left(\frac{[Na^+]}{[Na^+]+K}\right)^2$
I([Na$^+$],pH$_o$) / I(110mM,7.3)
[Na$^+$] / mM
0.0
0.2
0.4
0.6
0.8
1.0
0
20
40
60
80
100
120

solutions highly buffered to different pH values. Low series resistance (typically less than 4 MΩ) pipettes were used, and recordings were not made until the cell membrane had been broken for at least 5 minutes. This was intended to ensure that there had been adequate dialysis of the intracellular solution. A near-saturating dose of glutamate (200μM) was applied to determine the rate of glutamate uptake at each internal pH. Uptake currents in different cells were compared, so errors introduced by variability in the size of the cells were reduced by normalizing each cell's current to its capacitance (Barbour *et al.* 1991).

Control experiments were performed to test if the different buffers used to examine a wide pH range directly affected the internal surface of the glutamate uptake carrier. Internal solutions of the same pH, but with different buffers were used. The pH was chosen to be mid-way between the pK_a of the buffers concerned, so that the buffering power of the two solutions were approximately equal. For internal pH 6.8, buffered with either MES or HEPES, the maximal glutamate uptake currents (normalized by cell capacitance) were 0.39±0.04pA/pF and 0.38±.05pA/pF (mean±SEM of data from 5 cells) respectively. There is no significant difference between the currents recorded with these two buffers ($p=0.90$, two-tailed t-test). For internal pH 8.0, buffered with either TAPS or HEPES, the maximal glutamate uptake currents were 0.69±0.08pA/pF and 0.74±0.08pA/pF (mean±SEM of data from 6 cells) respectively. There is no significant difference between the currents recorded with these two buffers either ($p=0.68$, two-tailed t-test). Thus differences in uptake current seen at different internal pH values (figure 3.8) presumably reflect the altered pH rather than the altered buffer species or concentration.

Sample currents recorded from different cells at different internal pH values are shown in figure 3.8A. The uptake current was increased at more alkaline values of internal pH. Averaged values are plotted as a function of internal pH in figure 3.8B. The data are best-fit with a Michaelis-Menten dependence of current

Figure 3.8 - Internal pH-dependence of the maximal rate of forward uptake

A. Membrane currents recorded in whole-cell voltage-clamped Müller cells at different values of internal pH. The holding potential was -40mV. The black bar above each trace represents the bath application of a near-saturating dose of glutamate (200μM). Data for each different value of internal pH were obtained from different cells clamped using pipette solutions of different pH values.

B. The magnitude of the maximal forward uptake current plotted as a function of internal pH. The currents are normalized to the cells' capacitance. The data are fit with a Michaelis-Menten dependence on the internal hydroxide ion concentration, proportional to $[OH^-]_i/([OH^-]_i+K_M)$ with K_M=43nM The points are the mean±SEM of the data from at least 5 cells.

Solutions The external solution contained (in mM) KCl 2.5, NaCl 104.5, $MgCl_2$ 0.5, $CaCl_2$ 3, $BaCl_2$ 6, glucose 15 and HEPES 5. The pH was adjusted to 7.3 with NMDG.

Internal solutions contained (in mM) KCl 50, K_2EGTA 5, NaCl 5, Na_2ATP 5, $CaCl_2$ 1, $MgCl_2$ 7 and buffer. For pH 7.0, 71mM HEPES was used as the buffer and the pH was adjusted to 7.0 with 25mM NMDG. For pH values between 6.8 and 7.9 the concentrations of HEPES and NMDG were adjusted appropriately. For pH values less than 6.8, HEPES was replaced by MES. For pH values above 7.9, HEPES was replaced by TAPS.

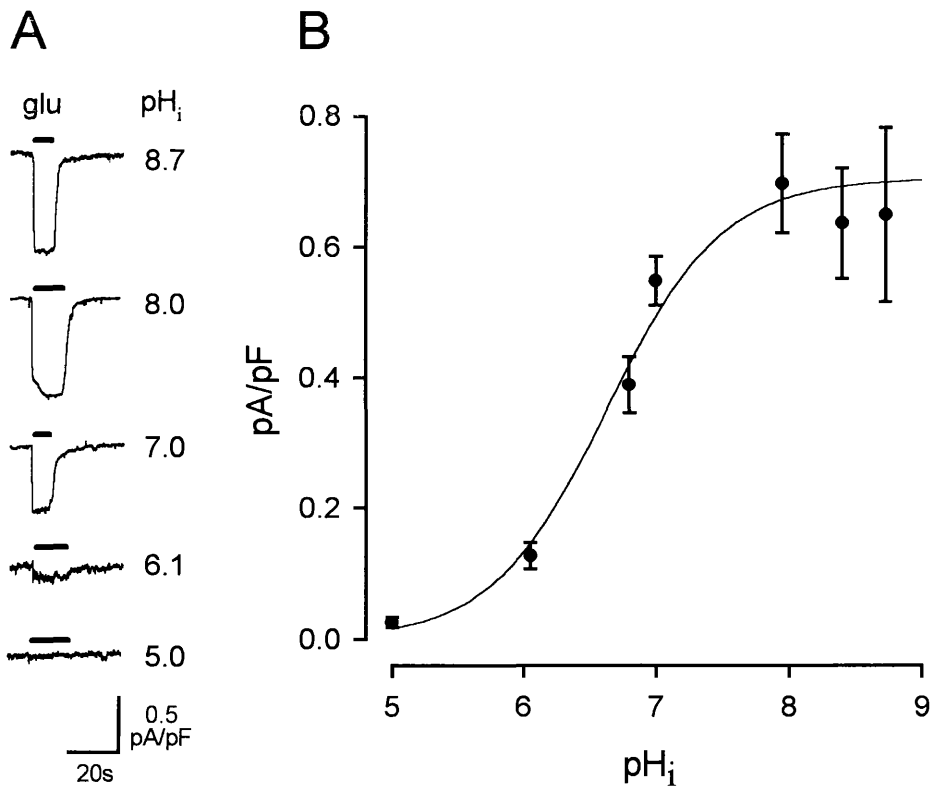
A
glu
pH$_i$
8.7
8.0
7.0
6.1
5.0
0.5
pA/pF
20s
B
0.8
0.6
0.4
0.2
0.0
pA/pF
5
6
7
8
9
pH$_i$

on internal hydroxide ion concentration. A half-maximal current was observed with an internal hydroxide ion concentration of 43nM, which corresponds to a pH of 6.63 (assuming $[OH^-][H^+]=10^{-14}M^2$).

An inhibition of glutamate uptake by an acid internal pH (low $[OH^-]_i$) is expected since internal hydroxide is one of the substrates for the carrier, although an additional inhibition due to protons titrating the internal surface of the carrier can not be ruled out. Possible effects of internal pH on the potassium-binding site were not tested.

3.8 Internal pH-dependence of the apparent affinity for external glutamate

The effect of changing the internal pH on the carriers' affinity for external glutamate was tested. Dose-response curves for glutamate were performed at different internal pH values. Figure 3.9A compares the currents produced by a near-saturating (200μM) dose of glutamate and by a non-saturating (30μM) dose of glutamate as the internal pH is changed. The complete dose-response curves are shown in figure 3.9B, where each point is normalized to the value produced by 200μM glutamate for each pH. The data were best-fit with Michaelis-Menten curves to determine the K_M for each internal pH. As the internal pH was made more acid, from 8.7 to 6.8, the K_M for external glutamate was reduced. The K_M is plotted as a function of the internal pH in figure 3.10A, and the relationship between the carrier's affinity for external glutamate and the maximal rate of uptake when varying internal pH is plotted in figure 3.10B.

3.9 Discussion

The results presented in this chapter demonstrate the effects of changing the internal and external pH on the forward glutamate uptake current.

Forward glutamate uptake was maximal at normal extracellular pH, and

Figure 3.9 - Internal pH dependence of the carrier's affinity for external glutamate

A. Whole-cell voltage-clamped Müller cells were held at -40mV. Membrane currents produced by a near-saturating (200μM) and a non-saturating (30μM) dose of glutamate at different internal pH values, are compared. Data from each internal pH value are from a different cell.

B Complete glutamate dose-response curves at different intracellular pH values. The currents are normalized to the maximum value at each pH. The data are best fit with Michaelis-Menten equations: $[glu]_o/([glu]_o+K_M)$. The data points are the mean±SEM of the data from at least 5 cells.

Solutions The external solution contained (in mM) KCl 2.5, NaCl 104.5, $MgCl_2$ 0.5, $CaCl_2$ 3, $BaCl_2$ 6, glucose 15 and HEPES 5. The pH was adjusted to 7.3 with NMDG.

Internal solutions contained (in mM) KCl 50, K_2EGTA 5, NaCl 5, Na_2ATP 5, $CaCl_2$ 1, $MgCl_2$ 7 and buffer. For pH 7.0, 71mM HEPES was used as the buffer and the pH was adjusted to 7.0 with 25mM NMDG. For pH values between 6.8 and 7.9, the concentrations of HEPES and NMDG were adjusted appropriately. For pH values less than 6.8, HEPES was replaced by MES. For pH values above 7.9, HEPES was replaced by TAPS.

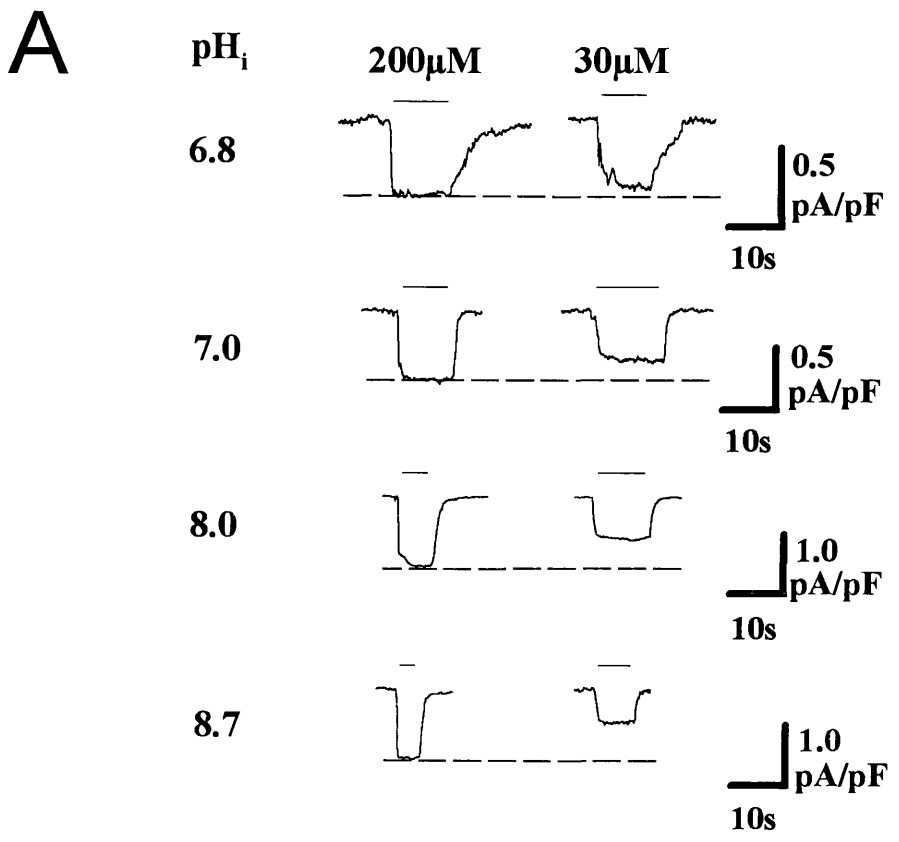
A
pH$_i$
200μM
30μM
6.8
0.5 pA/pF
10s
7.0
0.5 pA/pF
10s
8.0
1.0 pA/pF
10s
8.7
1.0 pA/pF
10s

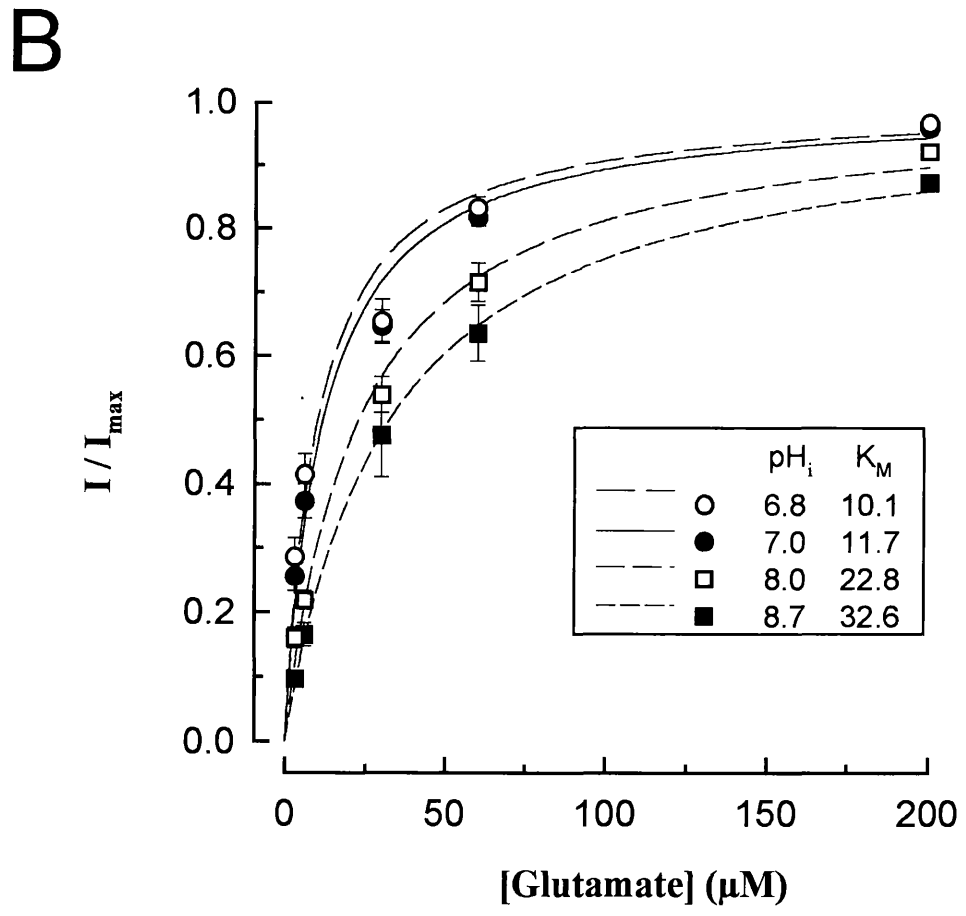
B
1.0
0.8
0.6
0.4
0.2
0.0
I / I$_{max}$
0
50
100
150
200
[Glutamate] (μM)
pH$_i$
K$_M$
6.8 10.1
7.0 11.7
8.0 22.8
8.7 32.6

Figure 3.10 - Relationship between internal pH, K_M and V_{max}

A. The K_M for glutamate (from figure 3.9) plotted as a function of internal pH.

B. The carrier's V_{max} at various internal pH values (from figure 3.8) plotted as a function of the K_M for glutamate at the same internal pH value (from figure 3.9).

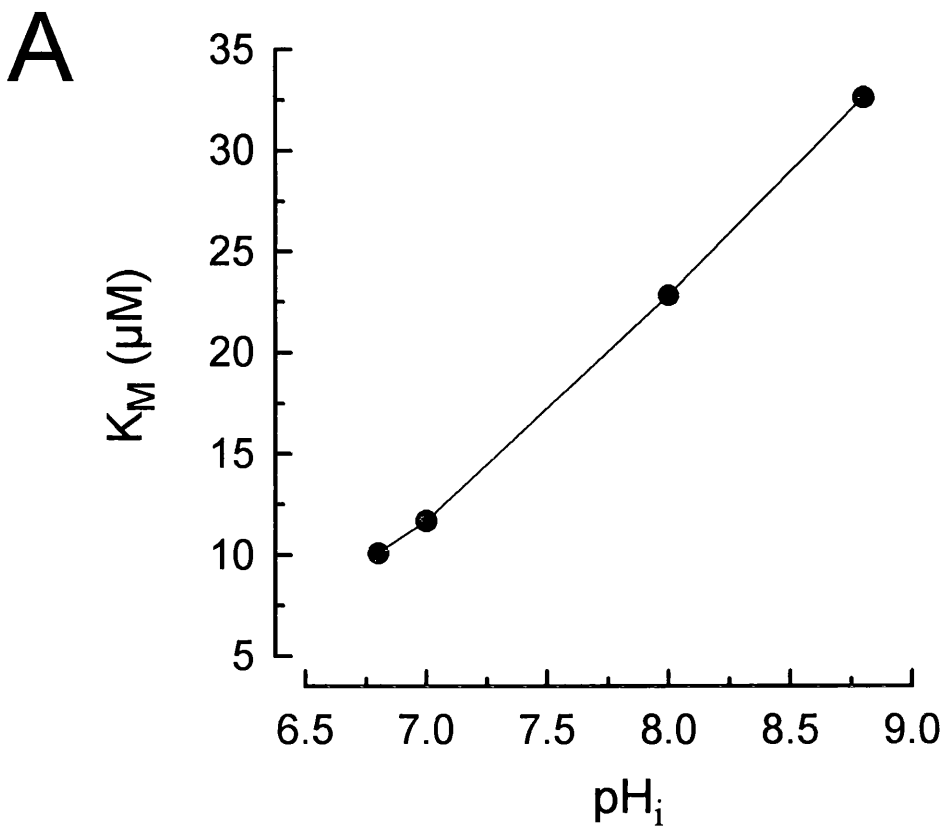
A
35
30
25
20
15
10
5
K_M (μM)
6.5
7.0
7.5
8.0
8.5
9.0
pH_i

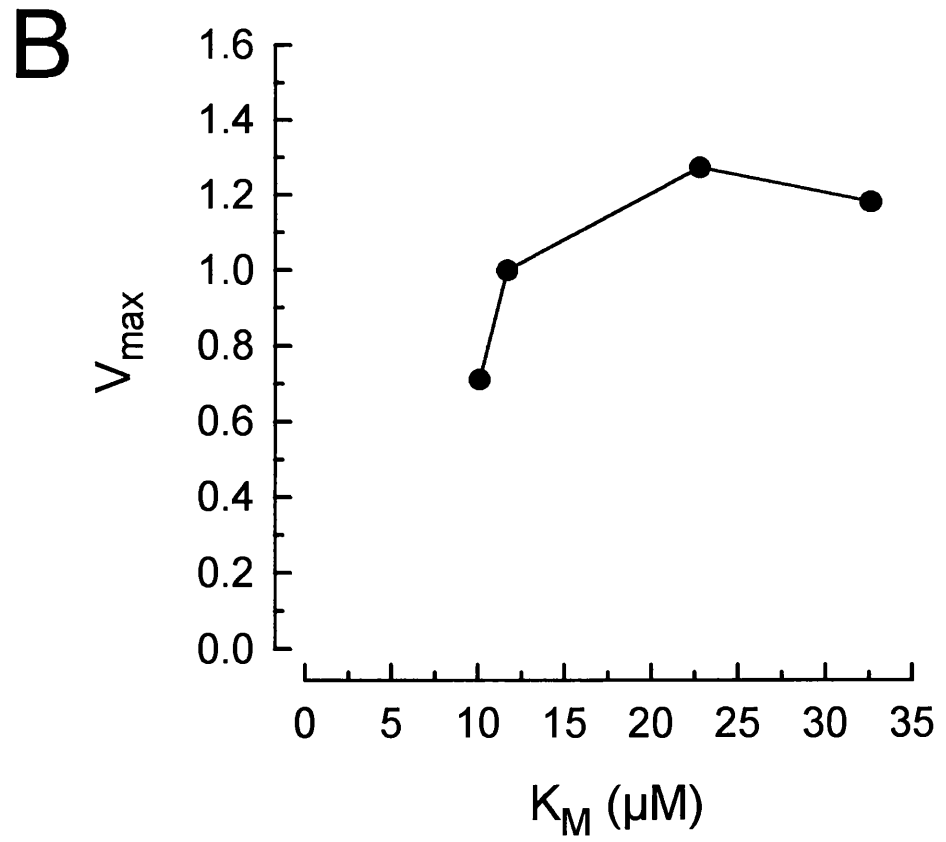
B
1.6
1.4
1.2
1.0
0.8
0.6
0.4
0.2
0.0
V_{max}
0
5
10
15
20
25
30
35
K_M (μM)

was inhibited by either an increase or decrease in external pH (figure 3.4). The inhibition at a high external pH is expected since forward uptake has been suggested to transport a hydroxide ion out of the cell (Bouvier *et al.*, 1992) and a more alkaline external pH would slow the loss of transported hydroxide from the outer face of the carrier. More recent work (see chapter 5) has shown that the carrier might transport a proton into the cell rather than a hydroxide ion out, but this would also be expected to be inhibited by an alkaline external pH. The inhibition of forward uptake at low external pH could reflect the titration of an amino acid on the outer surface of the carrier by the excess protons. Since the sodium affinity was reduced at an acid external pH (figure 3.7), protons could be competing with sodium for binding to the external sodium binding site. The K_M for glutamate increased with increasing external pH. This could reflect a secondary effect of a change in the concentration of transported hydroxide ions, or a direct effect of pH on the glutamate binding site. Since the majority of glutamate is present in the anionic form (figure 3.2), presumably glutamate binds, in part, to a positively charged region of the carrier. The lower affinity for glutamate at an alkali pH could reflect removal of protons from the glutamate binding site by the excess hydroxide ions. There was no simple relationship between the changes in K_M and V_{max}.

Changes in internal pH had a simpler effect on the forward uptake current than did changes in external pH. Possibly the only effect of internal pH was to alter the concentration of hydroxide (or protons) transported by the carrier. Internal acidification inhibited the forward glutamate uptake current, as expected since an acid internal pH would lower the concentration of counter-transported hydroxide (or slow the loss of co-transported protons from the carrier). The K_M for glutamate increased with increasing internal pH, and again there was no simple relationship between the changes in K_M and V_{max}.

The inhibition of forward glutamate uptake by an acid external or internal

pH could have implications during pathological conditions when the brain pH may be altered. Any condition which results in an internal or external acidification will reduce the glutamate uptake carrier's ability to remove glutamate from the external environment. This may cause changes in neuronal signal processing as a result of EPSCs being prolonged (Barbour et al., 1994; Takahashi et al., 1995) or the raised external glutamate concentration desensitizing glutamate receptors (Tang *et al.*, 1989). Furthermore, the increased external glutamate concentration could lead to cell death (Choi *et al.*, 1987).

During brain ischaemia the internal and external pH quickly become acid by up to 1 pH unit (Mutch and Hansen, 1984; Silver and Erecinska, 1992 and see section 1.3.3). Under these conditions the glutamate uptake carrier is predicted to operate in the reversed direction, releasing glutamate from cells (Szatkowski *et al.*, 1990). The influence of the internal and external pH on this reversed glutamate uptake are examined in the next chapter.

CHAPTER 4

Effects of pH on reversed glutamate uptake

4.1 Introduction

This chapter examines the effects of changing the extracellular pH on the reversed operation of glutamate uptake carriers. This is of interest for three reasons. First, reversed uptake is thought to release glutamate and trigger neuronal death in conditions like stroke (see section 1.2.6). Second, during stroke the pH of the brain shifts acid by about 1 pH unit (see section 1.3.3). Third, the proposed movement of hydroxide ions in the carrier stoichiometry (Bouvier *et al.*, 1992) suggests that the pH change occurring in stroke could modulate the release of glutamate by reversed uptake (section 1.3.3).

For the experiments in this chapter, reversed uptake was evoked in whole-cell voltage-clamped isolated Müller cells. It was stimulated by raising the external potassium ion concentration when the cell was held at a depolarized membrane potential, with sodium and glutamate present in the internal solution (via the whole-cell pipette). When the carrier runs backwards there is a movement of net positive charge outwards (section 1.2.6). Reversal of the transporter can thus be monitored as an outward membrane current in the voltage-clamped cells (Szatkowski *et al.*, 1990).

Accurate assessment of the effect of pH on glutamate release by measuring the reversed uptake current relies on several assumptions. First, the stoichiometry of reversed uptake must be constant, for example there must be one net positive charge moving out for each carrier cycle, independent of the pH. Second, there must be no electroneutral mode of reversed uptake, as proposed by Schwartz and Tachibana (1990). Finally, there must be no significant contamination of the

current by fluxes of ions through the anion channel associated with the carrier (Fairman *et al.*, 1995; Wadiche *et al.*, 1995 and see section 1.2.5: an investigation of anion conductance activation during reversed uptake is presented in chapter 5 of this thesis). To avoid these possible problems, reversed uptake was also monitored by directly detecting the glutamate released using glutamate-sensitive cells placed next to the Müller cells. Rat cerebellar neurons were used as glutamate sensors, as previously used to detect synaptic glutamate release from cochlear hair cells (Kataoka and Ohmori, 1994).

4.2 External pH-dependence of the reversed uptake current

Initially, the dependence of the reversed uptake current on external pH was tested. Reversed uptake was stimulated by raising the external potassium ion concentration from 0 to 30mM, while the cells were held at a depolarized membrane potential (+20mV) with pipettes containing sodium and glutamate, a protocol used previously by Szatkowski *et al.* (1990). The external pH was altered, and its effect on the outward reversed uptake current was observed.

Figure 4.1A shows specimen currents recorded at normal and acidic extracellular pH values. Averaged data are shown in figure 4.1B, where the reversed uptake current is plotted as a function of extracellular pH. An extracellular acidification resulted in a reduction of the reversed uptake current, the current at pH_o=6.1 being 7.3±1.5% (mean±SEM of data from 5 cells) of the current at pH_o=7.3. This suppression of reversed uptake by external acidification was still observed if the intracellular pH was made more acid (this is relevant to the events in ischaemia, as discussed later). With an internal pH of 6.1, the reversed uptake current at pH_o=6.1 was reduced to 8.7±1.6% (mean±SEM of data from 5 cells) of its magnitude at pH_o=7.3 (data not shown). This is not significantly different from the suppression of the reversed uptake current evoked at external

Figure 4.1 - pH-dependence of the reversed uptake current

A. Typical membrane currents recorded during reversed uptake in a whole-cell voltage-clamped Müller cell at different external pH values. The holding potential was 0mV. Reversed uptake was evoked at different external pH values, by raising the external potassium concentration from 0 to 30mM (represented by the black bar above each trace), in the presence of 10mM sodium and glutamate inside the whole-cell pipette and hence inside the cell. The external pH is indicated by the column of numbers on the right.

B. The magnitude of the reversed uptake current, from experiments like in A, is plotted as a function of external pH. The currents are normalized by the size of the current observed at pH 7.3, and are shown as the mean±SEM of data from 5 cells. The data are best-fit with a second order spline curve.

Solutions - External solutions contained (in mM) choline-chloride 30, NaCl 75, $MgCl_2$ 0.5, $CaCl_2$ 3, $BaCl_2$ 6, glucose 15, ouabain 0.1 (to block the Na^+/K^+ pump) and buffer 5. For solutions with pH < 6.7 the buffer used was MES; for pH 6.8 and 7.3 HEPES was used. The solutions were titrated to the appropriate pH using NMDG. To evoke reversed uptake, the choline-chloride was replaced by KCl.

The internal solution contained (in mM) Na-glutamate 10, choline-chloride 40, $(NMDG)_2EGTA$ 5, Na_2ATP 5, $CaCl_2$ 1, $MgCl_2$ 7, HEPES 70. It was titrated to pH 7.0 with 26mM NMDG.

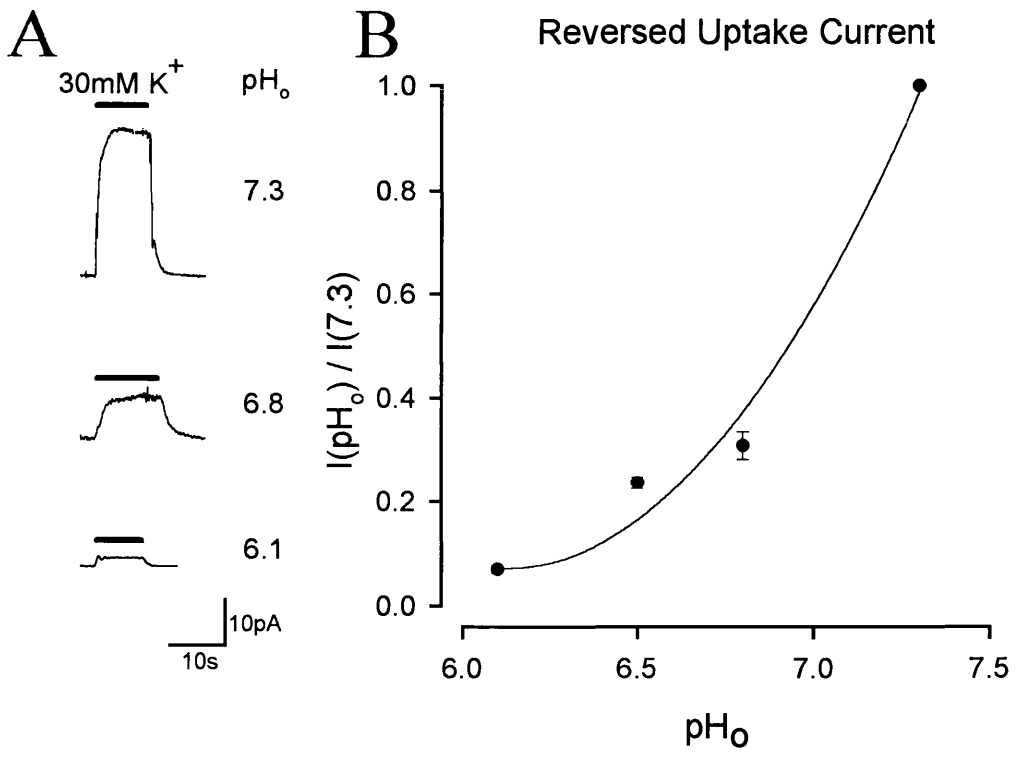
A
30mM K+
pHo
7.3
6.8
6.1
10pA
10s
B
Reversed Uptake Current
I(pHo) / I(7.3)
1.0
0.8
0.6
0.4
0.2
0.0
6.0
6.5
7.0
7.5
pHo

pH 6.1 with a normal intracellular pH ($p \approx 0.57$, two-tailed t-test).

The reduction of reversed uptake current by an acid extracellular pH, i.e. when the external hydroxide concentration is reduced, is consistent with the notion that hydroxide ions are transported into the cell during reversed uptake, so that lowering the concentration of external hydroxide substrate slows the rate at which the carrier can cycle in the reversed direction (see section 1.2.6).

4.3 Glutamate responses in isolated neurons used to sense glutamate release from Müller cells

To provide an independent measure of the amount of glutamate released by Müller cells when reversed uptake occurs, isolated neurons were whole-cell voltage-clamped and placed next to the Müller cells to act as glutamate sensors. Neurons dissociated with papain from cerebellar slices of 12 day old rat pups were used. Two main classes of neurons can be identified from this dissociation, granule cells and Purkinje cells. The more numerous granule cells express many NMDA receptors. These receptors have a high affinity for glutamate with an EC_{50} of 2.3μM for the steady state current seen during prolonged glutamate application (Patneau and Mayer, 1990). Purkinje cells do not express any functional NMDA receptors (Perkel *et al.*, 1990), but are thought to express both the AMPA and kainate types of non-NMDA receptor (Renard *et al.*, 1995). These receptors have a lower affinity for glutamate: the EC_{50} for AMPA receptors is 19μM for the steady state current seen during prolonged glutamate application (Patneau and Mayer, 1990) and normally desensitize within a few milliseconds when agonist is applied (Tang *et al.*, 1989). Purkinje cells were used in preference to granule cells to sense released glutamate because the experiments described below involve changing the extracellular pH, and the NMDA receptors in the granule cells are blocked by an acid pH much more potently than are the non-NMDA receptors in

Purkinje cells. The IC_{50} for protons acting on the NMDA receptor is at pH 7.3 (Traynelis and Cull-Candy, 1990), whereas for AMPA and kainate responses of non-NMDA receptors it is at pH 6.3 and 5.7 respectively (Traynelis and Cull-Candy, 1991).

To use non-NMDA receptors to sense glutamate release from Müller cells it is useful to increase the current generated by the receptors by blocking their desensitization. This can be achieved using a class of drugs known as benzothiadiazides (Yamada and Tang, 1993), the exact mechanism of which is unknown. One of two such compounds, trichlormethiazide or diazoxide, was added to the external solution to prevent the Purkinje cell glutamate-evoked current from desensitizing. The magnitude of the steady-state current evoked by 15μM quisqualate in rat cultured hippocampal neurons is approximately 14 fold larger in the presence of 0.5mM trichlormethiazide and 7 fold larger in the presence of 0.5mM diazoxide, compared to control (Yamada and Tang, 1993). With trichlormethiazide or diazoxide present, whole-cell currents evoked by 3μM external glutamate could usually be detected easily in the isolated Purkinje cells, whereas in their absence 3μM glutamate produced a barely detectable current change (data not shown; done on 4 Purkinje cells).

The Purkinje cell glutamate dose-response curve, in the presence of 1mM trichlormethiazide, is shown in figure 4.2 The data are fit with a Hill equation with an EC_{50} of 23μM and a Hill coefficient of 1.19.

4.4 Measuring glutamate release using isolated neurons

To detect glutamate release from Müller cells by reversed glutamate uptake, release was stimulated by bathing the cells in a medium containing 30mM potassium, and stepping the Müller cell membrane potential from a negative holding potential (typically -60mV) to a more positive one (typically +20mV).

Figure 4.2 - Glutamate sensitivity of isolated Purkinje cells

The membrane current evoked in whole-cell voltage-clamped isolated Purkinje cells is shown as a function of glutamate concentration. The currents are normalized to the current evoked by 300μM glutamate for each cell. The cells were held at a membrane potential of -60mV. 1mM trichlormethiazide was added to the external solution to prevent non-NMDA receptor desensitization. The data are the mean±SEM of data from 4 cells, and are fitted with the Hill equation shown in the inset.

Solutions - The external solution contained (in mM) KCl 30, NaCl 75, $MgCl_2$ 0.5, $CaCl_2$ 3, $BaCl_2$ 6, glucose 15, ouabain 0.1, trichlormethiazide (dissolved in DMSO. 0.05% in final solution) 1 and HEPES 5. The solution was titrated to pH 7.3 with NMDG.

The internal solution contained (in mM) CsCl 110, Na_2ATP 2, $CaCl_2$ 0.5, $MgCl_2$ 2, HEPES 10 and $(NMDG)_2EGTA$ 5. It was titrated to pH 7.0 with NMDG.

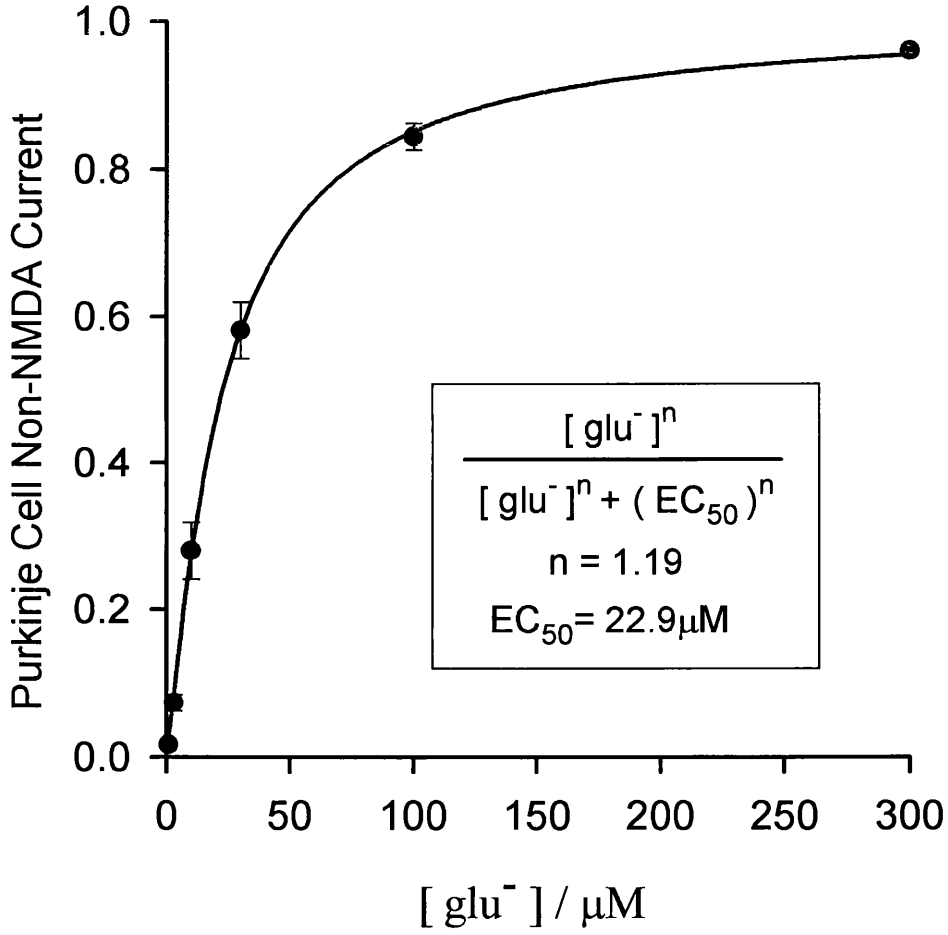
Purkinje Cell Non-NMDA Current
1.0
0.8
0.6
0.4
0.2
0.0
0
50
100
150
200
250
300
[glu⁻] / μM
[glu⁻]^n
[glu⁻]^n + (EC50)^n
n = 1.19
EC50= 22.9μM

Since reversed glutamate uptake is expected to be electrogenic, with net positive charge moving outwards with the glutamate, this manipulation will stimulate reversed uptake (Szatkowski *et al.*, 1990). Whole-cell voltage-clamped isolated Purkinje cells were placed next to the Müller cells to detect this release (figure 4.3). When the Müller cell was depolarized, a current was detected in the adjacent Purkinje cell (figure 4.4); an experiment done in 20 cell pairs This current was inward at negative Purkinje cell potentials, outward at positive Purkinje cell potentials and reversed at a Purkinje cell membrane potential of around 0mV (figure 4.4, typical of 3 cells studied at different Purkinje cell voltages). Furthermore the current was inhibited by the non-NMDA receptor antagonist CNQX (Drejer and Honore, 1988) (figure 4.5, typical of 4 cells), indicating that the membrane current observed in the Purkinje cells is a non-NMDA receptor mediated current.

The Purkinje cell current observed when reversed uptake in the Müller cell was evoked was also inhibited by the glutamate transport blocker PDC (Bridges *et al.*, 1991) (figure 4.6, typical of 4 cells). This is evidence that glutamate release from the Müller cells is by reversed glutamate uptake. Control experiments (figure 4.7) showed that the Purkinje cells' response to external glutamate was not affected by PDC: the current evoked by 3μM glutamate at -60mV with PDC present was 98±13% (mean±SEM of data from 3 cells) of its magnitude in the absence of PDC.

4.5 External potassium-dependence of glutamate release by reversed uptake, measured with sensing neurons

The glutamate release detected by the Purkinje cells when the Müller cells were depolarized was abolished when the external potassium was removed (figure 4.8, typical of 9 cells). Control experiments (figure 4.9) showed that lowering the

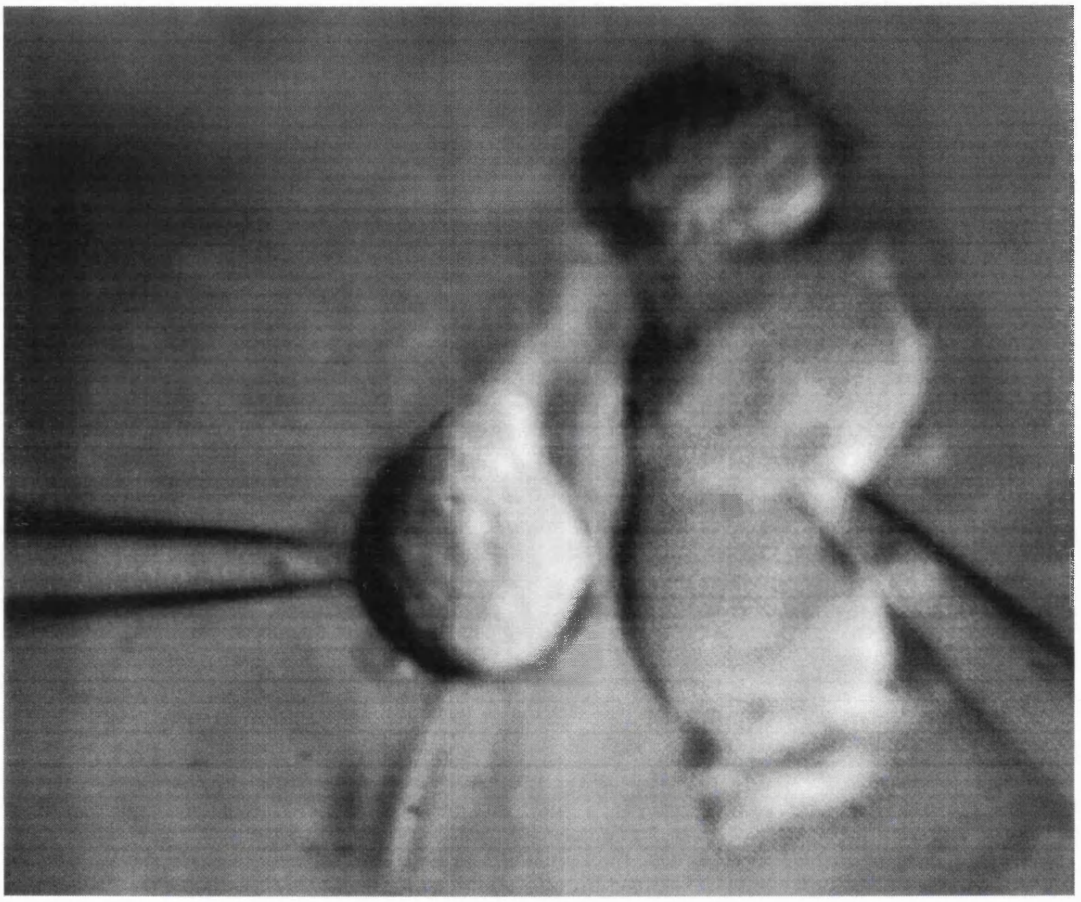

Figure 4.3 - Isolated Purkinje cell and Müller cell

Acutely isolated whole-cell voltage-clamped Purkinje cells and Müller cells were placed next to each other to enable the Purkinje cell to detect the glutamate released from the Müller cell by reversed uptake.

Figure 4.4 - Purkinje cell membrane currents produced by glutamate release from Müller cells

Depolarizing a Müller cell from -60 to +20mV (indicated by V_M - top trace) in the presence of 30mM external potassium and with sodium and glutamate in the whole-cell pipette, to evoke reversed glutamate uptake, produced membrane currents in an adjacent Purkinje cell (lower traces) that were inward at negative Purkinje cell membrane potentials (V_P) and outward at positive potentials.

Solutions - The external solution contained (in mM) KCl 30, NaCl 75, $MgCl_2$ 0.5, $CaCl_2$ 3, $BaCl_2$ 6, glucose 15, ouabain 0.1, trichlormethiazide 1 (dissolved in DMSO, 0.05% in final solution) and HEPES 5. The solution was titrated to pH 7.3 with NMDG.

The Müller cell internal solution contained (in mM) Na-glutamate 10, choline-chloride 40, $(NMDG)_2EGTA$ 5, Na_2ATP 5, $CaCl_2$ 1, $MgCl_2$ 7, HEPES 70. It was titrated to pH 7.0 with 26mM NMDG.

The Purkinje cell internal solution contained (in mM) CsCl 110, Na_2ATP 2, $CaCl_2$ 0.5, $MgCl_2$ 2, HEPES 10 and $(NMDG)_2EGTA$ 5. It was titrated to pH 7.0 with NMDG.

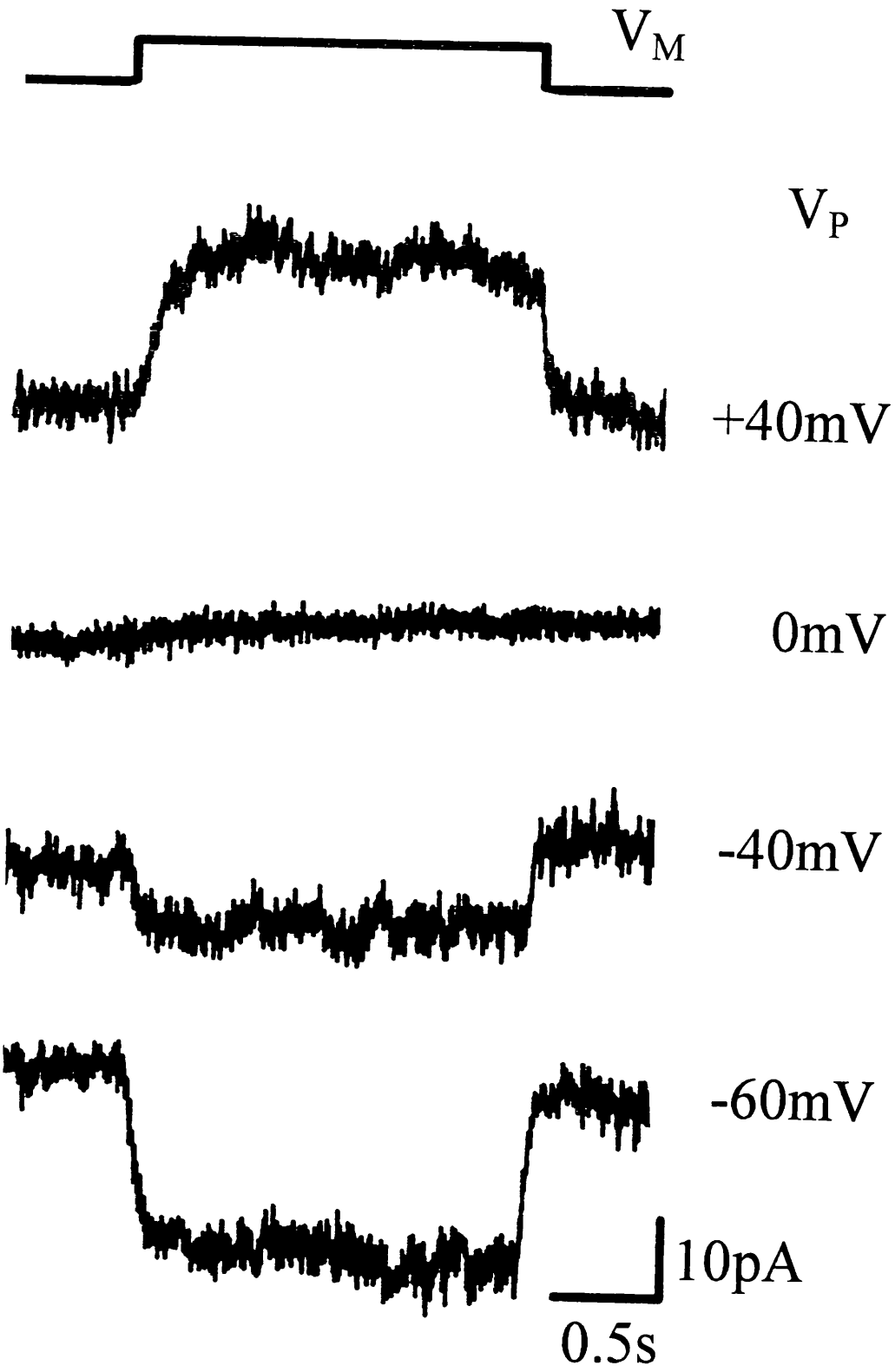
V_M
V_P
+40mV
0mV
-40mV
-60mV
10pA
0.5s

Figure 4.5 - Inhibition by CNQX of the Purkinje cell response to reversed uptake

Reversed uptake was stimulated in Müller cells by stepping the membrane potential (V_M) from -60 to +20mV (top trace) in the presence of 30mM extracellular potassium (with sodium and glutamate in the whole-cell pipette). The resulting membrane current in the adjacent Purkinje cell (V_P = -60mV) seen in the bottom trace was entirely inhibited by the presence of 10μM CNQX (middle trace), a non-NMDA receptor blocker. The same result was observed in 4 cells.

Solutions - The external solution contained (in mM) KCl 30, NaCl 75, $MgCl_2$ 0.5, $CaCl_2$ 3, $BaCl_2$ 6, glucose 15, ouabain 0.1, diazoxide 0.5 (dissolved in DMSO, 0.01% in final solution) and HEPES 5. The solution was titrated to pH 7.3 with NMDG.

The Müller cell internal solution contained (in mM) Na-glutamate 10, choline-chloride 40, $(NMDG)_2EGTA$ 5, Na_2ATP 5, $CaCl_2$ 1, $MgCl_2$ 7, HEPES 70. It was titrated to pH 7.0 with 26mM NMDG.

The Purkinje cell internal solution contained (in mM) CsCl 110, Na_2ATP 2, $CaCl_2$ 0.5, $MgCl_2$ 2, HEPES 10 and $(NMDG)_2EGTA$ 5. It was titrated to pH 7.0 with NMDG.

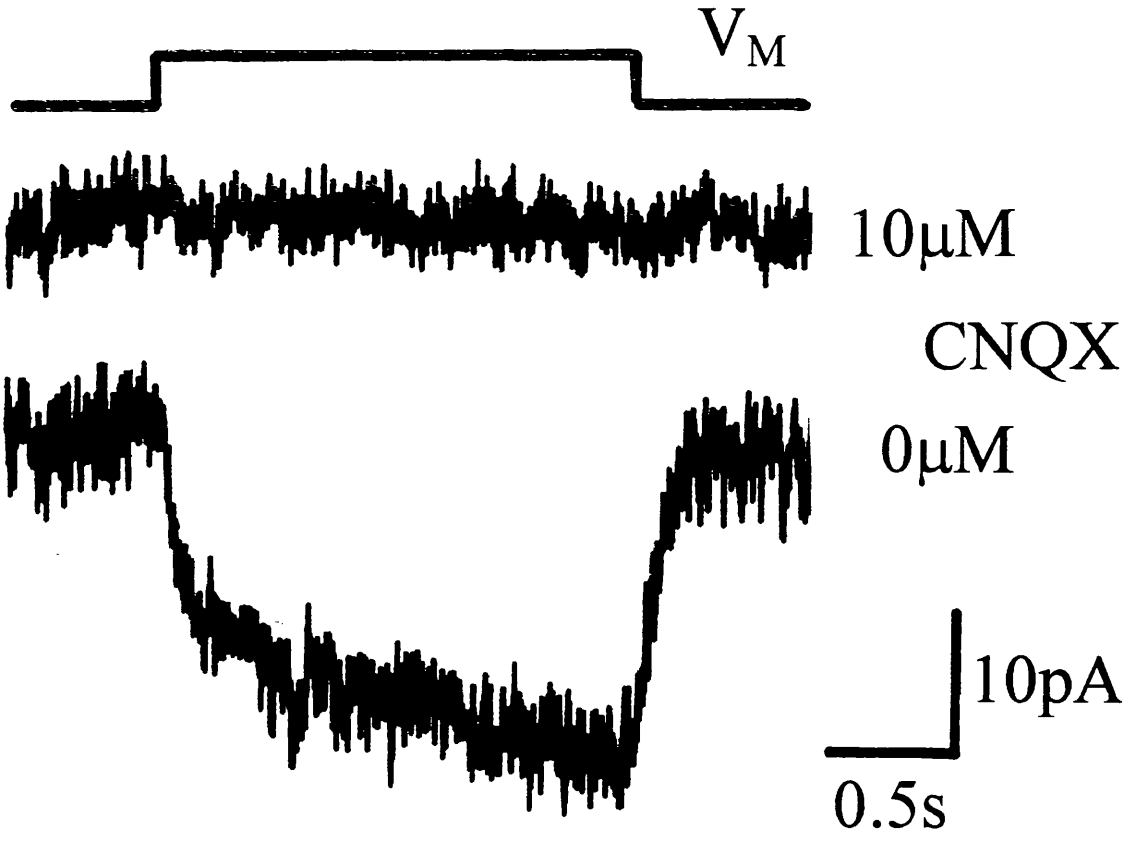
V_M
10μM
CNQX
0μM
10pA
0.5s

Figure 4.6 - Inhibition by PDC of glutamate release by reversed uptake

Reversed uptake was stimulated in Müller cells by stepping the membrane potential (V_M) from -60 to +20mV (top trace) in the presence of 30mM external potassium, and with sodium and glutamate in the whole-cell pipette. The resulting membrane current in the adjacent Purkinje cell (V_P = -60mV), seen in the bottom trace was entirely inhibited by the presence of 100μM PDC (middle trace), a glutamate uptake blocker. This result was observed in the same 4 cells as the inhibition of the current by CNQX (figure 4.5).

Solutions - The solutions used were the same as in figure 4.5.

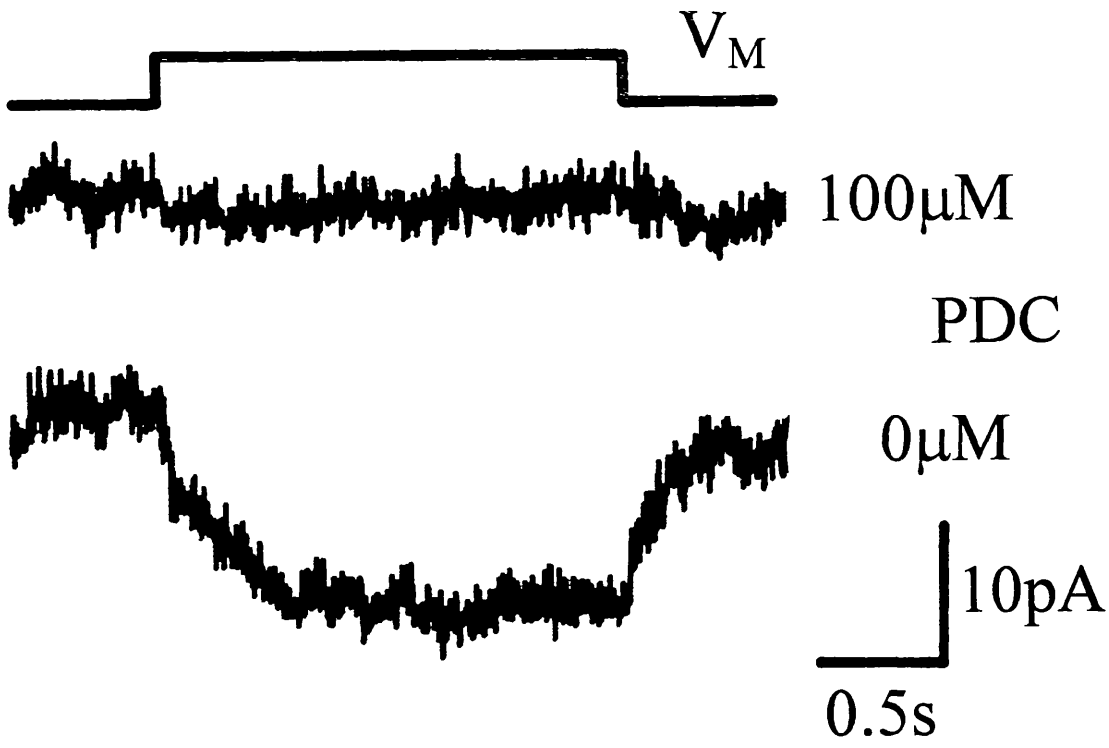
V_M
100μM
PDC
0μM
10pA
0.5s

Figure 4.7 - Lack of effect of PDC on the Purkinje cell sensitivity to glutamate

The membrane current evoked by 3μM glutamate (black bar) in a whole-cell voltage-clamped isolated Purkinje cell is shown in the presence and absence of PDC. The lack of effect of PDC on the Purkinje cell's glutamate sensitivity indicates that the effect of PDC on the Purkinje cells ability to detect glutamate release from the Müller cell (figure 4.6) must reflect an inhibition of the glutamate release from the Müller cell.

The Purkinje cell was held at a membrane potential of -60mV. The slower onset of the glutamate response in the absence of PDC is due to slower perfusion of the solution.

Solutions - The external solution contained (in mM) KCl 30, NaCl 75, $MgCl_2$ 0.5, $CaCl_2$ 3, $BaCl_2$ 6, glucose 15, ouabain 0.1, trichlormethiazide 1 (dissolved in DMSO, 0.05% in final solution) and HEPES 5. The solution was titrated to pH 7.3 with NMDG.

The internal solution contained (in mM) CsCl 110, Na_2ATP 2, $CaCl_2$ 0.5, $MgCl_2$ 2, HEPES 10 and $(NMDG)_2EGTA$ 5. It was titrated to pH 7.0 with NMDG.

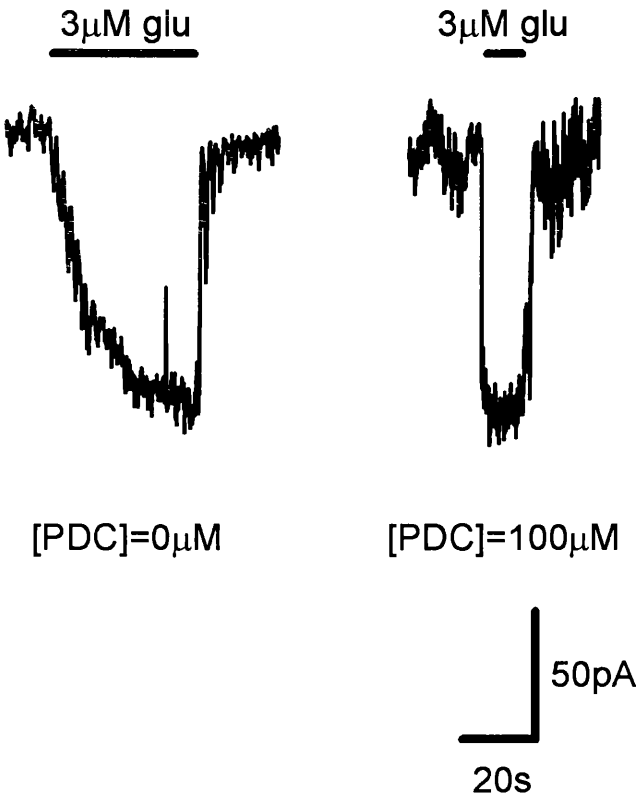
3μM glu
3μM glu
[PDC]=0μM
[PDC]=100μM
50pA
20s

Figure 4.8 - External potassium-dependence of glutamate release measured with sensing neurons

The membrane potential (V_M) of Müller cells was stepped from -60 to +20mV (top trace) in the presence of 30mM external potassium, and with sodium and glutamate in the whole-cell pipette. This evokes reversed uptake in the Müller cell, and the released glutamate evokes a membrane current (middle trace) in the adjacent Purkinje cell (clamped at V_P = -60mV). This current was inhibited when the external potassium was removed (replaced by choline: bottom trace), indicating that glutamate release by reversed glutamate uptake is entirely dependent on the presence of external potassium. The same result was observed in 9 cells.

Solutions - The solutions used were the same as in figure 4.4

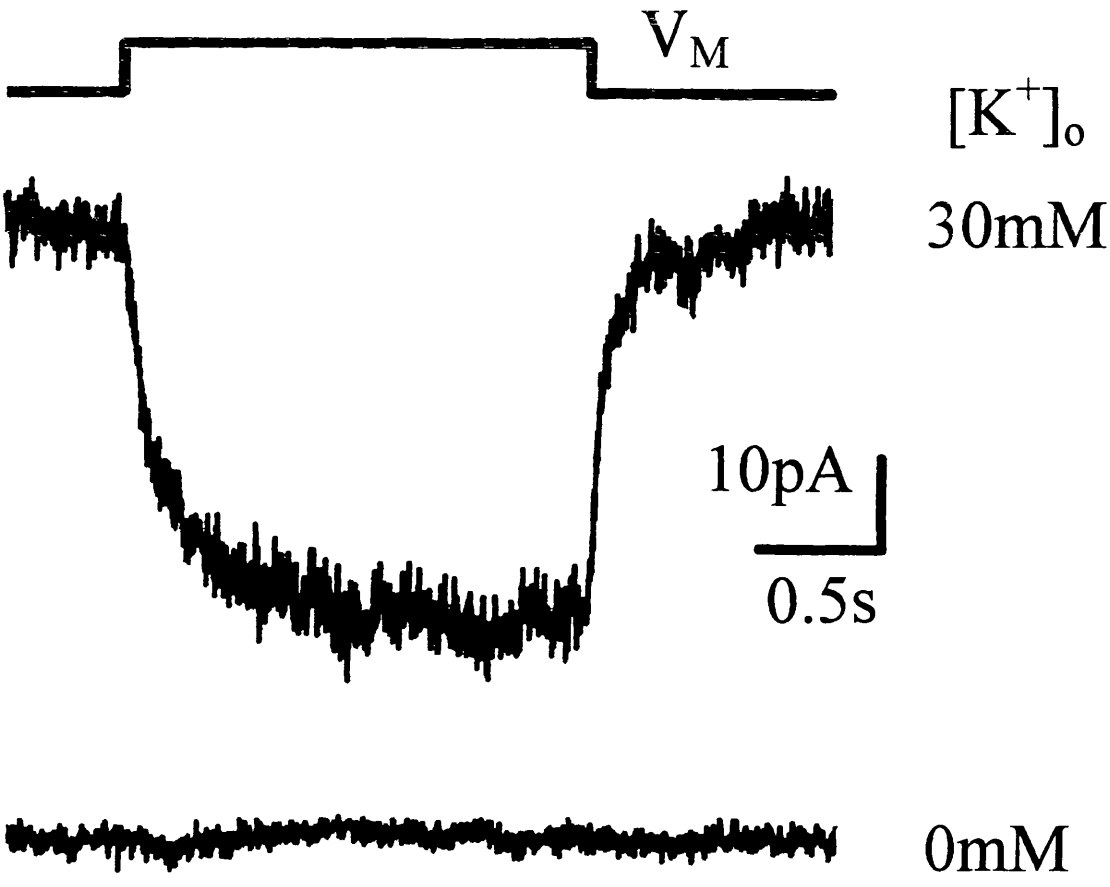
V_M
$[K^+]_o$
30mM
10pA
0.5s
0mM

Figure 4.9 - Lack of effect of removal of external potassium on the Purkinje cell glutamate sensitivity

Membrane currents evoked by 3μM glutamate (black bar) in a whole-cell voltage-clamped isolated Purkinje cell are shown in the presence and absence of external potassium ions. The lack of effect of the removal of external potassium on the Purkinje cell's sensitivity to glutamate indicate that the abolition of the Purkinje cell's response to stimulation of the Müller cell (figure 4.8) is caused by an effect of removing external potassium on the Müller cell's ability to release glutamate.

The Purkinje cell was held at a membrane potential of -60mV. Data typical of 5 cells.

Solutions - The external solution contained (in mM) KCl 30, NaCl 75, $MgCl_2$ 0.5, $CaCl_2$ 3, $BaCl_2$ 6, glucose 15, ouabain 0.1, trichlormethiazide 1 (dissolved in DMSO, 0.05% in final solution) and HEPES 5. The solution was titrated to pH 7.3 with NMDG. For the 0mM potassium solution, 30mM KCl was replaced by 30mM choline-chloride.

The internal solution contained (in mM) CsCl 110, Na_2ATP 2, $CaCl_2$ 0.5, $MgCl_2$ 2, HEPES 10 and $(NMDG)_2EGTA$ 5. It was titrated to pH 7.0 with NMDG.

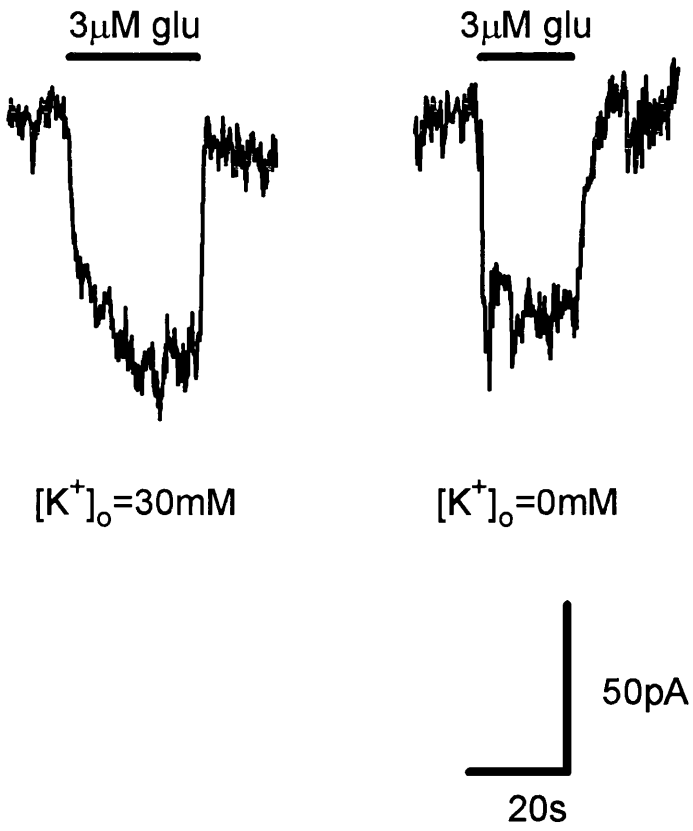
3μM glu
3μM glu
[K+]o=30mM
[K+]o=0mM
50pA
20s

external potassium ion concentration did not prevent the Purkinje cells from detecting external glutamate: the Purkinje cell current evoked by 3μM glutamate at -60mV in the absence of extracellular potassium was 94±9% (mean±SEM of data from 5 cells) of its magnitude in the presence of 30mM extracellular potassium. The abolition of the Purkinje cell response to Müller cell depolarization must therefore reflect an inhibition of reversed uptake. This would be expected from the stoichiometry of the glutamate uptake carrier (figure 1.1) which indicates that external potassium is required for reversed cycling of the carrier.

4.6 Müller cell reversed uptake current is proportional to the glutamate release measured with sensing neurons

To investigate the relationship between the reversed glutamate uptake current measured in the Müller cell and the amount of glutamate which is released, reversed uptake was stimulated to different degrees by depolarizing the Müller cell to different membrane voltages. To assess the magnitude of the reversed uptake current at these different membrane voltages, the external potassium concentration was raised while the cell was held at that particular voltage, and the resulting outward membrane current was measured (Szatkowski *et al.*, 1990). To assess the level of glutamate release at the different membrane voltages, the cells were bathed in an external solution with a high potassium concentration, then the Müller cell membrane potential was stepped from a negative potential to various more positive potentials, and the resulting change in Purkinje cell current was measured. The relationship between the glutamate release occurring (assessed as Purkinje cell current change), and the reversed uptake current measured in the Müller cell, for the difference Müller cell membrane voltages, is plotted in figure 4.10. These data (from 8 cell pairs) are well fitted with a curve which represents the reversed uptake current raised to the power 1.19, which is the Hill coefficient for the Purkinje cell

Figure 4.10 - Glutamate release measured with Purkinje cell sensors is proportional to the reversed uptake current measured in Müller cells

The Purkinje cell membrane current in response to glutamate released from a neighbouring Müller cell by reversed uptake, is plotted as a function of the reversed uptake current in that Müller cell. The Purkinje cell was held at -60mV in 30mM extracellular potassium solution, and the inward current evoked by stepping the Müller cell membrane potential from -80mV to the voltage indicated next to each point was recorded (plotted on the ordinate).

The Müller cell reversed uptake current at different membrane voltages (shown next to each point) was assessed by raising the external potassium concentration from 0 to 30mM at the different holding potentials (plotted on the abscissa).

The data are normalized to their values at 0mV, and represent the mean±SEM of data from 8 cell pairs. They are fitted with a line which corresponds to the reversed uptake current raised to the power 1.19, as expected if the glutamate concentration near the Purkinje cell is proportional to the reversed uptake current, and the Purkinje cell membrane current is proportional to $[\text{glutamate}]^{1.19}$ (as found at the low glutamate concentrations in figure 4.2).

Solutions - The solutions used were identical to those used in figure 4.5. To evoke reversed uptake in the Müller cells by raising the external potassium concentration (abscissa data), choline-chloride was used in place of the 30mM KCl for the low potassium solution.

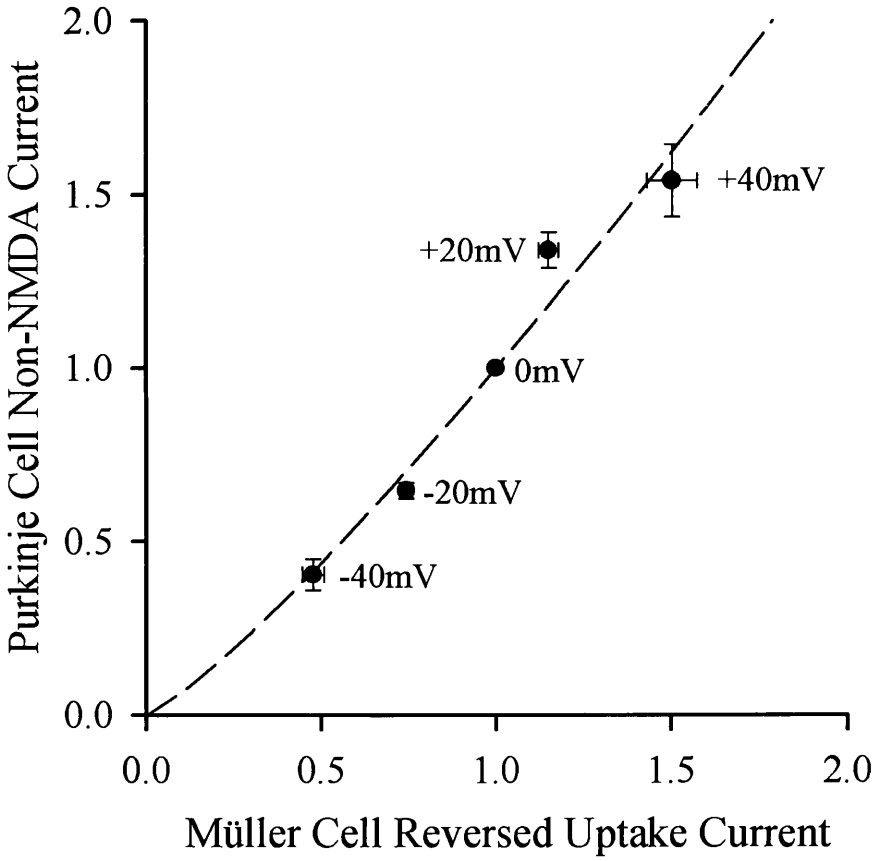
2.0
1.5
1.0
0.5
0.0
Purkinje Cell Non-NMDA Current
+40mV
+20mV
0mV
-20mV
-40mV
0.0
0.5
1.0
1.5
2.0
Müller Cell Reversed Uptake Current

glutamate dose-response curve (figure 4.2). Now the small size of the Müller cell membrane currents produced by reversed uptake (around 20pA) suggests that reversed uptake could only raise the external glutamate concentration at the Purkinje cell surface to a few micromolar, i.e. on the low concentration part of the glutamate dose-response curve in figure 4.2 where the Purkinje cell current is proportional to $[glu]^{1.19}$. Thus, since the Purkinje cell response during reversed uptake is proportional to $(\text{reversed uptake current})^{1.19}$, the reversed uptake current must be proportional to the glutamate concentration produced at the Purkinje cell, and thus is proportional to the amount of glutamate released by reversed uptake.

In the next chapter I will show that the current produced in the Müller cell by reversed operation of the glutamate uptake carrier is not solely produced by the transport of glutamate, sodium and the other transported ions, but also has a component generated by an anion channel present in the carrier. The fact that, nevertheless, the reversed uptake current is proportional to the amount of glutamate released implies either that the anion channel component is very small, or that it is proportional to the amount of glutamate release occurring.

4.7 Using Purkinje cells to test for electroneutral glutamate release from Müller cells

The voltage step protocol used to evoke reversed uptake in the experiments described above would not be expected to affect glutamate release by a non-electrogenic process. Schwartz and Tachibana (1990) have suggested that reversed glutamate uptake is electroneutral rather than electrogenic. To test for electroneutral release of glutamate, the Müller cell and Purkinje cell were placed next to each other, then quickly drawn apart. With the Müller cell and Purkinje cell adjacent to each other, the Purkinje cell would respond to any glutamate released with an inward current (at a negative Purkinje cell membrane potential),

irrespective of whether it was released by an electroneutral or an electrogenic mechanism. As the two cells are moved apart, the distance between them (>500μm) prevents the Purkinje cell responding to any glutamate which may be released from the Müller cell. The inward membrane current observed in the Purkinje cell will therefore be abolished, resulting in an outward deflection of the Purkinje cell membrane current. This was observed when the Müller cell was held at a depolarized membrane potential in the presence of a high concentration of external potassium (figure 4.11, top trace), i.e. conditions which favour electrogenic reversed uptake (see section 1.2.6). However, when the Müller cell was held at a more negative membrane potential (-80mV) (figure 4.11, second trace) or external potassium was removed (figure 4.11, bottom two traces), this outward deflection in the Purkinje cell current was not observed, indicating that under these conditions glutamate was not being released by the Müller cell (experiment done on 3 cell pairs). Thus, contrary to Schwartz and Tachibana (1990), I could not find any evidence for electroneutral reversed uptake - glutamate was only released in conditions favouring electrogenic reversed uptake.

4.8 External pH-dependence of glutamate release

In ischaemia the brain pH goes acid by about one pH unit (Mutch and Hansen, 1984; Silver and Erecinska, 1992). This is expected to affect the release of glutamate by reversed uptake, because of the involvement of external hydroxide ions in the stoichiometry of reversed uptake. To test this, recordings were made from Müller cells and Purkinje cells in an external solution of pH 6.1 (figure 4.12). Depolarization of the Müller cell in an external solution containing 30mM potassium, resulted in a Purkinje cell membrane current that was reduced by 97±3% (mean±SEM of data from 4 cells) at external pH 6.1 compared to its amplitude at pH 7.4. Control experiments (figure 4.13A) indicated that the

Figure 4.11 - Using Purkinje cells as glutamate sensors to test for electroneutral release of glutamate by Müller cells

Release of glutamate from Müller cells was assessed by rapidly moving the Purkinje cell from a position close to the Müller cell, to a distant position, at the time shown by the dotted vertical line. The Purkinje cell membrane potential was held at -60mV. With 30mM external potassium and at a Müller cell membrane potential (V_M) of 0mV, this operation resulted in an outward Purkinje cell membrane current (top trace) as the Purkinje cell was moved to a position where it could no longer sense the glutamate being released from the Müller cell. With a Müller cell membrane potential of -80mV, or if the external potassium was removed (replaced by choline: lower traces), this outward Purkinje cell membrane current was not observed, implying that the Müller cell was not releasing glutamate. This result was observed in 3 cells. The traces shown are averages of 3-7 trials.

Solutions - The solutions used were identical to those used in figure 4.4.

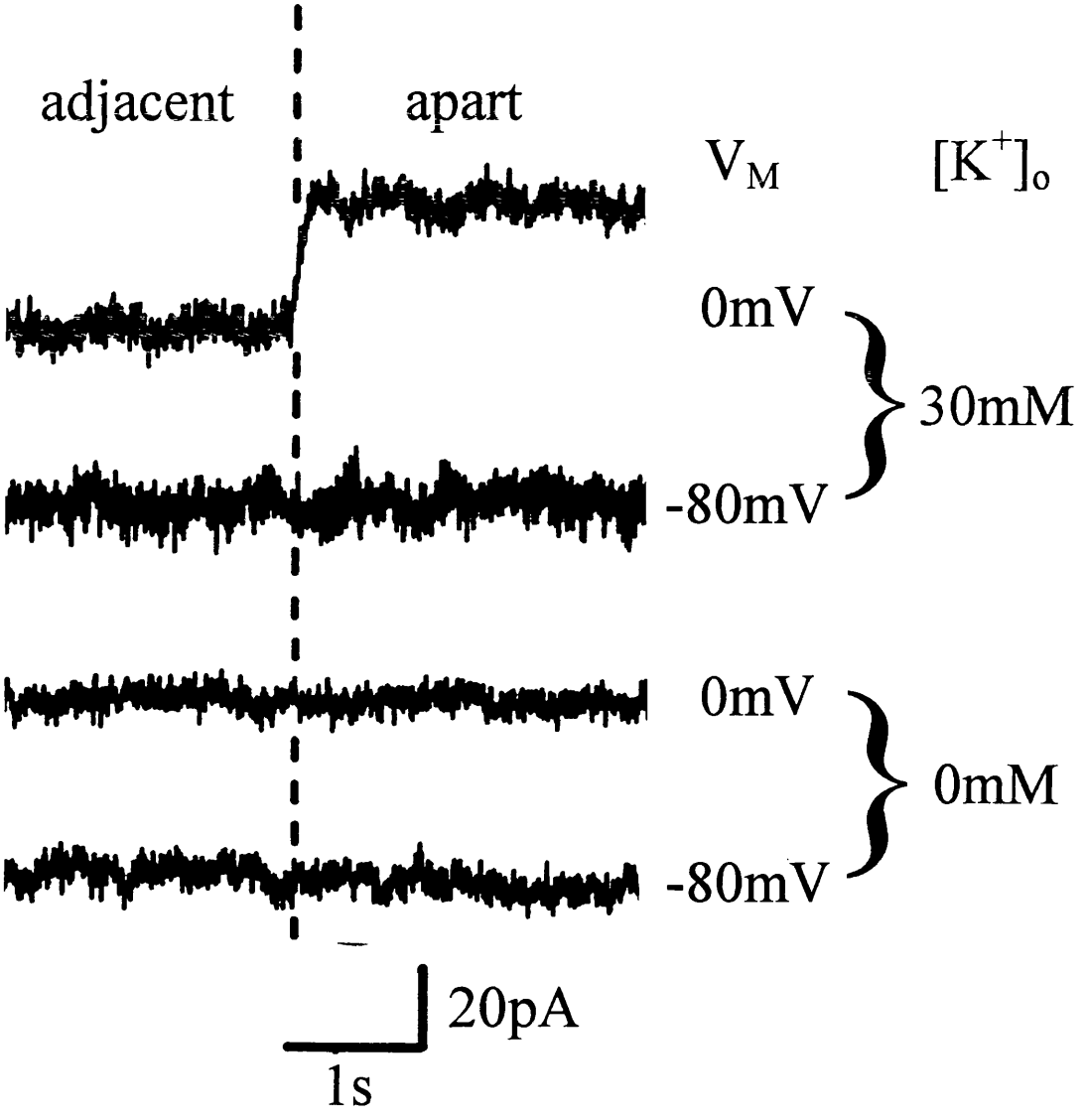
adjacent
apart
V_M
$[K^+]_o$
0mV
30mM
-80mV
0mV
0mM
-80mV
20pA
1s

Figure 4.12 - Using Purkinje cell sensors to measure the inhibition of glutamate release from Müller cells by external acidification

Reversed uptake was stimulated in Müller cells by stepping the membrane potential (V_M) from -60 to +20mV (top trace) in the presence of 30mM external potassium. The resulting membrane current change in the adjacent Purkinje cell (V_P = -60mV) was inhibited by lowering the external pH from 7.4 to 6.1 (middle and bottom traces). This result was observed in 4 cells.

Solutions - The external solution contained (in mM) KCl 30, NaCl 75, $MgCl_2$ 0.5, $CaCl_2$ 3, $BaCl_2$ 6, glucose 15, ouabain 0.1, trichlormethiazide 1 (dissolved in DMSO, 0.05% in final solution) and HEPES 5. For the external solution at pH 6.1 the buffer MES was used instead of HEPES. The solutions were titrated to the appropriate pH with NMDG.

The Müller cell internal solution contained (in mM) Na-glutamate 10, choline-chloride 40, $NMDG_2EGTA$ 5, Na_2ATP 5, $CaCl_2$ 1, $MgCl_2$ 7, HEPES 70. It was titrated to pH 7.0 with 26mM NMDG.

The Purkinje cell internal solution contained (in mM) CsCl 110, Na_2ATP 2, $CaCl_2$ 0.5, $MgCl_2$ 2, HEPES 10 and $NMDG_2EGTA$ 5. It was titrated to pH 7.0 with NMDG.

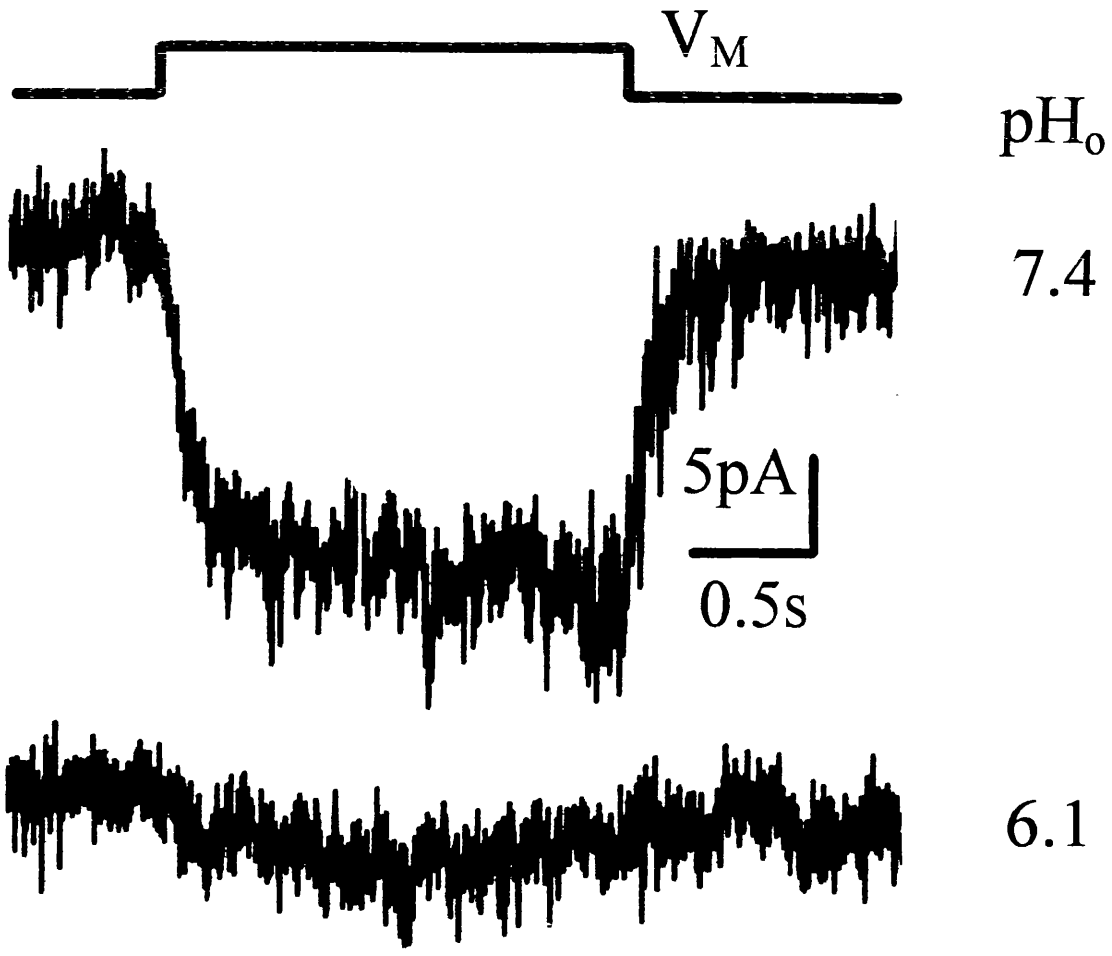
V_M
pH_o
7.4
5pA
0.5s
6.1

Figure 4.13 - Effect of external pH and bicarbonate on the Purkinje cell glutamate sensitivity

Membrane currents evoked by 3μM glutamate (black bars) in whole-cell voltage-clamped isolated Purkinje cells are shown at external pH 7.3 and 6.1, in the presence (A) and absence (B) of external bicarbonate ions. The cells were held at a membrane potential of -60mV. Data in B are from a different cell to A.

Solutions - For figure A the external solution contained (in mM) KCl 30, NaCl 75, $MgCl_2$ 0.5, $CaCl_2$ 3, $BaCl_2$ 6, glucose 15, ouabain 0.1, trichlormethiazide 1 (dissolved in DMSO, 0.05% in final solution) and HEPES 5. The solution was titrated to the appropriate pH with NMDG. For the solution at pH=6.1, the buffer MES replaced HEPES.

For figure B, the external solutions contained (in mM) KCl 30, $BaCl_2$ 6, $CaCl_2$ 3, $MgCl_2$ 0.5, glucose 15, ouabain 0.1, trichlormethiazide 1 (dissolved in DMSO, 0.05% in final solution), and for pH 7.3, NaCl 51 and $NaHCO_3$ 26, or for pH 6.1, NaCl 75.8 and $NaHCO_3$ 1.2. The solutions were bubbled with 95%O_2/5%CO_2.

The internal solution contained (in mM) CsCl 110, Na_2ATP 2, $CaCl_2$ 0.5, $MgCl_2$ 2, HEPES 10 and $(NMDG)_2EGTA$ 5. It was titrated to pH 7.0 with NMDG.

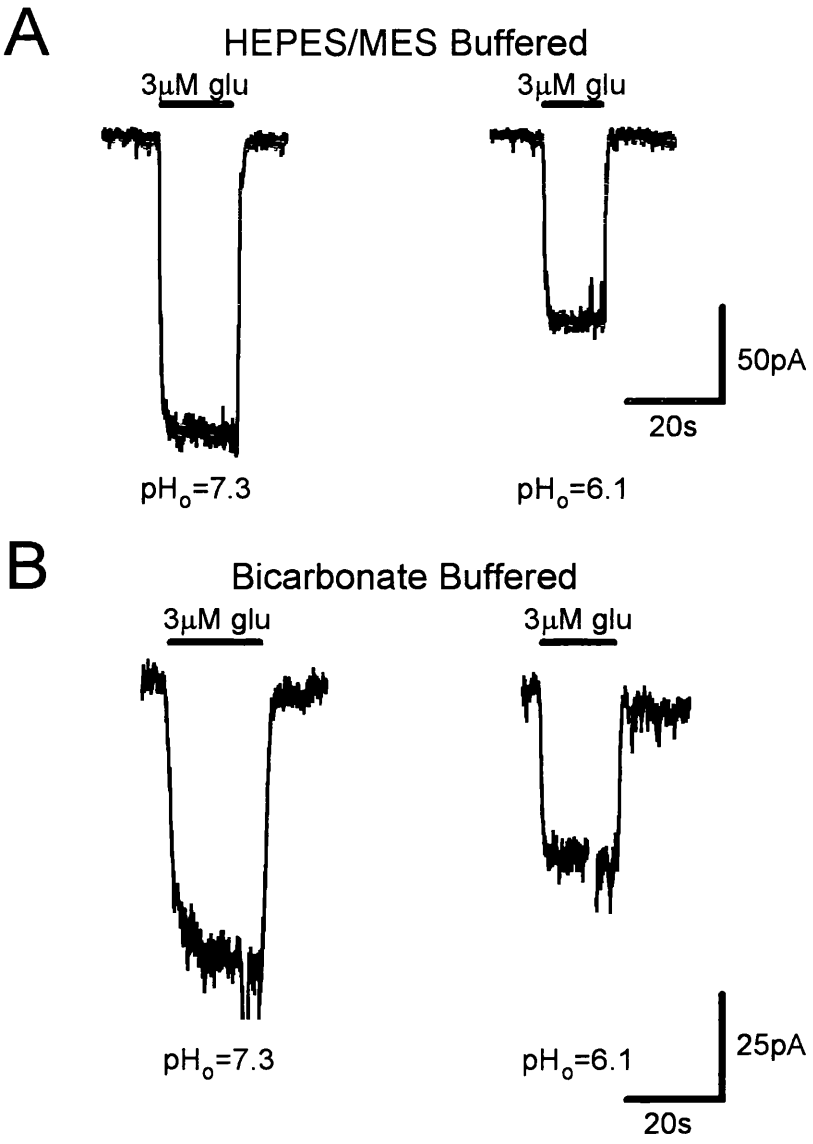
A
HEPES/MES Buffered
3μM glu
3μM glu
50pA
20s
pH$_o$=7.3
pH$_o$=6.1
B
Bicarbonate Buffered
3μM glu
3μM glu
pH$_o$=7.3
pH$_o$=6.1
25pA
20s

Purkinje cells' response to 3μM glutamate at external pH 6.1 was reduced to 68±8% (mean±SEM of data from 5 cells) of its magnitude at external pH 7.4. Correcting for the lower sensitivity of the Purkinje cells (and assuming that the Purkinje cell current is proportional to $[glu]^{1.19}$ as in figure 4.2), one can calculate that a 97% reduction at pH 6.1 of the Purkinje cell response during reversed uptake implies that the glutamate release by the Müller cells has been reduced to 7.3% of its control value by the acid external pH. This is consistent with the inhibition of reversed uptake current by acid pH seen in figure 4.1, where the current was reduced to 7.3±1.5% of its magnitude by a shift of external pH from 7.3 to 6.1.

The experiments above were all performed in HEPES or MES buffered solutions. A similar decrease in glutamate release was observed when the external solution was buffered with bicarbonate. A solution containing 1.2mM bicarbonate bubbled with 5% CO_2 (pH 6.1) reduced the Purkinje cell current, evoked by Müller cell depolarization in an external solution containing 30mM potassium, to 13±10% (mean±SEM of data from 4 cells) of its normal magnitude in a solution that contained 26mM bicarbonate (pH 7.4). Control experiments (figure 4.13B) determined that the Purkinje cells' response to 3μM glutamate at pH 6.1 in the presence of bicarbonate was reduced to 60±4% (mean±SEM of data from 5 cells) of its magnitude at pH 7.4.

4.9 Discussion

4.9.1 Stoichiometry of reversed uptake

The results presented above show that the glutamate which is released by Müller cells by reversed uptake can be detected by adjacent Purkinje cells. The glutamate release is inhibited by removing external potassium (figure 4.8) and external hydroxide ions (figure 4.12), consistent with the proposed stoichiometry

of reversed uptake.

Measuring glutamate release provides a useful assessment of reversed uptake since, unlike using whole-cell current measurements, it does not rely on the assumption that there is always one net positive charge moving out with each glutamate ion. This allows the suggestion that glutamate release by reversed uptake has an electroneutral component (Schwartz and Tachibana, 1990), which wouldn't be detectable using whole-cell current measurements, to be investigated. Figure 4.10 shows that the amount of glutamate release is proportional to the reversed glutamate uptake current over a wide voltage range (-40 to +40mV). This argues against the existence of a significant electroneutral component, since the quantity of electroneutral release might be expected to remain constant over this voltage range (or at least have a voltage-dependence different from that of electrogenic release). Combined with the observation that glutamate release can only be detected in the presence of external potassium, at a depolarized membrane potential (figure 4.11), I can find no evidence for electroneutral release of glutamate.

4.9.2 Predicting the rise of extracellular glutamate concentration in anoxia/ischaemia

The reduction by an acid extracellular pH of the rate glutamate release by reversed uptake, seen in figures 4.1 and 4.12 has implications for our understanding of the events in brain anoxia or ischaemia. During anoxia/ischaemia, the brain intracellular and extracellular pH both become acid by up to one pH unit (Mutch and Hansen, 1984; Silver and Erecinska, 1992). The other ionic changes occurring (a rise of $[K^+]_o$ and $[Na^+]_i$, a fall of $[Na^+]_o$ and $[K^+]_i$, and a depolarization of the membrane potential) will be expected to stimulate reversed uptake (see section 1.3.3). Thus, glutamate will be transported out of the cell until a new

equilibrium concentration of extracellular glutamate is attained. In this situation the minimum value at which uptake carriers can maintain the extracellular glutamate concentration is set by the stoichiometry of the transport process. For the stoichiometry in figure 1.1, it can be calculated using the equation:

$$[glu^-]_{o,t=\infty} = \frac{[Na^+]_i^2 \cdot [OH^-]_o \cdot [K^+]_o \cdot [glu^-]_i}{[Na^+]_o^2 \cdot [OH^-]_i \cdot [K^+]_i} e^{\left(\frac{V_m F}{RT}\right)} \quad [4.1]$$

(Attwell *et al.*, 1993), where V_m is the membrane potential, F is the Faraday constant, R is the gas constant and T is the absolute temperature. Under normal conditions, with $[Na^+]_o$=143mM, $[Na^+]_i$=25mM, $[K^+]_i$=66mM, $[K^+]_o$=2mM, $[glu^-]_i$=3mM and V_m=-87mV (Ballanyi *et al.*, 1987; Attwell *et al.*, 1993; Friedman and Haddad, 1994); the equilibrium concentration of extracellular glutamate achieved by the uptake carrier will be about 0.2μM. During anoxia the ion gradients are altered such that $[Na^+]_o$ falls to 87mM and $[K^+]_o$ rises to 60mM (Siesjo, 1990). Assuming a 7% extracellular volume fraction for the retina (Newman and Odette, 1984), $[Na^+]_i$ will rise to 29mM and $[K^+]_i$ will fall to 62mM. The membrane potential will thus depolarize to -20mV. The equilibrium external glutamate concentration (i.e. the lowest concentration that can be maintained by the carrier) will rise to 304μM (calculated from equation 4.1). The pH change, which precedes the other ionic changes occurring during ischaemia, is of a similar magnitude both inside and outside the cell (Mutch and Hansen, 1984; Silver and Erecinska, 1992), so the equilibrium glutamate concentration will not be greatly affected (from equation 4.1) because the $[OH^-]$ will change by a similar factor inside and outside. The rate at which this equilibrium is reached however, will be slowed.

The rate of the rise in extracellular glutamate concentration can be quantified using the equation:

$$Vol \cdot \frac{d[glu^-]_o}{dt} = efflux - influx \quad [4.2]$$

where Vol represents the extracellular volume per Müller cell, and efflux and influx

are the unidirectional fluxes of glutamate via the transporters. Equation 4.2 can be rearranged to give:

$$\text{Vol} \cdot \frac{d[glu^-]_o}{dt} = \text{efflux}\left(1 - \frac{\text{influx}}{\text{efflux}}\right) \qquad [4.3]$$

Influx and efflux can be assumed, simplistically, to be proportional to the concentration of the substrates present at the appropriate side of the membrane, viz.:

$$\text{influx} = k_i \cdot [Na^+]_o^2 \cdot [K^+]_i \cdot [OH^-]_i \cdot [glu^-]_o \qquad [4.4]$$

$$\text{efflux} = k_e \cdot [Na^+]_i^2 \cdot [K^+]_o \cdot [OH^-]_o \cdot [glu^-]_i \qquad [4.5]$$

where k_i and k_e are the rate constants for influx and efflux respectively. When equilibrium has been reached, at t=∞, influx equals efflux and (from equations 4.4 and 4.5) the external glutamate concentration is given by:

$$[glu^-]_{o,t=\infty} = \frac{k_e \cdot [Na^+]_i^2 \cdot [K^+]_o \cdot [OH^-]_o \cdot [glu^-]_i}{k_i \cdot [Na^+]_o^2 \cdot [K^+]_i \cdot [OH^-]_i} \qquad [4.6]$$

Now in general from equations 4.4 and 4.5,

$$\frac{\text{influx}}{\text{efflux}} = \frac{k_i \cdot [Na^+]_o^2 \cdot [K^+]_i \cdot [OH^-]_i \cdot [glu^-]_o}{k_e \cdot [Na^+]_i^2 \cdot [K^+]_o \cdot [OH^-]_o \cdot [glu^-]_i} \qquad [4.7]$$

so substituting into equation 4.6 gives:

$$\frac{\text{influx}}{\text{efflux}} = \frac{[glu^-]_o}{[glu^-]_{o,t=\infty}} \qquad [4.8]$$

Assuming that the reversed uptake current (I_{rev}) measured in a cell suspended in a large volume of fluid represents only the efflux of glutamate (since $[glu]_o$ is effectively zero), then

$$\text{efflux} = \frac{I_{rev}}{F} \qquad [4.9]$$

where F is the Faraday constant, so equation 4.3 can now be written (using equations 4.8 and 4.9) as:

$$\text{Vol} \cdot \frac{d[glu^-]_o}{dt} = \frac{I_{rev}}{F}\left(1 - \frac{[glu^-]_o}{[glu^-]_{o,t=\infty}}\right) \qquad [4.10]$$

The solution to this equation is:

$$[glu^-]_o = [glu^-]_{o,t=\infty} - \left([glu^-]_{o,t=\infty} - [glu^-]_{o,t=0}\right) \cdot e^{-\frac{t}{\tau}} \qquad [4.11]$$

where

$$\tau = \frac{Vol \cdot F \cdot [glu^-]_{o,t=\infty}}{I_{rev}} \qquad [4.12]$$

is the time constant with which the concentration of external glutamate rises. A plot of equation 4.11 is shown in figure 4.14 using values of I_{rev} and Vol (per Müller cell) from the salamander retina: the volume of the retina per Müller cell is $9x10^{-14}m^3$ (Mobbs *et al.*, 1988) of which 7% is extracellular (Newman and Odette, 1984). Raising the extracellular potassium concentration to 60mM depolarizes the cell to around -20mV and results in a reversed uptake current of the order of 20pA when the external pH is 7.3 and the internal pH is 7.0 (Szatkowski *et al.*, 1990). Disregarding the pH changes which occur, after 2 minutes of ischaemia when the external potassium concentration rises to around 60mM, the external glutamate concentration will rise from an initial value of $[glu^-]_{o,t=\infty}$ = 0.2μM to a final value of $[glu^-]_{o,t=\infty}$ =304μM (from equation 4.1) with a time constant of 9.2 seconds. This is indicated by the dashed line in figure 4.14. Since the pH changes by about 1 unit (Mutch and Hansen, 1984; Silver and Erecinska, 1992) inside and outside the cell, giving a decrease of $[OH^-]_i$ and $[OH^-]_o$ by the same factor of 10, the predicted equilibrium concentration of external glutamate is unaffected by the pH changes (from equation 4.1 or 4.6). However since I_{rev} is reduced at an acid pH (see figure 4.1), the time constant, τ, will be increased (equation 4.12). I_{rev} is postulated to be directly proportional to the external hydroxide concentration, $[OH^-]_o$ (from equations 4.5 and 4.9), so a change in external pH from 7.3 to 6.1 should decrease I_{rev} by a factor of 15.8. This is consistent with the 14 fold decrease seen experimentally in I_{rev} at external pH 6.1 (figure 4.1). Equation 4.12 thus predicts that τ will be increased from 9.2 to 127 seconds. The rise in external glutamate concentration over time in these conditions is indicated by the solid line in figure 4.14. The time taken for the external glutamate concentration to reach a neurotoxic level of 100μM is increased from 3.7 to 50.5 seconds by the extracellular acidification.

Figure 4.14 - Predicted rise in extracellular glutamate concentration over time

The dashed line represents the predicted time course of the rise in extracellular glutamate concentration after the large changes of ion concentrations occurring during the "anoxic depolarization" - which occurs roughly 2 minutes after the brain is made anoxic - but ignoring the effects of the pH changes which occur (from equation 4.11).

The solid line represents the prediction if the changes in pH are included: the slowing of reversed uptake by the acid pH in anoxia/ischaemia slows the rise in extracellular glutamate concentration.

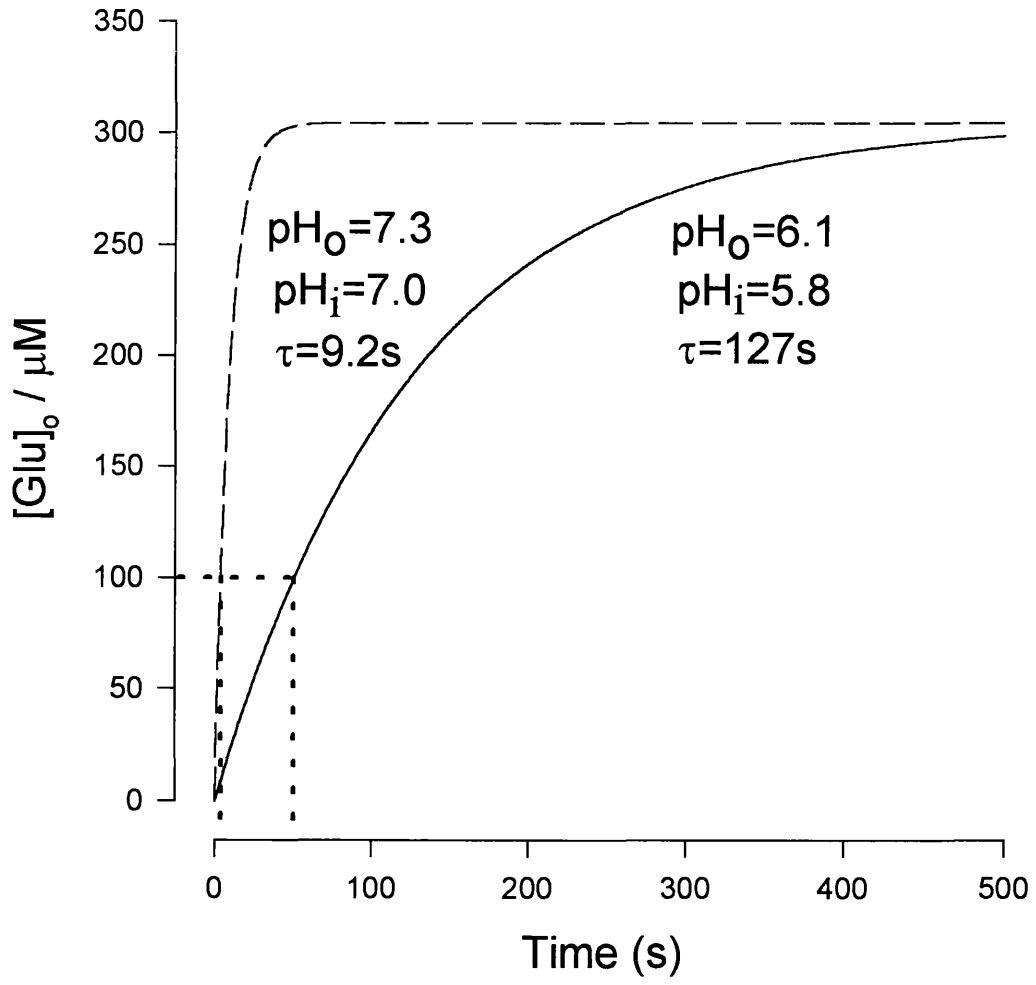
350
300
250
200
150
100
50
0
[Glu]o / μM
pHo=7.3
pHi=7.0
τ=9.2s
pHo=6.1
pHi=5.8
τ=127s
0
100
200
300
400
500
Time (s)

4.9.3 Neuroprotective effect of pH

The slowing of the rise in external glutamate concentration seen at more acid pH will be of little consequence in a long lasting period of ischaemia, since the equilibrium glutamate concentration remains unchanged and will eventually be reached. However, there may be a neuroprotective effect of the acid pH during brief periods of ischaemia.

Transient ischaemic attacks (TIAs) occur when the blood supply to part of the CNS is cut off for a period of several seconds to minutes (Lord, 1990; Nadeau, 1994). Clinically it is found that these short-term periods of ischaemia need not cause any lasting neuronal damage. In addition to the inhibition of NMDA receptors produced by an acid pH (Traynelis and Cull-Candy, 1990), the reduction in the rate of glutamate release by reversed uptake will prolong the time needed for the glutamate concentration to rise to a neurotoxic level and thus will help to prevent neuronal damage resulting from transient ischaemic attacks.

CHAPTER 5

Anion conductance associated with glutamate uptake

5.1 Introduction

The cloned mammalian glutamate uptake carriers (Fairman *et al.*, 1995; Wadiche *et al.*, 1995) and the transporters in salamander photoreceptors and fish bipolar cells (Sarantis *et al.*, 1988; Eliasof and Werblin, 1993; Grant and Dowling, 1995; Picaud *et al.*, Eliasof and Jahr, 1996) have been shown to activate an anion conductance when they bind external glutamate and sodium (see section 1.2.5). It remains unclear how the binding of glutamate to the carrier, or the movement of glutamate on the carrier, gates this anion conductance. Since during certain pathological conditions the glutamate uptake carrier will run backwards or be inhibited (see sections 1.2.6 and 4.1), it is of interest to determine if reversed uptake, or just the binding of glutamate to the carrier in the absence of transport, can activate the anion conductance. This chapter investigates the properties of the anion conductance in the salamander Müller cell glutamate transporter.

5.2 External chloride-dependence of the glutamate uptake current

The cloned mammalian glutamate uptake carrier EAAT4 (Fairman *et al.*, 1995) activates a high permeability to chloride ions, while the carriers EAAT1, EAAT2 and EAAT3 show much less chloride conductance. To determine whether the glutamate uptake carrier in Müller cells also activates a significant chloride conductance, the external chloride concentration was reduced and its effect on the glutamate-evoked current investigated.

Reducing the external chloride ion concentration increases the driving force

for the outward movement of chloride. If the Müller cell glutamate transporter activates a significant anion conductance, one would expect chloride removal to result in an extra glutamate-evoked inward current in whole-cell voltage-clamped Müller cells. When glutamate is applied to the outside of the cells, an inward membrane current is observed due to forward cycling of the glutamate uptake carrier, as described in chapter 3. This current was potentiated by a reduction in external chloride ion concentration (figure 5.1), indicating that the inward current may in part reflect chloride movement through an anion conductance. A similar result was reported recently by Eliasof and Jahr (1996).

The current-voltage relationship of the glutamate-evoked inward current, and its potentiation by a reduction in external chloride ion concentration, are shown in figure 5.2. The glutamate-evoked current was potentiated at all voltages, indicating that the anion conductance is active over the entire voltage range tested, even at positive voltages where uptake of glutamate is inhibited. At a membrane potential of -100mV, the current evoked by 200μM glutamate was increased by 15±6% (mean±SEM of data from 4 cells) by lowering the external chloride concentration. Interestingly, although one might expect the increase produced by chloride removal to be larger at positive potentials (where the driving force for chloride influx would be greatest), a larger change was seen at negative potentials. The current change at 0mV was 34±13% (mean±SEM of data from 4 cells) of that at -100mV. This might be attributable to more activation of the anion conductance occurring at more negative potentials when the carrier is cycling more often.

5.3 Permeability to NO_3^- and ClO_4^-

It has previously been shown that intracellular NO_3^-, SCN^- and ClO_4^- increase the inward current generated by the glutamate uptake carrier when glutamate is applied extracellularly (Bouvier *et al.*, 1992). Bouvier *et al.* (1992)

Figure 5.1 - External chloride-dependence of forward uptake current

The current evoked by 200μM glutamate (indicated by the black bar) in a whole-cell voltage-clamped Müller cell held at -60mV was increased by lowering the external chloride concentration from 126.5mM (left trace) to 19mM (centre trace). Changing the external chloride concentration back to 126.5mM (right trace) restored the current to its control amplitude. Similar results were observed in 4 cells.

Solutions - The external solution contained (mM) NaCl 105, KCl 2.5, $CaCl_2$ 3, $MgCl_2$ 0.5, glucose 15, HEPES 5, $BaCl_2$ 6. The pH was adjusted to 7.3 with NaOH. To lower the extracellular chloride concentration, NaCl and KCl were replaced with Na-gluconate and K-gluconate.

The internal solution contained (mM) KCl 95, NaCl 5, HEPES 5, $MgCl_2$ 7, Na_2ATP 5, $CaCl_2$ 1, K_2EGTA 5. The pH was adjusted to 7.0 with KOH.

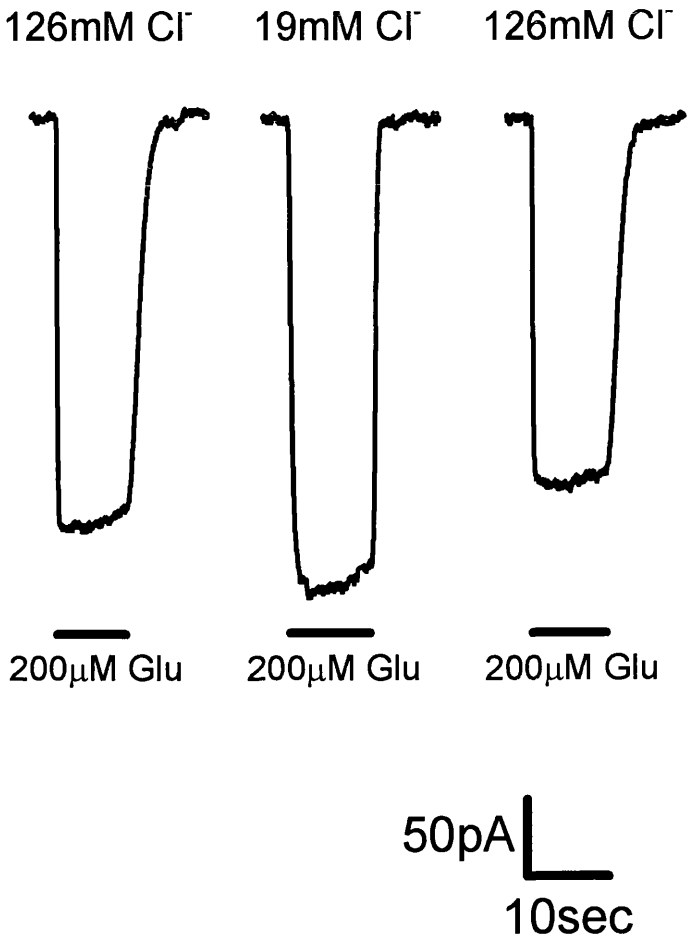
126mM Cl-
19mM Cl-
126mM Cl-
200μM Glu
200μM Glu
200μM Glu
50pA
10sec

Figure 5.2 - Voltage-dependence of glutamate-evoked current in high and low external chloride solutions

The voltage-dependence of the 200μM glutamate-evoked current, for the same cell as in figure 5.1, is shown. The current with 126.5mM external chloride is represented by the solid circles. The current with 19mM external chloride (replaced by gluconate) is represented by the solid squares. Similar results were observed in 4 cells.

Solutions - The external solution contained (mM) NaCl 105, KCl 2.5, $CaCl_2$ 3, $MgCl_2$ 0.5, glucose 15, HEPES 5, $BaCl_2$ 6. The pH was adjusted to 7.3 with NaOH. To lower the extracellular chloride concentration, NaCl and KCl were replaced with Na-gluconate and K-gluconate.

The internal solution contained (mM) KCl 95, NaCl 5, HEPES 5, $MgCl_2$ 7, Na_2ATP 5, $CaCl_2$ 1, K_2EGTA 5. The pH was adjusted to 7.0 with KOH.

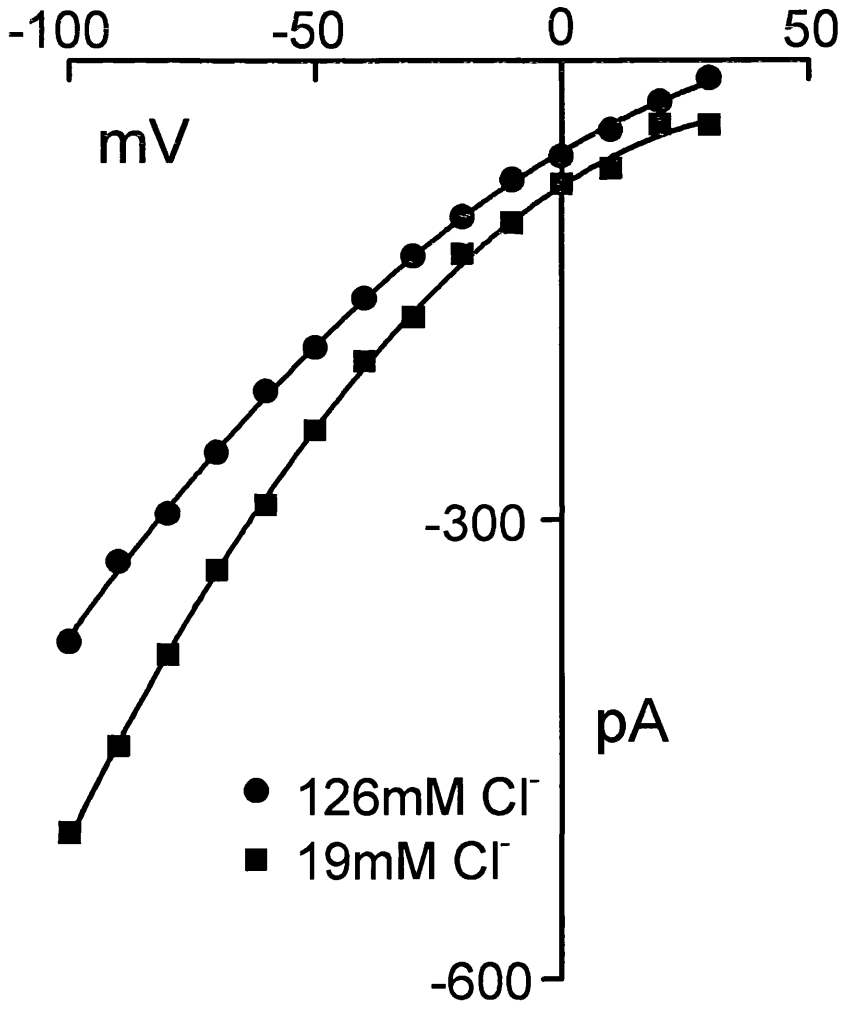
-100
-50
0
50
mV
-300
pA
126mM Cl-
19mM Cl-
-600

suggested that the increased current was due to these anions competing for transport on a hydroxide counter-transport site on the carrier, but another possibility is that these ions permeate the anion conductance gated by the glutamate uptake carrier. To test the latter idea, the effects of NO_3^- and ClO_4^- on the glutamate uptake current were examined in more detail.

With NO_3^- or ClO_4^- present extracellularly but not intracellularly, the glutamate-evoked current was outward at a depolarized membrane potential (figure 5.3). This is not expected if the current is generated only by a carrier with a stoichiometry such that net positive charge is transported inwards with each glutamate ion. This result could however be explained if NO_3^- or ClO_4^- can permeate the anion conductance activated during glutamate uptake (with a higher permeability than the Cl^- normally present). With one of these highly permeant anions present outside the cell, the current observed when glutamate is applied extracellularly would then be a combination of the inward current produced by glutamate uptake with two Na^+ ions (and movement of counter-transported ions as in figure 1.1) and the outward current generated by the negatively charged anion moving inwards. At a depolarized potential, the inward anion current dominates, producing the outward current observed. At a more negative potential, the glutamate uptake current is largest and a reduced inward current is seen when the highly permeant anion was added (figure 5.3).

The glutamate-evoked currents recorded with different concentrations of external ClO_4^- showed I-V relations with a reversal potential characteristic of an anion conductance with a relatively high permeability to ClO_4^- (figure 5.4A). Best-fitting a straight line to the dependence on $\log([ClO_4^-])$ of the reversal potential of the I-V relations gave an average shift of 55mV per 10-fold change in the concentration of ClO_4^- (figure 5.4B). Similar results were obtained with NO_3^- replacing Cl^- (figures 5.4C and 5.4D). On average the reversal potential shifted by 33mV per 10-fold change in the concentration of NO_3^-. Thus the anion

Figure 5.3 - Effects of external anions on glutamate-evoked current

Replacing 100mM external chloride with either NO_3^- or ClO_4^- caused the glutamate-evoked current in a whole-cell voltage-clamped Müller cell, held at 0mV, to reverse (top traces). The black bar represents application of 200μM glutamate. At a holding potential of -60mV (lower traces) the inward glutamate-evoked current seen in chloride Ringer's is reduced by the presence of external NO_3^- or ClO_4^-. Similar results were obtained from 5 cells.

Solutions - The external solution contained (mM) NaCl 105, KCl 2.5, $CaCl_2$ 3, $MgCl_2$ 0.5, glucose 15, HEPES 5, $BaCl_2$ 6. The pH was adjusted to 7.3 with NaOH. For NO_3^- and ClO_4^- ringers, 100mM NaCl was replaced by 100mM $NaNO_3$ or 100mM $NaClO_4$ respectively.

The internal solution contained (mM) KCl 95, NaCl 5, HEPES 5, $MgCl_2$ 7, Na_2ATP 5, $CaCl_2$ 1, K_2EGTA 5. The pH was adjusted to 7.0 with KOH.

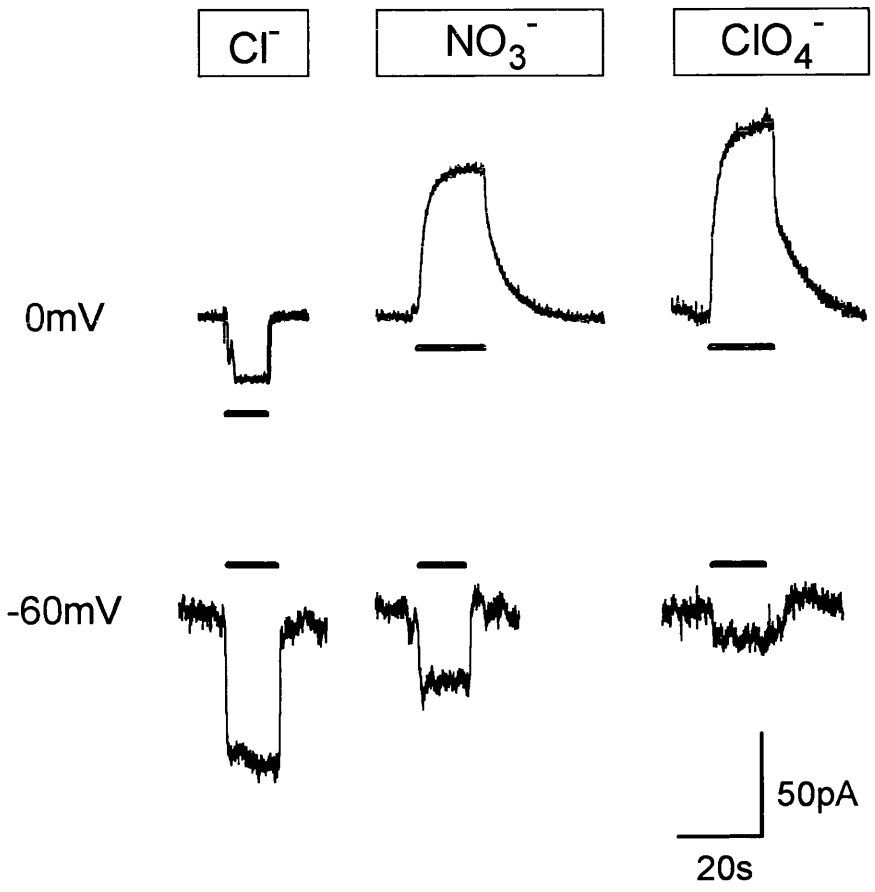
Cl-
NO3-
ClO4-
0mV
-60mV
50pA
20s

Figure 5.4 - Voltage-dependence of effects of external anions on glutamate-evoked current

A Specimen I-V data for the 200μM glutamate-evoked current (as in figure 5.3) show that with chloride outside (0mM ClO_4^-) the current is inward at all potentials but decreases towards zero at positive potentials because glutamate transport into the cell (with two sodium ions) is inhibited at positive potentials. With ClO_4^- outside the current reverses at depolarized membrane potentials because ClO_4^- influx through the carrier's anion conductance generates a significant membrane current.

B Dependence on $[ClO_4^-]_o$ (log scale) of the reversal potential of the currents in A. The points represent the mean±SEM of data from 4 or more cells. The data are best-fit with a straight line which represents a reversal potential change of 55mV per 10-fold change in $[ClO_4^-]_o$.

C Specimen data for an experiment like in A, but with NO_3^- replacing Cl^-.

D Dependence on $[NO_3^-]_o$ (log scale) of the reversal potential of currents studied in C. The point represent mean±SEM of data from 5 or more cells. The data are best-fit with a straight line which represents a reversal potential change of 33mV per 10-fold change in $[NO_3^-]_o$.

Solutions - The external solution contained (mM) NaCl 105, KCl 2.5, $CaCl_2$ 3, $MgCl_2$ 0.5, glucose 15, HEPES 5, $BaCl_2$ 6. The pH was adjusted to 7.3 with NaOH. Cl^- replacement was performed by replacing NaCl with $NaNO_3$ or $NaClO_4$ as required.

The internal solution contained (mM) KCl 95, NaCl 5, HEPES 5, $MgCl_2$ 7, Na_2ATP 5, $CaCl_2$ 1, K_2EGTA 5. The pH was adjusted to 7.0 with KOH.

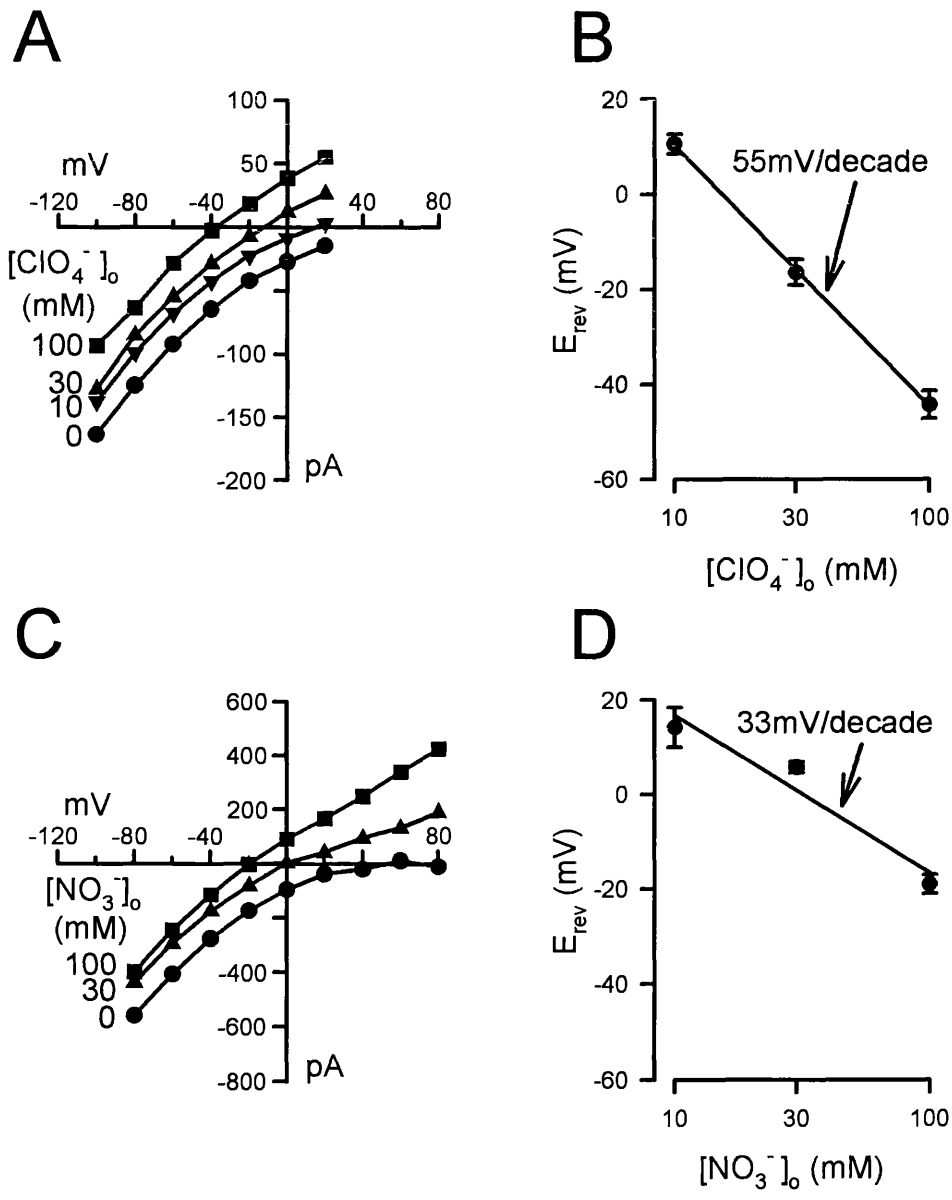
A
100
50
mV
-120
-80
-40
40
80
[ClO4-]o
(mM)
100
30
10
0
-100
-150
-200
pA
B
20
0
-20
-40
-60
55mV/decade
Erev (mV)
10
30
100
[ClO4-]o (mM)
C
600
400
200
mV
-120
-80
-40
80
[NO3-]o
(mM)
100
30
0
-400
-600
-800
pA
D
20
0
-20
-40
-60
33mV/decade
Erev (mV)
10
30
100
[NO3-]o (mM)

conductance is most permeable to ClO_4^-, less permeable to NO_3^- and much less permeable to Cl^-. With Cl^- as the main anion present, anion flux through the carrier's anion conductance makes only a small contribution to the total current flowing (too small, for example, to produce a net outward current at positive voltages).

5.4 Dependence of the anion conductance on external sodium

A requirement for binding of external sodium to the carrier for activating the anion conductance was tested by looking at the external sodium dependence of the outward glutamate-evoked membrane current produced when ClO_4^- is present in the extracellular solution. With sodium replaced by choline in the extracellular solution, the outward current was abolished (figure 5.5A). The current-voltage relation of the block of the current by removal of external sodium is shown in figure 5.5B. Both the outward anion channel current seen at a positive membrane potential, and the inward current made up of anion flux and glutamate transport currents seen at a negative membrane potential, were inhibited by removal of external sodium. Similar results were found in 5 cells with NO_3^- replacing Cl^-. Activation of the anion conductance, like the transport of glutamate (Brew and Attwell, 1987), is thus entirely dependent on the presence of external sodium. Experiments described below (section 5.8) investigate the sodium-dependence of the anion channel activation in more detail.

5.5 Dependence of the anion conductance on internal potassium

The dependence on internal potassium of the activation of the anion conductance was tested by removing potassium from the intracellular pipette solution. With 95mM K^+ inside the cell, the I-V relation of the glutamate-evoked current in the presence and absence of external NO_3^- is shown in figure 5.6A. As

Figure 5.5 - Sodium-dependence of glutamate-evoked current with external ClO_4^-

A The outward glutamate-evoked current at a holding potential of 0mV in the presence of 105mM extracellular ClO_4^- (left-hand trace), reflecting ClO_4^- entry through the transporter's anion conductance, was abolished by the removal of external sodium (right-hand trace). The black bars represent the application of 200μM glutamate. External sodium was replaced by choline. The same result was seen in 5 cells.

B Current-voltage relation of the glutamate-evoked current in the presence and absence of external sodium. The data points represent the mean±SEM of the data from 3 cells, and are normalized by cell capacitance to compensate for differences in cell size (Barbour *et al.*, 1991).

Solutions - The external solution contained (mM) $NaClO_4$ 105, KCl 2.5, $CaCl_2$ 3, $MgCl_2$ 0.5, glucose 15, HEPES 5, $BaCl_2$ 6. The pH was adjusted to 7.3 with NaOH. External sodium was removed by replacing the $NaClO_4$ with choline-ClO_4.

The internal solution contained (mM) KCl 95, NaCl 5, HEPES 5, $MgCl_2$ 7, Na_2ATP 5, $CaCl_2$ 1, K_2EGTA 5. The pH was adjusted to 7.0 with KOH.

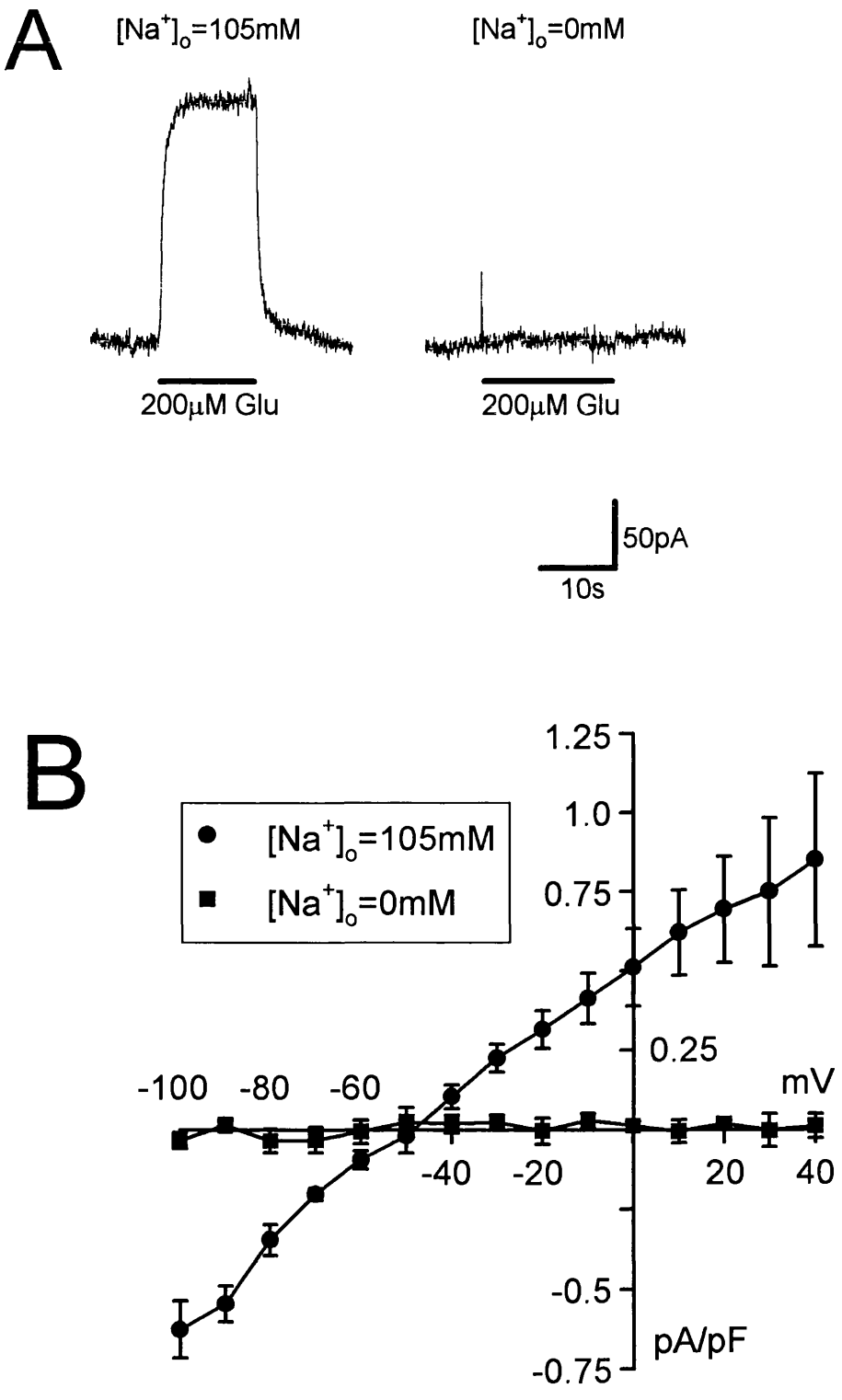
A
[Na+]o=105mM
[Na+]o=0mM
200μM Glu
200μM Glu
50pA
10s
B
[Na+]o=105mM
[Na+]o=0mM
1.25
1.0
0.75
0.25
-0.5
-0.75
pA/pF
-100
-80
-60
-40
-20
20
40
mV

Figure 5.6 - Internal potassium-dependence of glutamate-evoked current with external NO_3^-

The current evoked by 200μM glutamate in Müller cells voltage-clamped between -90 and +50mV, in the presence and absence of 50mM external NO_3^- (A), was greatly inhibited by removal of internal potassium (B, different cells to those in A). The data points represent the mean±SEM of data from 5 cells. The currents are normalized to the cell capacitance to minimize differences in current magnitude due to cell size differences (Barbour *et al.*, 1991).

Solutions - The external solution contained (mM) NaCl 75, choline-Cl 30, KCl 2.5, $CaCl_2$ 3, $MgCl_2$ 0.5, glucose 15, HEPES 5, $BaCl_2$ 6. The pH was adjusted to 7.3 with NaOH. For the NO_3^- solution, 50mM NaCl was replaced by $NaN0_3$.

The internal solution contained (mM) KCl 95, NaCl 5, HEPES 5, $MgCl_2$ 7, Na_2ATP 5, $CaCl_2$ 1, $(NMDG)_2EGTA$ 5. The pH was adjusted to 7.0 with NMDG. For the 0mM K^+ solution, KCl was replaced by choline-Cl.

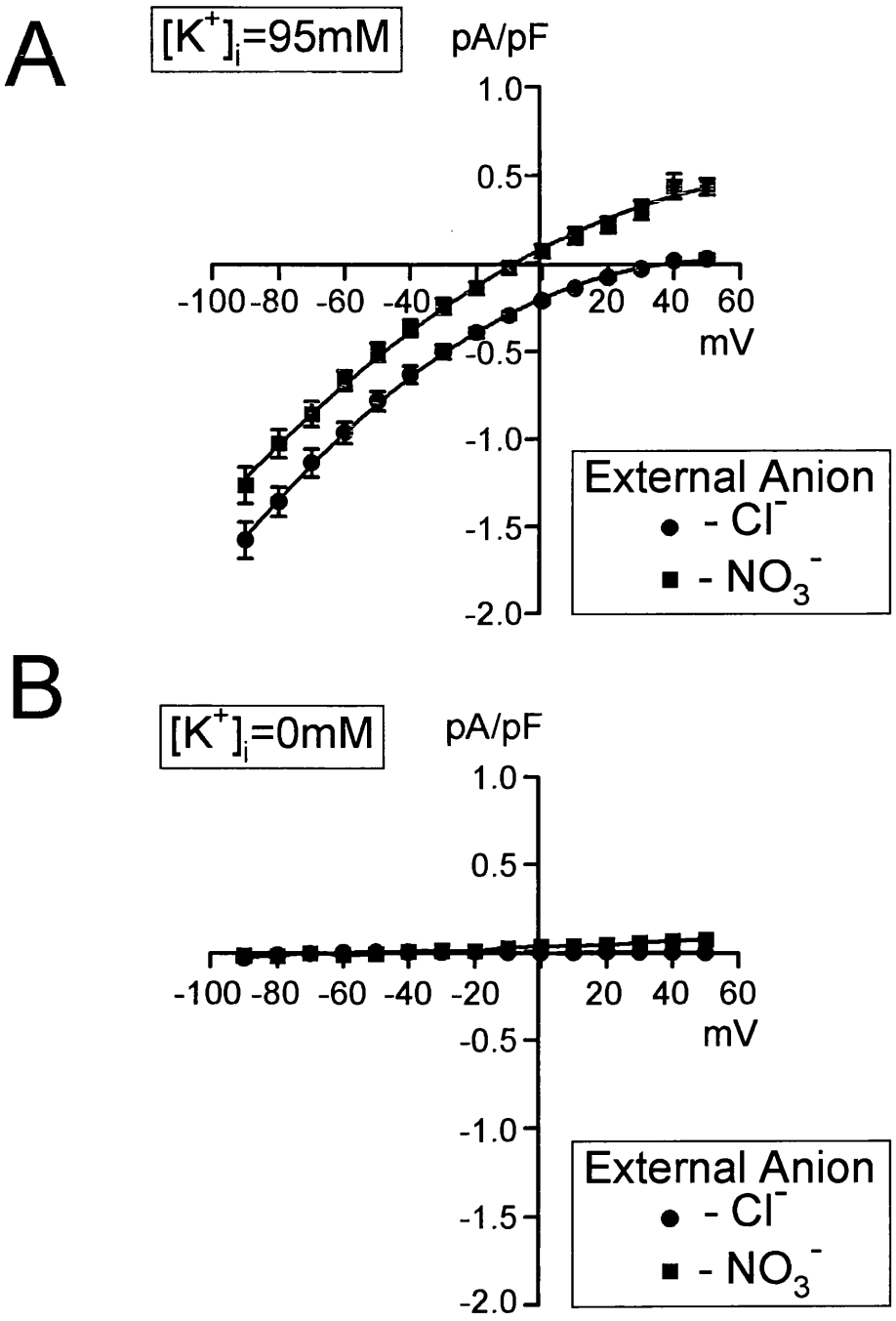
A
[K+]i=95mM
pA/pF
1.0
0.5
-100 -80 -60 -40
20 40 60
mV
-0.5
-1.0
-1.5
-2.0
External Anion
- Cl-
- NO3-
B
[K+]i=0mM
pA/pF
1.0
0.5
-100 -80 -60 -40 -20
20 40 60
mV
-0.5
-1.0
-1.5
-2.0
External Anion
- Cl-
- NO3-

was seen in figure 5.4C, the presence of extracellular NO_3^- leads to an outward glutamate-evoked current at depolarized membrane potentials, presumably due to entry of NO_3^- through the anion conductance. When internal potassium was removed (by recording from different cells with pipettes filled with a solution lacking potassium) the glutamate transport current was abolished (data in Cl^-), and the anion current carried by NO_3^- was greatly inhibited at all membrane potentials (figure 5.6B). The outward glutamate-evoked current observed at +40mV with 50mM NO_3^- in the extracellular solution was reduced by 86±3% (mean±SEM of data from 5 cells) by the removal of internal potassium. As for the transport of glutamate (Kanner and Sharon, 1978; Barbour *et al.*, 1988), therefore, internal potassium is required for the activation of the anion conductance.

5.6 Activation of the anion conductance by reversed glutamate uptake

With sodium and glutamate present inside the cell, raising the external potassium concentration evokes an outward membrane current which can be attributed to the reversed operation of the glutamate uptake carrier, transporting net positive charge out of the cell (Szatkowski *et al.*, 1990 and see chapter 4). Confirmation that this manipulation releases glutamate was shown in figure 4.4, by the detection of glutamate using glutamate-gated ion channels present in whole-cell voltage-clamped neurons placed next to the Müller cell. To determine if stimulating the glutamate transporter to run backwards will also gate the anion conductance, the effects of external NO_3^- and ClO_4^- on the potassium-evoked current were examined.

When extracellular Cl^- was replaced by ClO_4^- or NO_3^-, the outward membrane current evoked by raising the external potassium concentration from 0 to 30mM was increased (figure 5.7). Replacing 50mM of the external Cl^- by NO_3^- increased the potassium-evoked current by a factor of 1.58±0.06 (mean±SEM of

Figure 5.7 - Effects of external anions on the reversed uptake current

Reversed glutamate uptake was activated by raising the external potassium concentration from 0 to 30mM (black bars) in Müller cells voltage-clamped at 0mV, with 20mM sodium and 10mM glutamate in the internal solution (via the patch pipette). The effect of different external anions was studied by applying normal chloride-containing solution , followed by solution in which 50mM chloride was replaced by NO_3^- or ClO_4^- and then by normal chloride-containing solution again.

Solutions - The external solution contained (mM) NaCl 75, choline-Cl 30, $CaCl_2$ 3, $MgCl_2$ 0.5, glucose 15, HEPES 5, $BaCl_2$ 6, ouabain 0.1. The pH was adjusted to 7.3 with NaOH. For the NO_3^- and ClO_4^- solutions, 50mM NaCl was replaced by $NaNO_3$ or $NaClO_4$. To evoke reversed uptake 30mM choline-Cl was replaced by 30mM KCl.

The internal solution contained (mM) Na-glutamate 10, choline-Cl 40, HEPES 71, $MgCl_2$ 7, Na_2ATP 5, $CaCl_2$ 1, $(NMDG)_2EGTA$ 5. The pH was adjusted to 7.0 with 25mM NMDG.

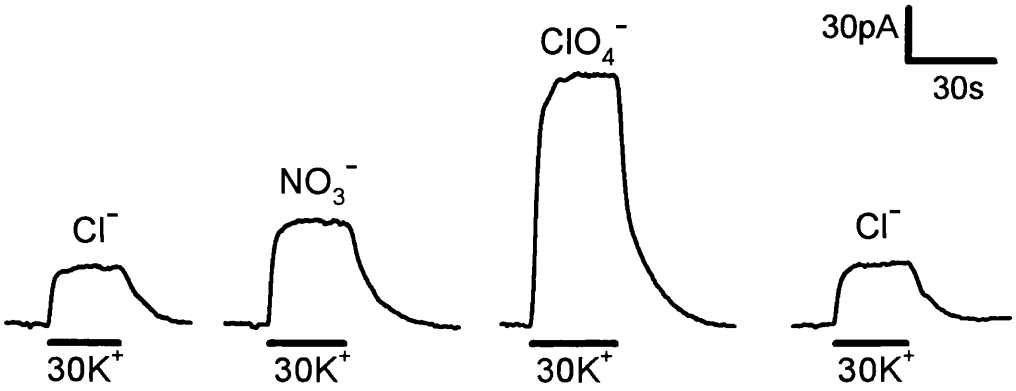
30pA
30s
Cl^-
NO_3^-
ClO_4^-
Cl^-
$30K^+$
$30K^+$
$30K^+$
$30K^+$

data from 6 cells), while replacing 50mM Cl^- by ClO_4^- increased the current by a factor of 3.34±0.41 (mean±SEM of data from 5 cells) (figure 5.8B). These results are consistent with the anion conductance being activated when reversed uptake is stimulated: an inward movement of the more permeant negatively charged ions through the anion conductance enhances the outward current.

Replacing 50mM intracellular Cl^- by ClO_4^- resulted in an inward current being evoked when the external potassium concentration was raised (figure 5.8A). The reversal in polarity of the current is consistent with an outward movement of ClO_4^- through the anion conductance producing an inward membrane current larger than the outward current resulting from the net positive charge efflux accompanying reversed transport of glutamate.

All of the current produced by raising external potassium in the presence of extracellular NO_3^- was inhibited by the removal of internal sodium and glutamate (figure 5.9). This is consistent with the binding of internal sodium and glutamate being a requirement for activating the anion conductance, as well as for the reversed transport of glutamate (Szatkowski *et al.*, 1990).

5.7 Coupling of glutamate transport and anion movement

The experiments described in the previous section showed that the anion flux through the carrier's anion conductance can be greatly increased by replacing Cl^- with NO_3^- or ClO_4^-. To determine whether this altered anion flux results in an alteration of the transport of glutamate, or whether the anion movement is independent of the movement of glutamate, glutamate transport was assessed by measuring the efflux of glutamate using glutamate-gated ion channels in adjacent whole-cell voltage-clamped neurons (see section 4.4).

With 10mM sodium and glutamate inside the cell and 30mM potassium in the external solution, depolarizing the Müller cell from -60 to +20mV induces the

Figure 5.8 - Effects of internal anions (A), and summary of effects of internal and external anions (B), on the reversed uptake current

A Specimen data from two different cells showing the potassium-evoked reversed uptake current in Müller cells voltage-clamped at 0mV, with 10mM sodium and glutamate inside, with (right-hand trace) or without (left-hand trace) 50mM internal ClO_4^-.

B The effect of external NO_3^- and ClO_4^-, and internal ClO_4^- on the potassium-evoked reversed uptake current (as in figures 5.7 and 5.8A). The currents are normalized to the current with only Cl^- present, and are the mean±SEM of data from 5 or more cells.

Solutions - The external solution contained (mM) NaCl 75, choline-Cl 30, $CaCl_2$ 3, $MgCl_2$ 0.5, glucose 15, HEPES 5, $BaCl_2$ 6, ouabain 0.1. The pH was adjusted to 7.3 with NaOH. To evoke reversed uptake, 30mM choline-Cl was replaced by 30mM KCl.

The internal solution for (A) contained (mM) Na-glutamate 10, choline-Cl 85, NaCl 5, HEPES 5, $MgCl_2$ 7, Na_2ATP 5, $CaCl_2$ 1, $(NMDG)_2EGTA$ 5. The pH was adjusted to 7.0 with NMDG. For 50mM internal ClO_4^- solution, 50mM choline-Cl was replaced by choline-ClO_4.

A

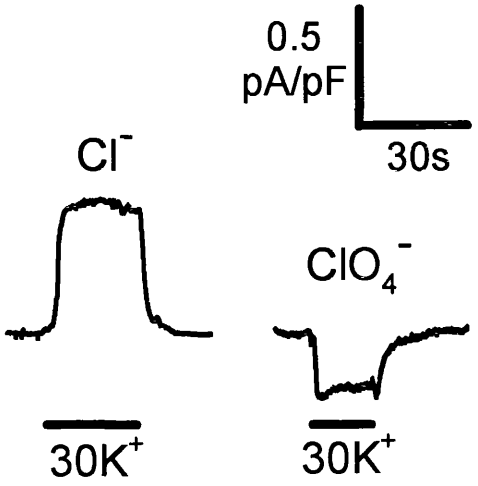
0.5
pA/pF
30s
Cl⁻
ClO4⁻
30K+
30K+

B

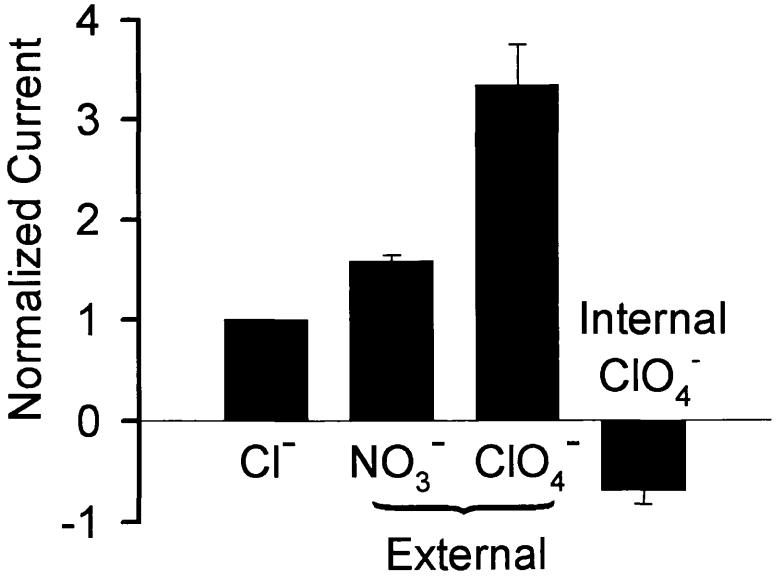
Normalized Current
4
3
2
1
0
-1
Cl⁻
NO3⁻
ClO4⁻
External
Internal
ClO4⁻

Figure 5.9 - Reversed uptake activation of anion conductance - intracellular sodium- and glutamate-dependence

The reversed uptake current evoked by raising the external potassium concentration (black bars) in the presence of external chloride (Cl^-), and larger current observed in the presence of 50mM external nitrate (NO_3^-) (see figure 5.7), and the current recorded in chloride again in Müller cells voltage-clamped at 0mV. Data are shown in a cell clamped with a pipette containing sodium and glutamate (bottom trace, from figure 5.7) and from another cell clamped with a pipette lacking sodium and glutamate (top trace).

Solutions - The external solution contained (mM) NaCl 75, choline-Cl 30, $CaCl_2$ 3, $MgCl_2$ 0.5, glucose 15, HEPES 5, $BaCl_2$ 6, ouabain 0.1. The pH was adjusted to 7.3 with NaOH. For the NO_3^- solution, 50mM NaCl was replaced by $NaNO_3$. To evoke reversed uptake 30mM choline-Cl was replaced by 30mM KCl.

The internal solution contained (mM) choline-Cl 100, HEPES 5, $MgCl_2$ 2, MgATP 5, $CaCl_2$ 1, $(NMDG)_2EGTA$ 5, malonic acid 0.2 (to block succinate dehydrogenase), L-methionine-sulphoximine 2 (to block glutamine synthetase). The pH was adjusted to 7.0 with NMDG. The two blockers of glutamate metabolizing enzymes were included to try to control the concentration of intracellular glutamate better. For the cells with sodium and glutamate inside, the internal solution contained (mM) Na-glutamate 10, choline-Cl 40, HEPES 71, $MgCl_2$ 7, Na_2ATP 5, $CaCl_2$ 1, $(NMDG)_2EGTA$ 5. The pH was adjusted to 7.0 with 25mM NMDG.

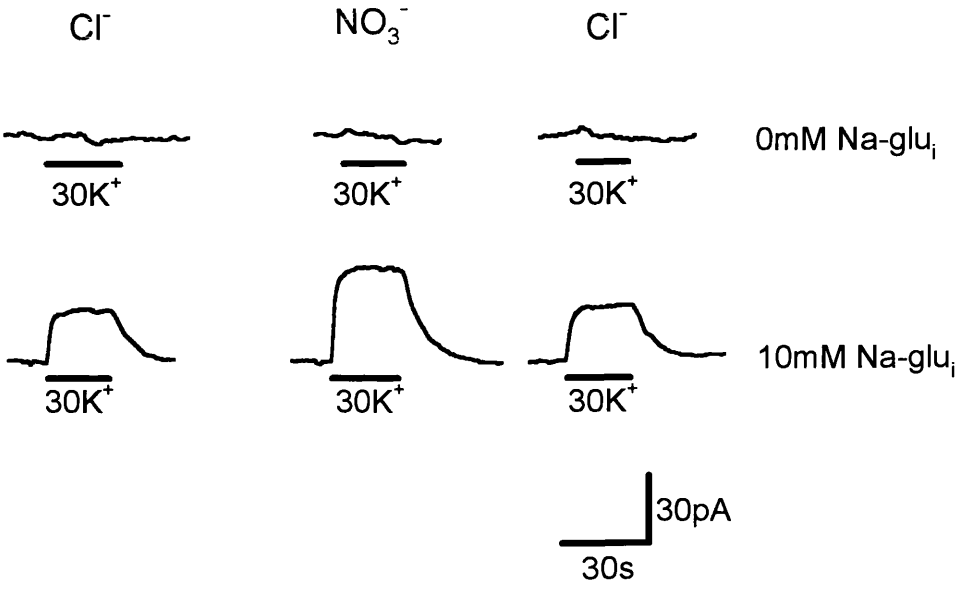
Cl-
NO3-
Cl-
0mM Na-glui
30K+
30K+
30K+
10mM Na-glui
30K+
30K+
30K+
30pA
30s

release of glutamate by reversed glutamate uptake, which can be detected by adjacent Purkinje cells (see section 4.4). Replacement of 50mM Cl^- in the external solution by NO_3^- reduced the resulting Purkinje cell membrane current to 69±4% (mean±SEM of data from 3 cells) of its value with only Cl^- present (figure 5.10A). Replacement of 50mM Cl^- by ClO_4^- reduced the Purkinje cell current to 98±10% of its value with only Cl^- present (figure 5.10B).

To interpret these data in is necessary to know how the presence of extracellular NO_3^- and ClO_4^- affected the sensitivity of Purkinje cells to external glutamate. Control experiments showed that the membrane current evoked in whole-cell voltage-clamped Purkinje cells by the application of 3μM extracellular glutamate was reduced to 76±18% (mean±SEM of data from 3 cells) of its control value when 50mM extracellular Cl^- was replaced by NO_3^-, and increased to 233±29% (mean±SEM of data from 3 cells) of its value with only Cl^- present when 50mM Cl^- was replaced by ClO_4^- (data not shown). The potentiation by ClO_4^- is consistent with the effect of chaotropic ions like ClO_4^- which increase the affinity of AMPA receptors (Honore and Drejer, 1988).

Taking into account these changes in Purkinje cell sensitivity produced by the substituted anions, 50mM external NO_3^- resulted in an insignificant change in glutamate release from the potassium-stimulated Müller cell. Glutamate release was 0.92±0.22 (mean±SEM, calculated from the above figures i.e. 0.69/0.76) of its value with only Cl^- present in the extracellular solution. Similarly, replacement of Cl^- by ClO_4^- resulted in a reduction in the amount of glutamate released from the stimulated Müller cell, to 0.42±0.06 (mean±SEM) of its value in Cl^- (it is uncertain why ClO_4^- slows carrier cycling in this way). When compared to the 1.58 and 3.34 fold increases in potassium-evoked current produced by the presence of external NO_3^- and ClO_4^- respectively (see figure 5.7), it is clear that the amount of glutamate transported is not proportional to the movement of charge through the anion conductance part of the carrier molecule. Thus, there is no tight coupling

Figure 5.10 - Effect of different external anions on glutamate release from Müller cells, sensed by adjacent Purkinje cells

Glutamate release by reversed uptake was assessed as the current (noisy traces) evoked in a whole-cell voltage-clamped Purkinje cell held at -60mV, placed next to a Müller cell. Glutamate release from the Müller cell was stimulated by stepping the membrane potential (V_M, top trace) from -60 to +20mV in the presence of 30mM external potassium and with 20mM sodium and 10mM glutamate inside the cell.

A Left: Purkinje cell response in normal chloride-containing external solution . Right: Purkinje cell response after switching to an external solution with 50mM chloride replaced by NO_3^-.

B Data from another cell pair, like A except that ClO_4^- was the substituted anion.

Solutions - The external solution contained (mM) NaCl 75, KCl 30, $CaCl_2$ 3, $MgCl_2$ 0.5, glucose 15, HEPES 5, $BaCl_2$ 6, ouabain 0.1 and trichlormethiazide 1 (dissolved in DMSO, 0.05% in final solution). The pH was adjusted to 7.3 with NaOH. For the NO_3^- and ClO_4^- solutions, 50mM NaCl was replaced by $NaNO_3$ or $NaClO_4$. Trichlormethiazide was used to increase the Purkinje cell's glutamate sensitivity by removing desensitization of non-NMDA receptors (see section 4.3).

The Müller cell internal solution contained (mM) Na-glutamate 10, choline-Cl 40, HEPES 71, $MgCl_2$ 7, Na_2ATP 5, $CaCl_2$ 1, $(NMDG)_2EGTA$ 5. The pH was adjusted to 7.0 with 25mM NMDG.

The Purkinje cell internal solution contained (mM) CsCl 110, Na_2ATP 2, $CaCl_2$ 0.5, $MgCl_2$ 2, HEPES 10 and $(NMDG)_2EGTA$ 5. It was titrated to pH 7.0 with NMDG.

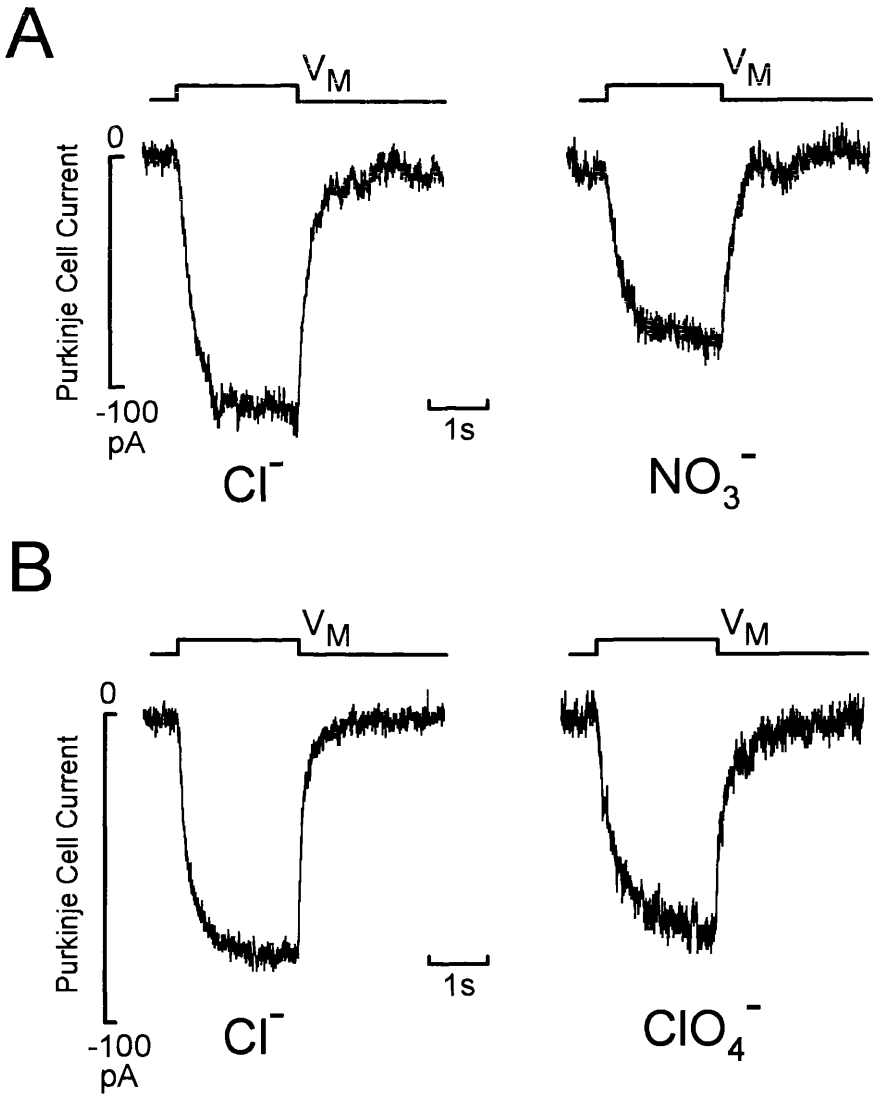
A
V_M
V_M
0
Purkinje Cell Current
-100
pA
1s
Cl^-
NO_3^-
B
V_M
V_M
0
Purkinje Cell Current
1s
-100
pA
Cl^-
ClO_4^-

between anion flux and glutamate flux.

5.8 Activation of the anion conductance in the absence of glutamate transport

In the absence of intra- and extracellular potassium both forward and reversed transport of glutamate are inhibited (see section 4.5, and Kanner and Sharon, 1978; Barbour *et al.*, 1988; Szatkowski *et al.*, 1990). However, when sodium and glutamate are present inside the cell, a small glutamate-evoked membrane current was still observed in the absence of intra- and extracellular potassium. This current was inward at negative membrane potentials, outwards at positive membrane potentials, and showed the pharmacology of glutamate uptake (figure 5.11), being activated by L-glutamate, L-aspartate and D-aspartate, but not by the agonists of glutamate's ionotropic and metabotropic receptors (NMDA, kainate and quisqualate). Removal of either sodium or glutamate from the internal solution greatly inhibited this current (figure 5.12). Relative values of the glutamate-evoked current (normalized to cell capacitance) at +20mV with 10mM Na-glu, 10mM glu^- but no Na^+, 10mM Na^+ but no glu^-, or no Na^+ and no glu^-, were (respectively) 1.0, 0.014±0.024, -0.041±0.031 and 0.0±0.0 (mean±SEM of data from 6 or 7 cells).

Changing the external chloride concentration (replaced with gluconate) revealed that the glutamate-evoked current was produced by activation of an anion conductance (figure 5.13A). Best-fitting a straight line to the dependence on $\log([Cl^-]_o)$ of the reversal potential of the I-V relations in figure 5.13A showed a shift of 28mV per 10-fold change of chloride concentration (figure 5.13B).

With ClO_4^- instead of Cl^- as the major anion present inside and outside the cell, the glutamate-evoked conductance seen in the absence of potassium (but with sodium and glutamate present inside the cell) was greatly increased (figure 5.14).

Figure 5.11 - Pharmacology of the glutamate-evoked current in Müller cells clamped with pipettes containing sodium and glutamate, in the absence of intra- and extracellular potassium

Currents evoked by 100μM glutamate and analogues (black bars) in a Müller cell voltage-clamped at -5 and -65mV. Similar results were obtained in five cells.

Solutions - The external solution contained (mM) NaCl 100, choline-Cl 10, $MgCl_2$ 0.5, $CaCl_2$ 3, $BaCl_2$ 6, HEPES 5, glucose 15, ouabain 0.1. The pH was set to 7.3 with NaOH.

The internal solution contained (mM) Na-glu 100, MgATP 5, HEPES 5, $CaCl_2$ 1, $MgCl_2$ 2, $(NMDG)_2EGTA$ 5. The pH was set to 7.0 with NMDG.

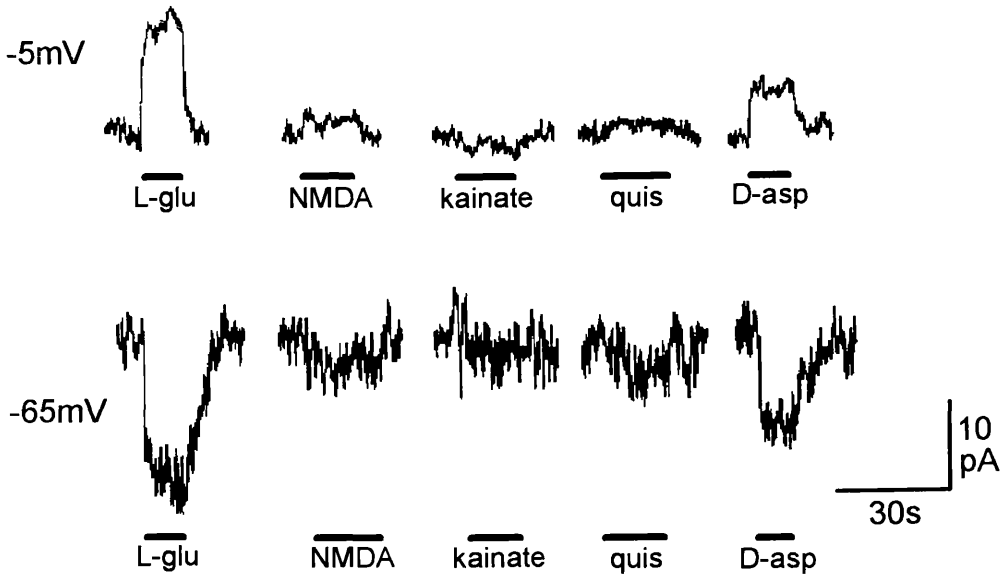
-5mV
L-glu
NMDA
kainate
quis
D-asp
-65mV
L-glu
NMDA
kainate
quis
D-asp
10
pA
30s

Figure 5.12 - Internal sodium- and glutamate-dependence of the glutamate-evoked current seen with sodium and glutamate inside the cell but in the absence of intra- and extracellular potassium

Currents evoked by 200μM glutamate in four different Müller cells voltage-clamped at +20 and -40mV with pipette solutions containing different sodium and glutamate concentrations (as stated over each record). The currents are normalized to the cell capacitance to minimize the differences in current magnitude due to cell size (Barbour *et al.*, 1991).

Solutions - The external solution contained (mM) NaCl 100, choline-Cl 10, $MgCl_2$ 0.5, $CaCl_2$ 3, $BaCl_2$ 6, HEPES 5, glucose 15, ouabain 0.1. The pH was set to 7.3 with NaOH.

The 10mM Na-glu internal solution contained (mM) NaCl 10, NMDG-glutamate 10, choline-Cl 80, $(NMDG)_2EGTA$ 5, MgATP 5, HEPES 5, $CaCl_2$ 1, $MgCl_2$ 2, aminooxyacetic acid 5 (to block glutamate transaminase), L-methionine-sulphoximine 2 (to block glutamine synthetase). The pH was set to 7.0 with NMDG. The two blockers of glutamate metabolizing enzymes are used to give more accurate control of the internal glutamate concentration. For removal of either the sodium or the glutamate or both, the NaCl and/or the NMDG-glutamate were replaced by choline-Cl.

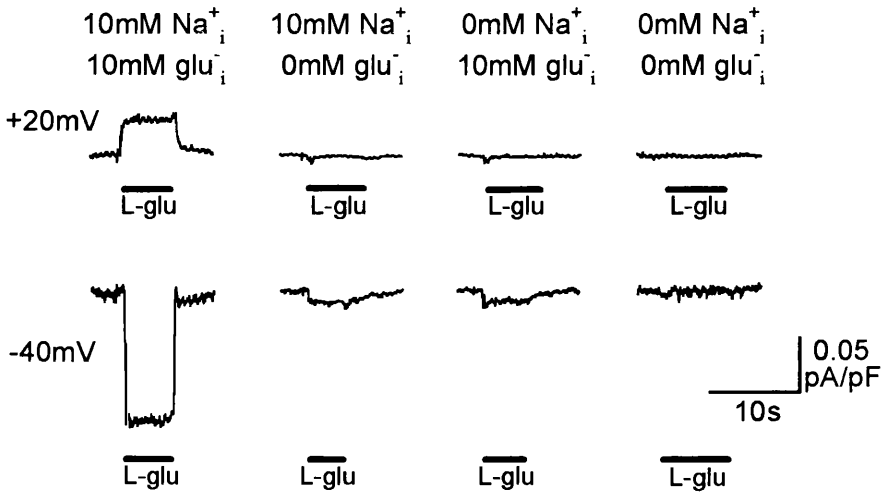
10mM Na^+_i
10mM glu^-_i
10mM Na^+_i
0mM glu^-_i
0mM Na^+_i
10mM glu^-_i
0mM Na^+_i
0mM glu^-_i
+20mV
L-glu
L-glu
L-glu
L-glu
-40mV
0.05
pA/pF
10s
L-glu
L-glu
L-glu
L-glu

Figure 5.13 - Chloride-dependence of the glutamate-evoked current with internal and external potassium removed and sodium and glutamate present inside the cell

A Specimen I-V relationships of the glutamate-evoked current in a Müller cell, with various values of external chloride concentration (replaced with gluconate). The triangles, squares and circles represent external chloride concentrations of 126, 60 and 27mM respectively.

B The reversal potential of the data obtained as in A, plotted as a function of $[Cl^-]_O$ on a log scale. The data points represent the mean±SEM of data from 5 or more cells, and are best-fitted with a straight line which represents a change in reversal potential of 28mV per 10-fold change in $[Cl^-]_O$. E_{Cl} with 126mM chloride outside (and 56mM chloride inside) is -21mV

Solutions - The external solution contained (mM) NaCl 107, $MgCl_2$ 0.5, $CaCl_2$ 3, $BaCl_2$ 6, HEPES 5, glucose 15. The pH was set to 7.3 with NaOH. For removal of external chloride, NaCl was replaced by Na-gluconate.

The internal solution contained (mM) Na-glutamate 10, choline-Cl 40, HEPES 71, $MgCl_2$ 7, Na_2ATP 5, $CaCl_2$ 1, $(NMDG)_2EGTA$ 5. The pH was adjusted to 7.0 with 25mM NMDG.

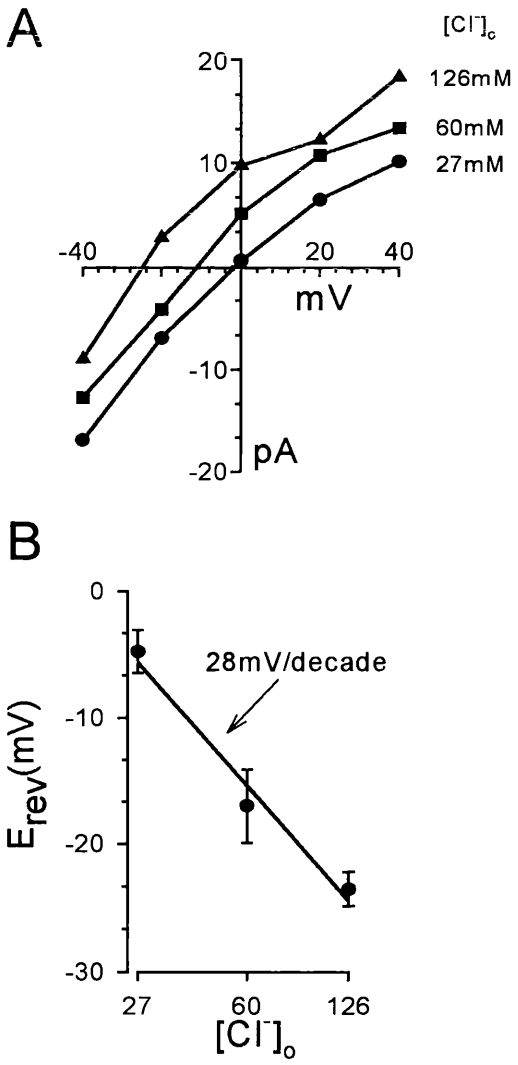
A
[Cl⁻]o
126mM
60mM
27mM
20
10
-10
-20
-40
20
40
mV
pA
B
0
-10
-20
-30
28mV/decade
Erev(mV)
27
60
126
[Cl⁻]o

Figure 5.14 - Effect of ClO_4^- on the glutamate-evoked current seen with potassium absent intra- and extracellularly, and with sodium and glutamate present inside the cell

Specimen I-V data for the glutamate-evoked current in two different Müller cells. The solid circles are the currents seen in a cell with chloride as the main intra- and extracellular anion. The solid squares are the currents in a different cell with 50mM intra- and extracellular ClO_4^-. The currents are normalized to cell capacitance to minimize the differences in current magnitude due to cell size (Barbour *et al.*, 1991). The data points represent the mean±SEM of data from 5 cells.

Solutions - The external solutions contained (mM) NaCl 75, choline-Cl 30, $CaCl_2$ 3, $MgCl_2$ 0.5, glucose 15, HEPES 5, $BaCl_2$ 6. The pH was adjusted to 7.3 with NaOH. For the ClO_4^- solution, 50mM NaCl was replaced by $NaClO_4$.

The internal solution contained (mM) Na-glutamate 10, choline-Cl 85, NaCl 5, HEPES 5, $MgCl_2$ 7, Na_2ATP 5, $CaCl_2$ 1, $(NMDG)_2EGTA$ 5. The pH was adjusted to 7.0 with NMDG. For 50mM internal ClO_4^- solution, 50mM choline-Cl was replaced by choline-ClO_4.

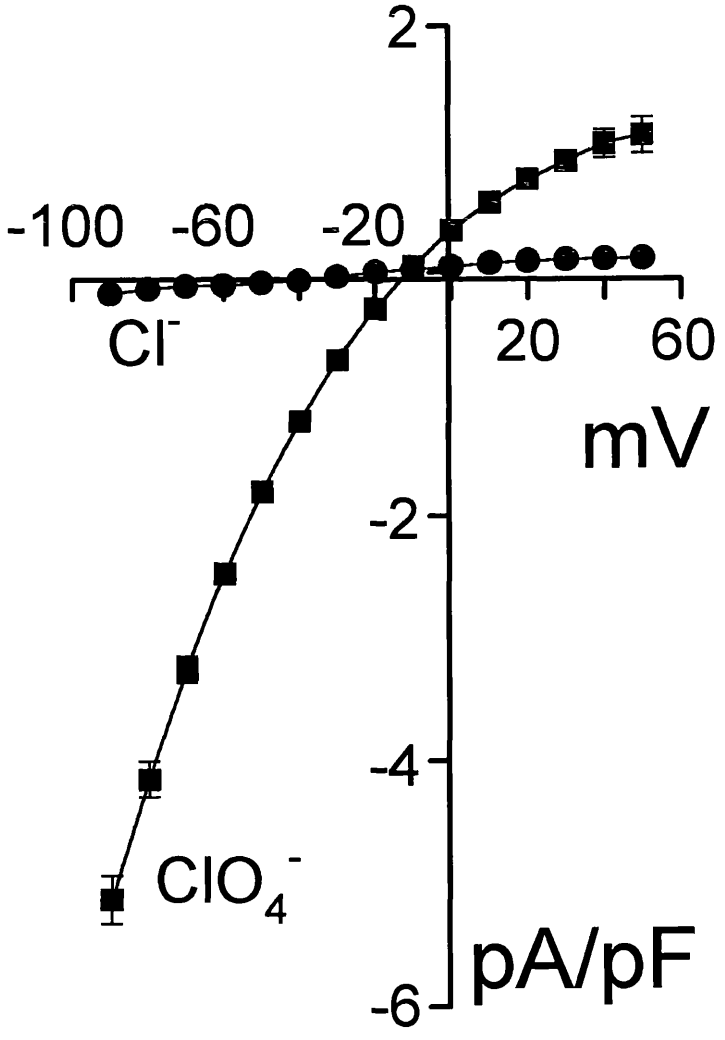
2
-100
-60
-20
20
60
Cl-
mV
-2
-4
ClO4-
pA/pF
-6

The current was increased by a factor of 30.1±6.5 and 9.7±1.8 (mean±SEM of data from 4 cells) at -80 and +40mV respectively. A similar, though smaller increase in outward current was seen when NO_3^- replaced Cl^- outside the cell. Thus, the anion selectivity of the conductance activated with glutamate transport inhibited is similar to that for the anion conductance activated during forward or reversed glutamate transport (figures 5.3 and 5.7). This result suggests that the anion conductance can be activated, at least in part, independently of whether the carrier molecule is transporting glutamate across the membrane. The fact that a large anion current can be seen at positive potentials (figure 5.4) where glutamate transport is slow, reinforces this point.

Activation of the anion conductance in the absence of glutamate transport was found to have a dependence on external sodium and glutamate similar to that for glutamate transport, providing further evidence that the two processes are activated by similar mechanisms. The affinity for glutamate of glutamate transport was assessed as in chapter 3, by measuring the K_M of a Michaelis-Menten curve fitted to the dependence on glutamate concentration of the current associated with glutamate uptake. This was measured at -40mV with potassium inside and chloride as the anion present (figure 5.15, dashed line), assuming that with chloride present the contribution of anion flux to the current is negligible. The affinity for glutamate of activation of the anion conductance was assessed by measuring the K_M of a Michaelis-Menten curve fitted to the dependence on glutamate concentration of the outward current observed at +20mV in the presence of external NO_3^-, with glutamate transport inhibited by the removal of internal and external potassium (figure 5.15, solid line). The K_M for glutamate activating transport was 9.1±0.7μM (mean±SEM of data from 5 cells), while the K_M for glutamate activating the anion conductance was 15.1±0.3μM (mean±SEM of data from 5 cells). The difference ($p<0.001$, 2-tailed t-test) between these two affinities could be due to the different membrane voltages used in the two experiments, the

Figure 5.15 - Glutamate-dependence of uptake measured with potassium present, and of the anion conductance measured in the absence of potassium

The solid circles represent the inward forward glutamate uptake current (with potassium present) recorded in Müller cells voltage-clamped at -40mV, plotted as a function of external glutamate concentration. The data points are normalized to the current evoked by 300μM glutamate and represent the mean±SEM of data from 5 cells. The data are best-fitted with a Michaelis-Menten equation (dotted line), with a K_M of 9.1±0.7μM. The solid triangles represent the outward glutamate-evoked anion current (produced by NO_3^- influx) recorded in Müller cells voltage-clamped at +20mV, with glutamate transport inhibited by the removal of intra- and extracellular potassium and in the presence of 100mM extracellular NO_3^-. The data points are normalized to the current evoked by 300μM glutamate and represent the mean±SEM of data from 5 cells. The data are best-fitted with a Michaelis-Menten equation (solid line), with a K_M of 15.1±0.3μM.

Solutions - For studying the forward uptake current the external solution contained (mM) NaCl 107.5, $CaCl_2$ 3, $MgCl_2$ 0.5, $BaCl_2$ 6, HEPES 5, glucose 15 and ouabain 0.1. The pH was adjusted to 7.3 with NMDG. For studying the anion channel current 100mM NaCl was replaced by $NaNO_3$.

For studying the forward uptake current the internal solution contained (mM) KCl 95, NaCl 5, $(NMDG)_2EGTA$ 5, Na_2ATP 5, HEPES 5, $CaCl_2$ 1 and $MgCl_2$ 7. The pH was adjusted to 7.0 with NMDG. For studying the anion channel current the 95mM KCl was replaced by 85mM choline-chloride and 10mM Na-glutamate.

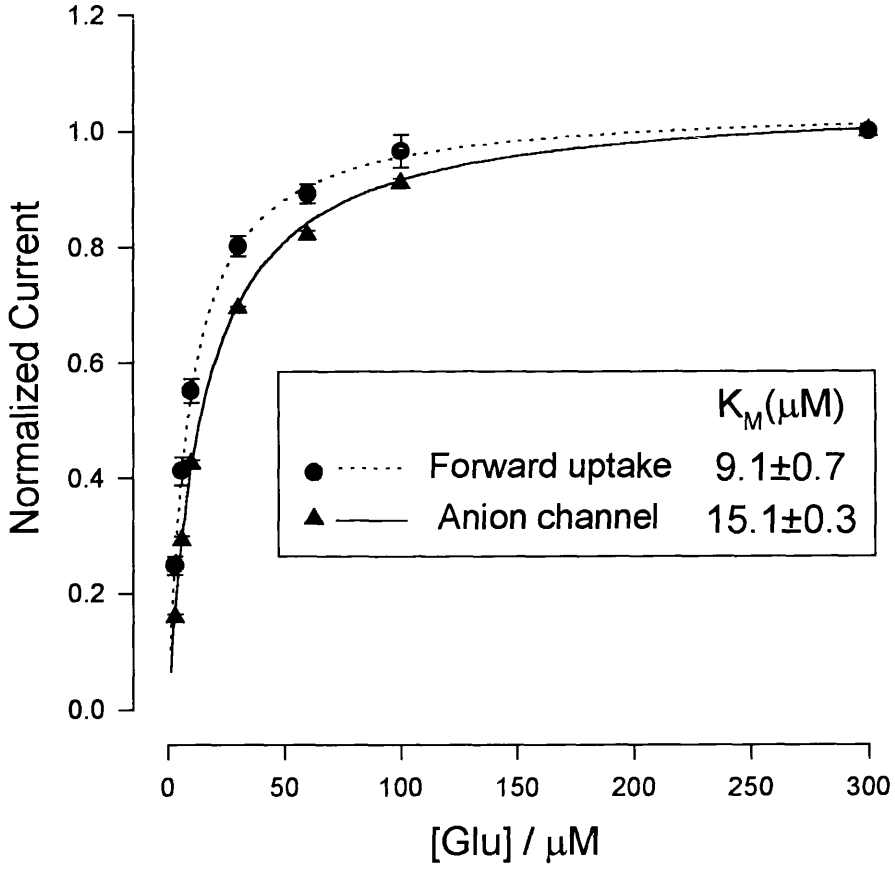
1.2
1.0
0.8
0.6
0.4
0.2
0.0
Normalized Current
0
50
100
150
200
250
300
[Glu] / μM
K_M(μM)
Forward uptake 9.1±0.7
Anion channel 15.1±0.3

fact that the experiments were performed on different cells, or some mechanistic difference in the details of how glutamate binding leads to activation of transport and of the anion channel.

The dependence of the anion channel current on the external sodium concentration (figure 5.16) demonstrated that at low external sodium concentrations the magnitude of the glutamate-evoked current (with external and internal potassium absent) increased in proportion to the 2.4^{th} power of the external sodium concentration. This implies that, as for glutamate uptake (Barbour *et* al., 1991 and see figure 3.7), activation of the anion channel requires the binding of two sodium ions to the external carrier surface.

5.9 pH-dependence of the anion conductance activated in the absence of potassium

The reversed glutamate uptake current, and the release of glutamate stimulated by raising the external potassium concentration in the presence of internal sodium and glutamate, are greatly reduced when the external pH is acidified by around 1 pH unit (see figures 4.1 and 4.12). However, in the absence of glutamate transport, the glutamate-evoked anion current did not show such a pH-dependence. With sodium and glutamate present in the intracellular solution, and in the absence of internal and external potassium, the outward glutamate-evoked current seen at a depolarized membrane potential, which is produced by the an anion conductance (see figure 5.11), was not greatly affected when the external pH was made more acid (figures 5.17 and 5.18). This result again suggests that the anion conductance function of the transport molecule can be activated independently of the transport of glutamate. A kinetic model consistent with these observations is presented in section 5.11.

Figure 5.16 - Sodium-dependence of the anion conductance measured with glutamate transport inhibited by removal of potassium and with sodium and glutamate inside the cell

The graph shows the currents evoked by 200μM glutamate in the presence of 110mM external NO_3^-, in Müller cells held at -40mV, as a function of external sodium concentration. The currents are normalized to the current observed with 110mM external sodium. The points represent the mean±SEM of the data from 5 cells, and are fitted with a Hill equation (inset) with a Hill coefficient of 2.4 and EC_{50} for sodium (K) of 22mM.

Solutions - The external solution contained (mM) $NaNO_3$ 110, $CaCl_2$ 3, $MgCl_2$ 0.5, $BaCl_2$ 6, HEPES 5, glucose 15 and ouabain 0.1. The pH was adjusted to 7.3 with NMDG. For reduced concentrations of sodium, $NaNO_3$ was replaced by choline-NO_3.

The internal solution contained (mM) choline-chloride 85, $(NMDG)_2EGTA$ 5, NaCl 5, Na_2ATP 5, HEPES 5, $CaCl_2$ 1, $MgCl_2$ 7 and Na-glu 10. The pH was adjusted to 7.0 with NMDG.

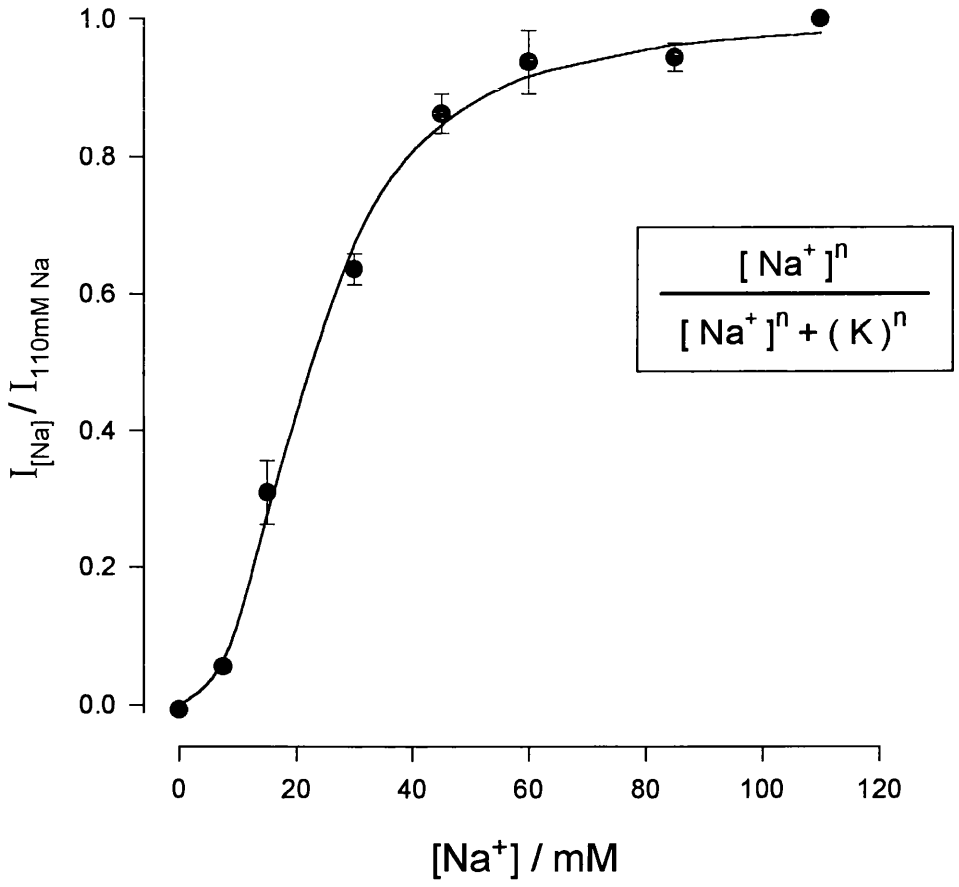
1.0
0.8
0.6
0.4
0.2
0.0
$I_{[Na]} / I_{110mM\ Na}$
0
20
40
60
80
100
120
$[Na^+]$ / mM
$\frac{[Na^+]^n}{[Na^+]^n + (K)^n}$

Figure 5.17 - Effect of an acid external pH on the glutamate-evoked anion current in the absence of potassium with sodium and glutamate inside the cell

Currents evoked by 1mM external glutamate in Müller cells voltage-clamped at +20 and -40mV, in external solutions of pH 7.3 and 6.1.

Solutions - The external solutions contained (mM) NaCl 75, choline-Cl 30, $CaCl_2$ 3, $MgCl_2$ 0.5, glucose 15, HEPES 5 and $BaCl_2$ 6. The pH was adjusted to 7.3 with NMDG. For external pH 6.1 the solution was buffered with MES in place of HEPES.

The internal solution contained (mM) Na-glutamate 10, choline-Cl 40, HEPES 71, $MgCl_2$ 7, Na_2ATP 5, $CaCl_2$ 1 and $(NMDG)_2EGTA$ 5. The pH was adjusted to 7.0 with 25mM NMDG.

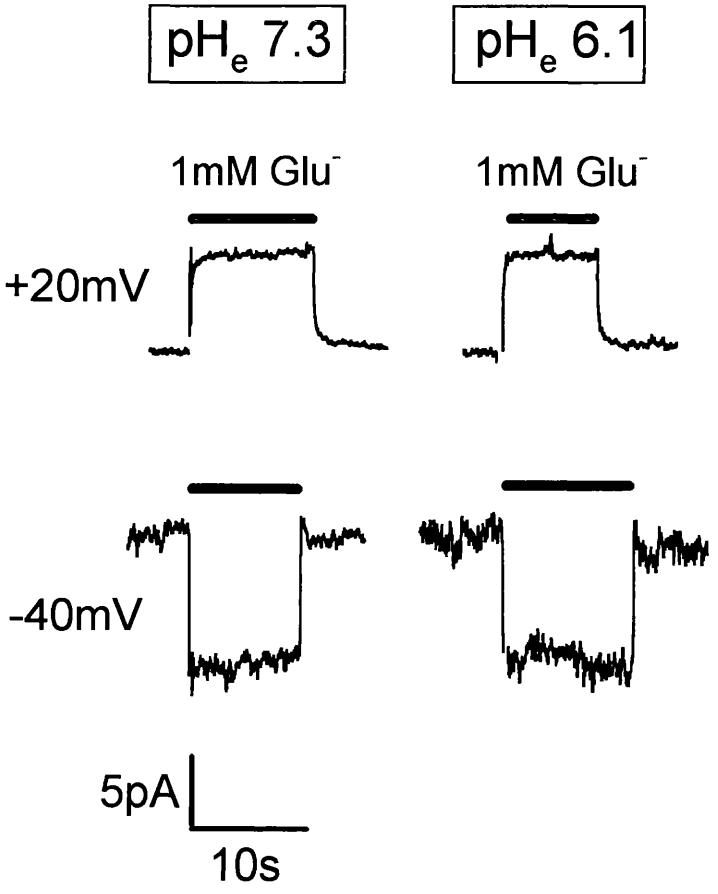
pH$_e$ 7.3
pH$_e$ 6.1
1mM Glu$^-$
1mM Glu$^-$
+20mV
-40mV
5pA
10s

Figure 5.18 - External pH-dependence of the glutamate-evoked current

Current evoked by 1mM external glutamate in Müller cells voltage-clamped at -40mV (as in figure 5.17), plotted as a function of external pH. The data points (open squares) represent the mean±SEM of the current in 5 cells, normalized to the current at pH 7.3. The data are best fit with a straight line. For comparison, the effect of external pH on the reversed glutamate uptake current is shown (solid circles), from figure 4.1.

Solutions - For the anion conductance experiments the external solutions contained (mM) NaCl 75, choline-Cl 30, $CaCl_2$ 3, $MgCl_2$ 0.5, glucose 15, $BaCl_2$ 6 and buffer 5. The pH was adjusted to 7.3 with NMDG. For external pH >6.9, the buffer HEPES was used. For external pH < 6.9 the buffer MES was used.

The internal solution contained (mM) Na-glutamate 10, choline-Cl 40, HEPES 71, $MgCl_2$ 7, Na_2ATP 5, $CaCl_2$ 1 and $(NMDG)_2EGTA$ 5. The pH was adjusted to 7.0 with 25mM NMDG.

For the reversed uptake experiments the solutions were as in figure 4.1.

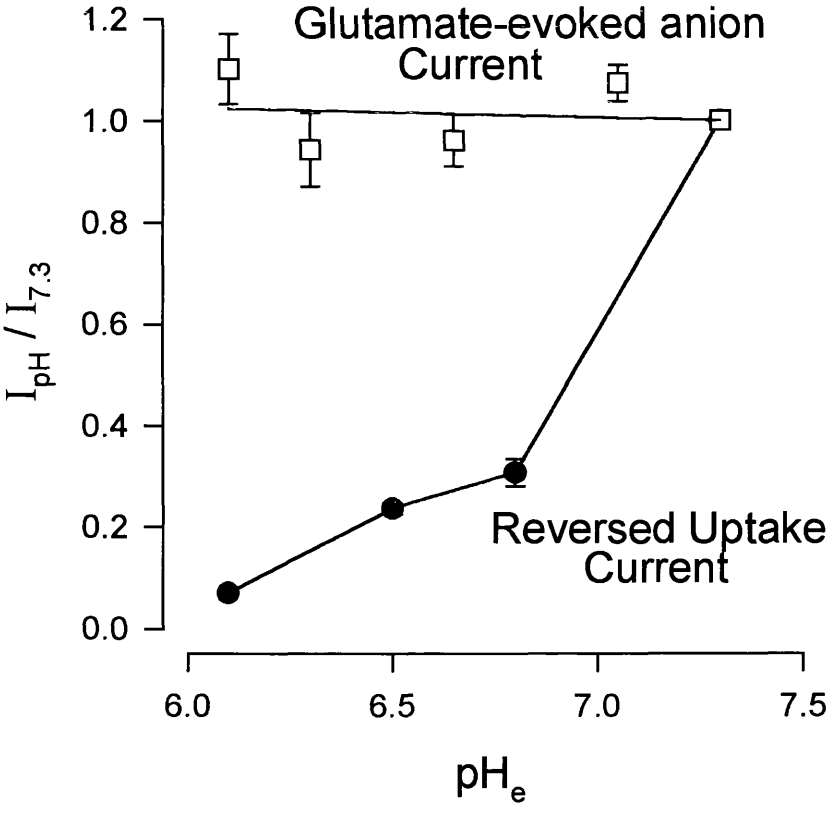
Glutamate-evoked anion Current
Reversed Uptake Current
1.2
1.0
0.8
0.6
0.4
0.2
0.0
$I_{pH} / I_{7.3}$
6.0
6.5
7.0
7.5
pH_e

5.10 Fluorescence measurement of pH to test if the movement of pH-changing ions is coupled to the movement of glutamate

During glutamate uptake the inside of the Müller cell goes acid, and this has been attributed to hydroxide ions being transported out of the cell by the glutamate transporter (Bouvier *et al.*, 1992). However, the existence of an anion channel in the structure of the glutamate uptake carrier opens up the possibility that the pH change observed during glutamate uptake could be a result of hydroxide ions permeating the anion conductance, rather than being a substrate for transport. To investigate this possibility, the internal pH of the Müller cell was monitored fluorescently using the pH-sensitive dye BCECF (see section 2.9). Müller cells were voltage-clamped at different membrane potentials to reverse the polarity of the electrochemical gradient for hydroxide. With an intracellular pH of 7.0 and an extracellular pH of 7.7, the reversal potential for hydroxide is -41mV. At potentials more negative than -41mV, if hydroxide was moving passively through the anion conductance external glutamate would therefore evoke an intracellular acidification, while at potentials more positive than -41mV glutamate would evoke an intracellular alkalinization. If hydroxide movement is coupled to glutamate movement as in figure 1.1, however, then an internal acidification would be expected at all membrane potentials. Experimentally, the latter was found to be the case (figure 5.19). The ratio of the rate of acidification to the glutamate-evoked current was similar at 0mV and -60mV (0.27±.04 and 0.23±0.05 pH units/sec/nA (mean±SEM of data from 6 cells) respectively). The slightly (though not significantly, $p=0.55$, 2-tailed t-test) smaller value at -60mV might be expected, because the inward glutamate-evoked current, but not the pH change, is increased at more negative potentials by chloride efflux through the anion conductance. This result provides evidence that the movement of a pH-changing ion is coupled to glutamate transport, rather than occurring through the anion conductance.

Figure 5.19 - Internal pH changes produced by the glutamate transporter

A Currents evoked by 200μM glutamate in a Müller cell voltage-clamped at -60 and 0mV, i.e. potentials below and above the reversal potential for OH^- (or H^+).

B Glutamate-evoked intracellular pH changes recorded simultaneously with the currents A. The pH was monitored fluorescently using the pH-sensitive dye BCECF.

Similar results were obtained in 4 cells.

Solutions - The external solution contained (mM) NaCl 105, KCl 2.5, $CaCl_2$ 3, $MgCl_2$ 0.5, glucose 15, HEPES 5 and $BaCl_2$ 6. The pH was adjusted to 7.7 with NaOH.

The internal solution contained (mM) KCl 95, NaCl 5, HEPES 0.5, $MgCl_2$ 7, Na_2ATP 5, $CaCl_2$ 1, K_2EGTA 5 and BCECF 0.1. The pH was adjusted to 7.0 with KOH.

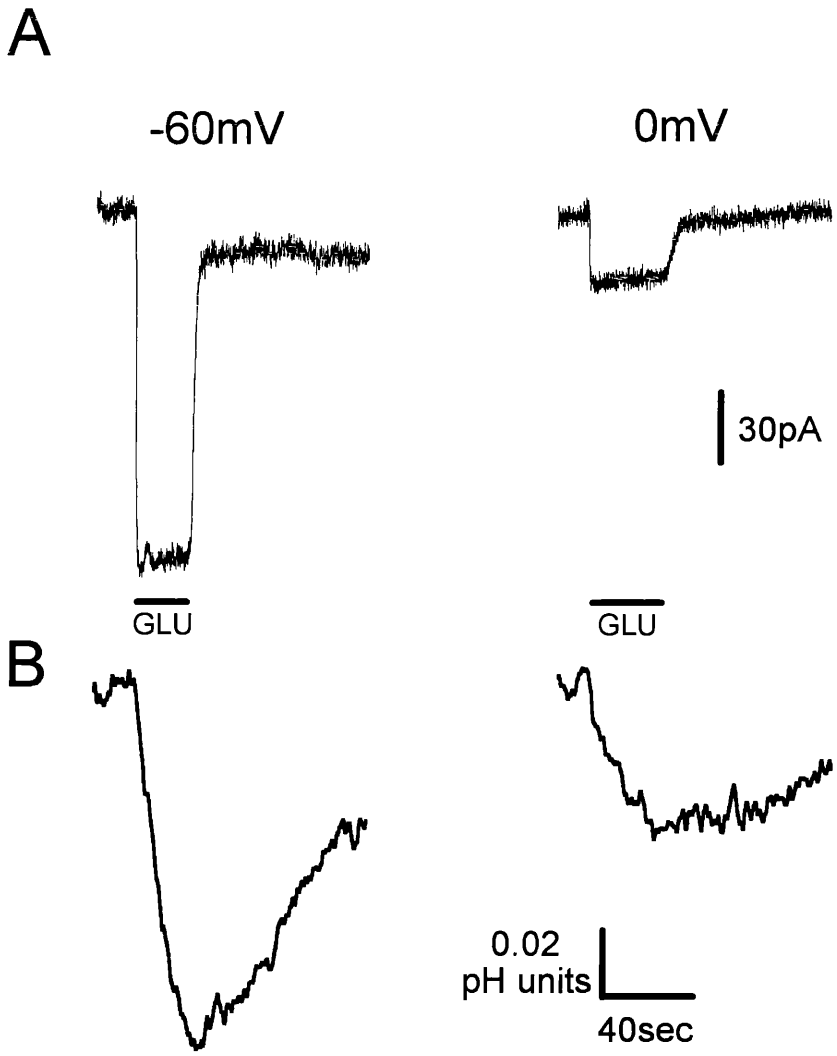
A
-60mV
0mV
30pA
GLU
GLU
B
0.02
pH units
40sec

5.11 Discussion

5.11.1 The salamander Müller cell glutamate transporter has an anion conductance

The data presented here show that the glutamate transporter in salamander retinal glial cells activates an anion conductance (see also Eliasof and Jahr, 1996). Removing external chloride increases the glutamate-evoked current (figure 5.1 and 5.2), consistent with the results of Wadiche *et al.* (1995) on cloned mammalian glutamate transporters. With chloride as the main ion inside and outside the cell, the glutamate-evoked current remains inward at positive potentials, presumably because it is dominated by the current associated with glutamate transport rather that that generated by the anion conductance. Anions with a higher permeability than chloride, such as NO_3^- or ClO_4^-, enhance the contribution of the anion conductance, resulting in an outward glutamate-evoked current at depolarized membrane potentials (figure 5.3 and 5.4).

Unlike in figure 5.1, Barbour *et al.* (1991) found an insignificant difference in the glutamate-evoked current on removal of external chloride. The reason for this is unclear but it may be due to the use of a non-saturating dose of glutamate (30μM), or the presence of internal acetate in the experiments of Barbour *et al.* (1991).

5.11.2 Permeability sequence of the anion conductance

The data presented here (figures 5.3 and 5.4) and by Bouvier *et al.* (1992) suggest a permeability sequence $SCN^- > ClO_4^- > NO_3^- > Cl^- \approx Br^- \approx I^-$ for the anion conductance. This is similar to the theoretical permeability sequence of an anion channel (sequence 1 of Wright and Diamond, 1977). For this theoretical sequence, however, ClO_4^- is more permeant than SCN^-. The difference in the

ranking of ClO_4^- could arise as a result of ClO_4^- slowing the cycling of the glutamate uptake carrier (see section 5.7), and thus inhibiting the opening of the anion channel. It is uncertain why ClO_4^- slows the operation of the transporter.

5.11.3 A kinetic model for activation of the anion channel

The glutamate-evoked anion conductance is activated by the simultaneous presence of external sodium and glutamate and internal potassium (figure 5.5) when the carrier operates in the forward direction. However, it is also activated by the simultaneous presence of internal sodium and glutamate and extracellular potassium when the carrier transports glutamate out of the cell (fig 5.7). These results suggest that activation of the anion conductance occurs when a particular state of the carrier cycle is reached, independent of whether that state is reached by the carrier cycling in the forward or reversed direction. An example of such a scheme is shown in figure 5.20. This scheme is consistent with the observation (figure 5.16) that two sodium ions have to bind to activate the anion conductance.

Which particular state of the carrier cycle activates the anion conductance is constrained by the observation that the anion conductance can be activated when glutamate transport is inhibited by removal of intracellular and extracellular potassium (provided that glutamate and sodium are present on both sides of the membrane: section 5.8). This implies that the anion conductance is activated by a state in the carrier cycle which does not have potassium bound. If, as previously suggested (Kanner and Bendahan, 1982), and as shown in figure 5.20, the potassium translocating part of the carrier cycle is distinct from the sodium and glutamate translocating part, then activation of the anion conductance must presumably occur from one of the states of the glutamate/sodium transporting limb. The need for intracellular sodium and glutamate to be present, for anion conductance activation to be produced by external glutamate in the absence of

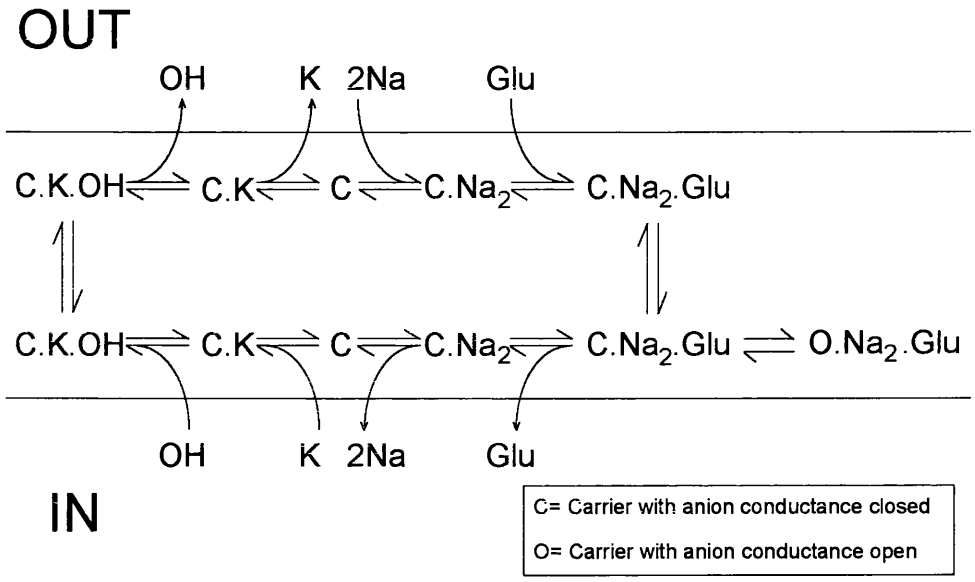

Figure 5.20 - Proposed kinetic scheme for the glutamate uptake carrier and anion conductance

C represents the carrier in conformations for which the anion conductance is not activated (closed). In these conformations the carrier binds extracellular glutamate and two sodium ions, transports them to the inner face of the membrane, then binds a potassium and a hydroxide ion at the inner membrane surface and transports them to the outside of the cell, shifting one net positive charge into the cell during the carrier cycle. O represents the carrier in a conformation of the carrier which the anion conductance is activated (open). I propose that the open state can be accessed from the closed conformation that has the sodium and glutamate ions bound at the inner face of the membrane. The data are also consistent with the open state being accessed from the closed state with sodium and glutamate bound at the outer membrane surface (or from both $C.Na_2.Glu$ conformations).

intra- and extracellular potassium, could be explained by the carrier spending more time in the state with glutamate and two sodium ions bound which is suggested in figure 5.20 to activate the anion conductance. Similarly external glutamate is needed to prevent the carrier accumulating in the state at the external surface with sodium but no glutamate bound.

Figure 5.20 proposes that the hydroxide transporting part of the carrier cycle is associated with the potassium transporting rather that the sodium/glutamate transporting limb of the molecule. This would explain the fact that an acid extracellular pH does not affect the activation of the anion conductance seen in the absence of intra- and extracellular potassium, although it does block the reversed uptake of glutamate (figures 5.17 and 5.18).

If the anion conductance only opens once per carrier cycle (during forward uptake) its open probability could be larger at negative membrane potentials when the carrier cycles more rapidly. This might explain why the change in glutamate-evoked current produced by a reduction of external chloride concentration is larger at more negative potentials (figure 5.2) rather than at positive potentials where the driving force for chloride entry is greatest. Similarly it may explain why the outward shift of glutamate-evoked current produced by external ClO_4^- or NO_3^- (figure 5.4) is only slightly larger at positive potentials.

5.11.4 Re-interpretation of the effects of intracellular ClO_4^- and NO_3^-

Bouvier *et al.* (1992) found that intracellular ClO_4^- and NO_3^- increased the inward current evoked by external glutamate, that ClO_4^- came out of the cell when glutamate was applied, and that the presence of these ions intracellularly reduced the ratio of the pH change generated by the carrier to the current that it generated. Those results were interpreted as showing that the glutamate-evoked pH changes were generated by the transport of hydroxide ions out of the cell, and that ClO_4^-

and NO_3^- could compete for transport at the hydroxide site. It is now clear that the effects of ClO_4^- and NO_3^- were due to these ions leaving the cell (at a much higher rate than Cl^-) through the anion conductance associated with the uptake carrier, generating an extra inward current. This invalidates the earlier conclusion that the pH changes generated by the carrier are due to the transport of hydroxide out of the cell rather than the (thermodynamically equivalent) transport of protons into the cell. This re-opens the possibility that protons are co-transported with glutamate.

Figure 5.19 shows that, irrespective of whether hydroxide ions or protons are transported, movement of the pH-changing ion is coupled to glutamate transport. Thus, glutamate uptake does derive energy from the transmembrane pH gradient, consistent with the observation that, in the kidney, a pH gradient alone can power uptake (Nelson *et al.*, 1983).

5.11.5 Therapeutic possibilities offered by the existence of the anion conductance

The ability of the anion conductance to be activated in the absence of glutamate transport suggests some degree of independence between these two functions of the molecule, and hence they may be modulated separately by pharmacological agents. This suggest a possible strategy for developing drugs to treat conditions in which excessive glutamate is released, such as epilepsy. If, for glutamate transporters in presynaptic terminals, the anion conductance activation could be greatly enhanced, then whenever glutamate is released, activation of the anion conductance during re-uptake would tend to clamp the presynaptic terminal at a negative potential. This would have the effect of reducing further exocytotic release (by making it harder for action potentials to invade the synaptic terminal and activate calcium channels) and potentiating the (voltage-dependent) re-uptake, Interestingly, in the retina at least, the glutamate transporter which is expressed in

the cone synaptic terminals expresses a particularly large anion conductance (Sarantis *et al.*, 1988; Eliasof and Werblin, 1993), like the human EAAT4 carrier (Fairman *et al.*, 1995), suggesting that evolution might already have arrived at this strategy for controlling glutamate release. Recently it has been shown that preventing the expression of neuronal EAAC1 carriers leads to epileptic behaviour of neurons (while prevention of expression of glial glutamate transporters leads to a rise in extracellular glutamate concentration but no epilepsy) (Rothstein *et al.*, 1996). It is not yet known if the anti-epileptic properties of the EAAC1 carriers derive solely from their ability to take up glutamate, or whether their contribution to the anion conductance of the neurons is also involved.

During brain ischaemia the glutamate concentration in glial cells rises (Storm-Mathisen *et al.*, 1992). Since activation of the anion conductance in glial uptake carriers can be potentiated by intracellular glutamate (figure 5.12), it is possible that the uptake carrier might contribute to the glial cell chloride conductance which, by allowing Cl^- influx, could facilitate glial swelling in ischaemia (Walz *et al.*, 1993).

Chapter 6

Effects of zinc on glutamate uptake and associated anion channel

6.1 Introduction

There is strong evidence that endogenous zinc may play a role as either a neurotransmitter or neuromodulator in the central nervous system, although its physiological function at present remains unclear. Synaptic vesicles containing zinc have been shown to be present in synaptic boutons of the rat forebrain (olfactory bulb, septum, caudate-putamen, amygdaloid complex, neocortex and entorhinal cortex) and hippocampus (subiculum, stratum radiatum, CA1, CA3, mossy fibres and dentate gyrus) (Perez-Clausell and Danscher, 1985). In the salamander retina, zinc containing vesicles are observed in the photoreceptors (Wu *et al.*, 1993). Electrical activity stimulates release of zinc from mossy fibre terminals *in vitro,* in a calcium-dependent manner (Assaf and Chung, 1984; Howell *et al.*, 1984). Spontaneous zinc release has also observed from the mossy fibre terminals *in vivo* (Charton *et al.*, 1985). These data suggest the presence of a vesicular release mechanism. The extracellular concentration of zinc has been estimated to reach a peak level of almost 300μM during convulsive electrical activity (Assaf and Chung, 1984).

Extracellular zinc may modulate synaptic transmission either pre- or postsynaptically. It may reduce transmitter release by its inhibitory effect (IC_{50} < 69μM) on presynaptic voltage-activated calcium channels (Sim and Cherubini, 1990; Busselberg *et al.*, 1992). Postsynaptic NMDA receptors are inhibited by zinc with an IC_{50} value of 3-100μM, and AMPA receptors are potentiated with an EC_{50} value of 13-30μM. Some studies indicate that $GABA_A$ receptors are inhibited by zinc (IC_{50} values from 0.6-320μM), while others report a potentiation

or that zinc has no effect. These differences could arise from heterogeneity in the population of $GABA_A$ receptors, such as would be caused by different sub-unit composition. The effects of zinc on GABA and glutamate receptors have recently been reviewed by Smart *et al.*, (1994).

There are thought to be two distinct systems to facilitate the uptake of zinc into cells, a low-affinity and a high-affinity system with K_M values of 402μM and 12μM respectively (Howell *et al.*, 1984). A high-affinity zinc transporter protein, Zrtlp, has been cloned in yeast. It has eight potential transmembrane domains and a K_M for zinc of 0.6μM (Zhao and Eide, 1996).

Zinc may play a role during pathological situations. Its reduction of inhibition mediated by GABA receptors has been suggested to cause epilepsy (Buhl *et al.*, 1996). Furthermore, the release of presynaptic zinc observed during brain ischaemia, and its subsequent entry into postsynaptic cells has been suggested to trigger the death of the postsynaptic cells (Koh *et al.*, 1996).

High doses of extracellular zinc have previously been shown to inhibit glutamate uptake (Gabrielsson *et al.*, 1986). However the radiotracing methods employed by Gabrielsson *et al.* (1986) do not allow for control of the membrane voltage, and zinc could have had an indirect effect on uptake mediated by an alteration of transmembrane ion gradients. Indeed, zinc has been suggested to inhibit the Na^+/K^+-ATPase (Donaldson *et al.*, 1971; Mustafa *et al.*, 1971; Hexum, 1974; Watson and Beamish, 1981). To examine in more detail the effects of zinc on forward and reversed uptake, glutamate uptake was studied in whole-cell voltage-clamped Müller cells while zinc was applied.

6.2 Calculation of free zinc concentration

Zinc binds to glutamate, and this interaction must be considered when adding zinc to glutamate-containing solutions. The free concentrations of zinc and

glutamate can be calculated by considering the following reactions:

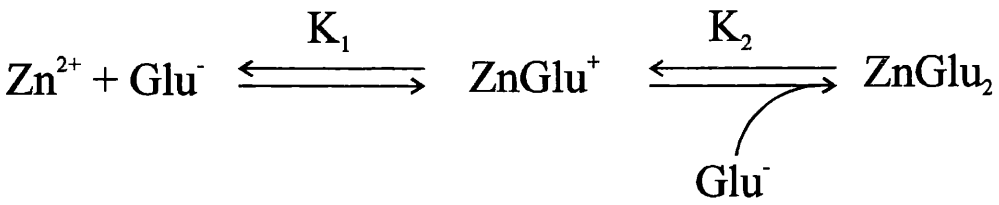

Figure 6.1 Binding of zinc and glutamate

The total concentrations of zinc, $[Z]_{total}$, and glutamate, $[G]_{total}$, present are:

$$[Z]_{total} = [Zn^{2+}] + [ZnGlu^+] + [ZnGlu_2] \quad [6.1]$$

$$[G]_{total} = [Glu^-] + [ZnGlu^+] + 2[ZnGlu_2] \quad [6.2]$$

Defining the stability constants K_1 and K_2 as:

$$K_1 = \frac{[ZnGlu^+]}{[Zn^{2+}] \cdot [Glu^-]} \quad [6.3]$$

$$K_2 = \frac{[ZnGlu_2]}{[Glu^-] \cdot [ZnGlu^+]} \quad [6.4]$$

and the cumulative constant as:

$$\beta = K_1 \cdot K_2 \quad [6.5]$$

one gets

$$[Z]_{total} = [Zn^{2+}] \cdot \left(1 + K_1[Glu^-] + \beta[Glu^-]^2\right) \quad [6.6]$$

and

$$[G]_{total} = [Glu^-] + K_1[Zn^{2+}][Glu^-] + 2\beta[Zn^{2+}][Glu^-]^2 \quad [6.7]$$

These equations were used to calculate the total amounts of zinc and glutamate needed to give the desired concentrations of free ions in the solutions used. The values of K_1 and β (Dawson *et al.*, 1986), corrected for the pH of the solution, were $10^{3.13}M^{-1}$ and $10^{4.76}M^{-2}$ respectively. For example, if the free glutamate concentration is 3 or 200 μM, the free zinc concentration is 0.4% or 21%, respectively, less than the total zinc concentration. For 8 or 80μM free zinc and 200μM free glutamate, the free glutamate concentration is 1% or 10%, respectively, less than the total glutamate concentration,

6.3 Zinc inhibits forward glutamate uptake

The effects of zinc on forward glutamate uptake were studied in whole-cell voltage-clamped isolated Müller cells. Glutamate uptake was stimulated by the application of external glutamate, and the effects of including zinc in the external solution examined.

Externally applied zinc inhibited the glutamate-evoked current in a reversible manner (figure 6.2A). Higher concentrations of zinc produced more inhibition, and the percentage reduction is shown in figure 6.2B (solid symbols) as a function of the concentration of free zinc, calculated from equation 6.6. The data were fitted by a Michaelis-Menten relation with a K_M of 140±38nM and a maximum fractional reduction, R_{max}, of 0.33±0.03 (mean±SEM of data from 4 cells). Fitting the curve to the total zinc concentration, rather than the free zinc concentration, gave a K_M of 179μM.

To eliminate the possibility that zinc affects the glutamate-evoked current by inhibiting the anion conductance associated with the glutamate uptake carrier, the experiment was repeated using chloride-free external and internal solutions (figure 6.2B - open symbols). At free zinc concentrations of <10μM there was no significant difference in the ability of zinc to inhibit the glutamate-evoked current in the presence or absence of chloride. This result indicates that zinc has an inhibitory effect on the glutamate uptake carrier, which is independent of any effect on the anion channel component of the current. The somewhat greater inhibition seen with 100μM zinc using chloride-free solutions could just reflect variability in the effects of zinc on different batches of cells.

The inhibition of the glutamate uptake carrier by such low concentrations of free zinc could mean that trace amounts of zinc in the control solutions tonically inhibit uptake. To test this possibility, glutamate-evoked currents in the control solution were compared to currents evoked in a solution containing 1mM EDTA, a strong zinc-chelating agent. 1mM EDTA would reduce a free zinc concentration

Figure 6.2 - Inhibition of forward uptake by external zinc

A Specimen data from one cell showing the current evoked by 200μM glutamate (black bars) at -60mV in control solution and in solutions containing 0.1μM and 100μM free zinc, followed by another response in control solution.

B Dose-response curve for the effects of external zinc on the forward uptake current, as shown in A. The data points represent the mean±SEM of the data from 4 cells. They are fitted with a Michaelis-Menten curve (see inset). The filled symbols were obtained with normal (chloride-containing solutions). The open symbols were obtained with chloride-free solutions to remove any contribution of the anion channel current to the glutamate-evoked current.

Solutions - For the filled symbols the external solution contained (mM) NaCl 75, choline-Cl 30, $CaCl_2$ 3, $MgCl_2$ 0.5, $BaCl_2$ 6, HEPES 5 and glucose 15. The pH was adjusted to 7.3 using NMDG. For the open symbols, recorded in the absence of chloride, the external solution contained (mM) Na-gluconate 105, $Ca(gluconate)_2$ 3, $Mg(gluconate)_2$ 0.5, $Ba(OH)_2$ 6, gluconic acid 12, HEPES 5 and glucose 15. The pH was adjusted to 7.3 using NMDG.

For the filled symbols the internal solution contained (mM) KCl 95, $(NMDG)_2EGTA$ 5, NaCl 5, Na_2ATP 5, $CaCl_2$ 1, $MgCl_2$ 7 and HEPES 5. The pH was adjusted to 7.0 using NMDG. For the open symbols, recorded in the absence of chloride, the internal solution contained (mM) K-gluconate 104, Na-gluconate 5, $Mg(gluconate)_2$ 2 and HEPES 5. The pH was adjusted to 7.0 using NMDG.

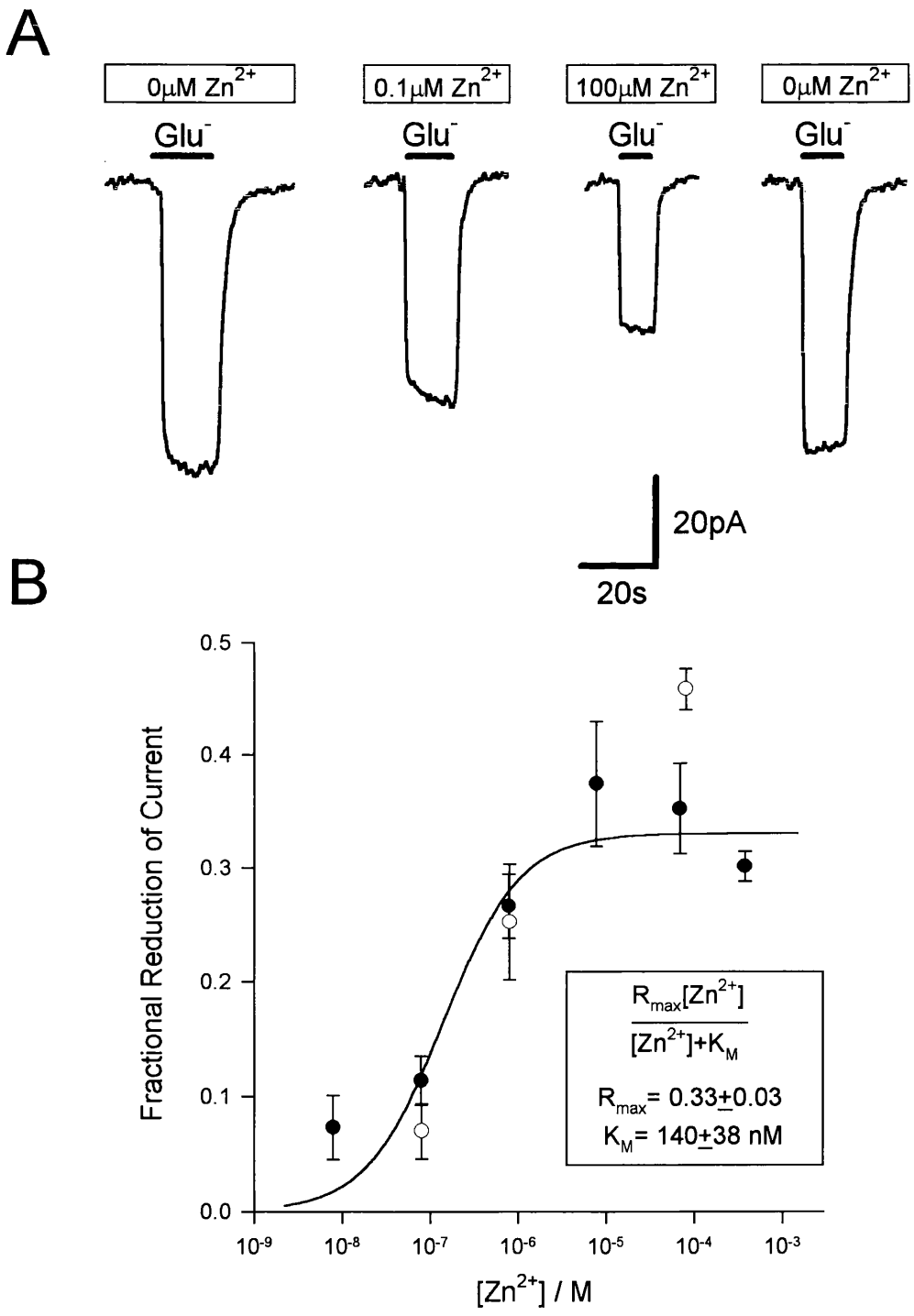
A
0μM Zn2+
0.1μM Zn2+
100μM Zn2+
0μM Zn2+
Glu-
Glu-
Glu-
Glu-
20pA
20s
B
Fractional Reduction of Current
0.5
0.4
0.3
0.2
0.1
0.0
10-9
10-8
10-7
10-6
10-5
10-4
10-3
[Zn2+] / M
Rmax[Zn2+]
[Zn2+]+KM
Rmax= 0.33±0.03
KM= 140±38 nM

of 1μM to $6.5x10^{-17}$M (calculated using the program MAXC). 1mM EDTA will also reduce the extracellular free calcium concentration from 3mM to 2mM, so the calcium concentration in the control solution was decreased to 2mM. Currents evoked by 200μM glutamate in EDTA-containing solution were reduced by 1.5±3.2% (mean±SEM of data from 3 cells) compared to the currents evoked in control solution, indicating that trace levels of zinc in the control solution were too low to significantly affect glutamate uptake.

6.4 Zinc inhibits reversed glutamate uptake

Reversed glutamate uptake was stimulated in isolated Müller cells by raising the external potassium concentration in the presence of internal sodium and glutamate (Szatkowski *et al.*, 1990, and see chapter 4). Externally applied zinc inhibited this reversed glutamate uptake current (figure 6.3). The data were fitted by a Michaelis-Menten relation with a K_M of 1.0±0.4μM (i.e. 7-fold higher than for the inhibition of forward uptake) and a maximum reduction of 0.41±.02 (mean±SEM of data from 7 cells).

6.5 Zinc is not a competitive inhibitor of glutamate binding

Since the amino group of the glutamate molecule (see figure 3.1) is positively charged at physiological pH, and presumably binds to a negative charge on the glutamate uptake carrier, zinc's action on the uptake carrier could be by competitive inhibition at the glutamate binding site. To investigate this possibility the effect of zinc on the carrier's affinity for glutamate was studied (figure 6.4A). The glutamate dose-response curves in the presence and absence of 8μM free zinc are shown in figure 6.4B. The Michaelis-Menten fits revealed an increase in the K_M for glutamate from 7.3±0.7μM to 13.1±1.9μM (mean±SEM of data from 6 cells) by the presence of zinc. This increase in K_M is statistically significant with a

Figure 6.3 - Inhibition of reversed glutamate uptake by external zinc

A Specimen data from one cell showing the reversed uptake currents, evoked at +20mV by raising the external potassium concentration (black bars) from 0 to 30mM, in control solution and in the presence of various free zinc concentrations. **B** Dose-response curve for the effects of external zinc on the reversed uptake current, as shown in A. The data points represent the mean±SEM of the data from 4 or more cells. They are fitted with a Michaelis-Menten curve (see inset).

Solutions - The external solution contained (mM) NaCl 75, choline-Cl 30, $CaCl_2$ 3, $MgCl_2$ 0.5, $BaCl_2$ 6, HEPES 5, glucose 15 and ouabain 0.1. The pH was adjusted to 7.3 using NMDG. To stimulate reversed uptake the 30mM choline-Cl was replaced by 30mM KCl.

The internal solution contained (mM) choline-Cl 85, $(NMDG)_2EGTA$ 5, NaCl 5, Na_2ATP 5, $CaCl_2$ 1, $MgCl_2$ 7, HEPES 5 and Na-glutamate 10. The pH was adjusted to 7.0 using NMDG.

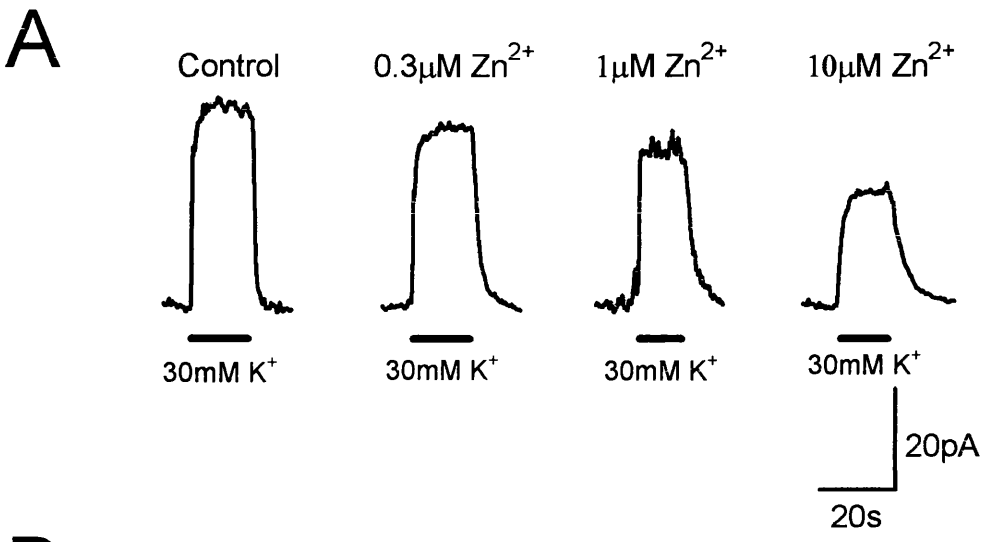
A
Control
0.3μM Zn2+
1μM Zn2+
10μM Zn2+
30mM K+
30mM K+
30mM K+
30mM K+
20pA
20s

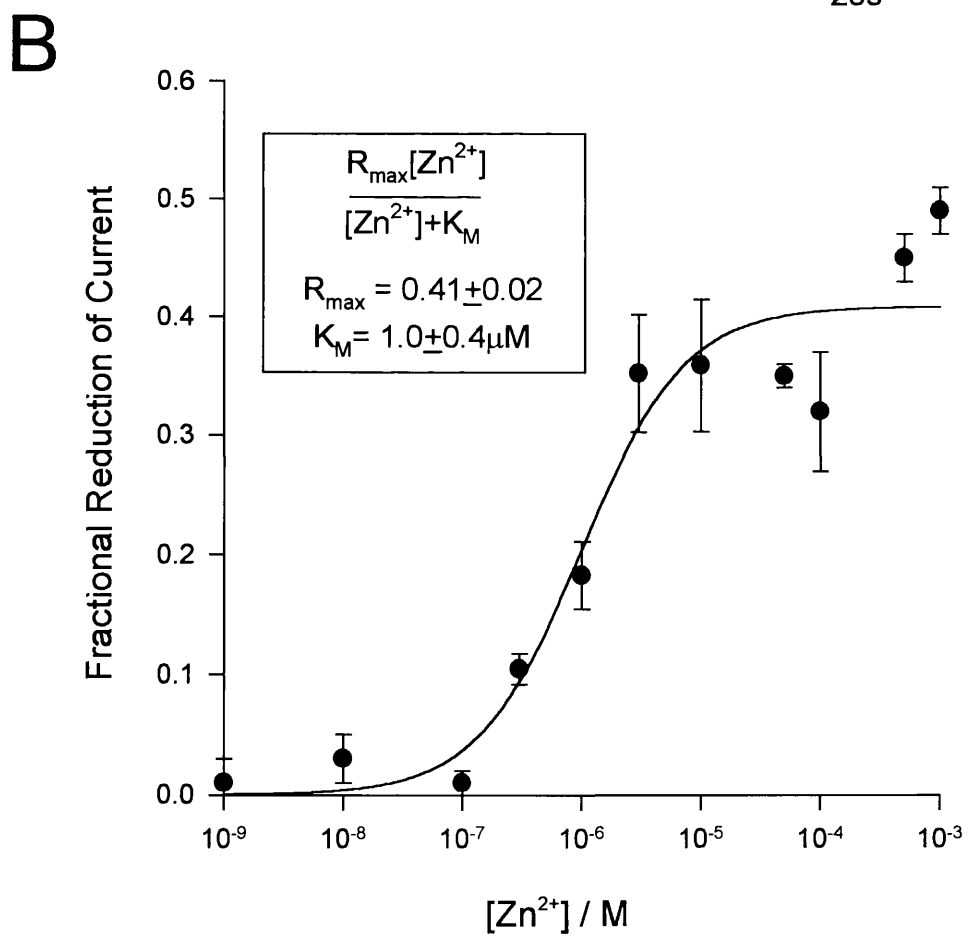
B
Fractional Reduction of Current
0.6
0.5
0.4
0.3
0.2
0.1
0.0
Rmax[Zn2+]
[Zn2+]+KM
Rmax = 0.41±0.02
KM= 1.0±0.4μM
10-9
10-8
10-7
10-6
10-5
10-4
10-3
[Zn2+] / M

Figure 6.4 - Effect of external zinc on the glutamate-dependence of the forward uptake current

A Specimen data from one cell showing the responses to saturating (300μM) and sub-saturating (30μM) doses of external glutamate, evoked at -60mV, in the presence and absence of 8μM free zinc. The fractional response to 30μM glutamate is smaller in the presence of zinc, indicating a decrease in the apparent glutamate affinity (increase in K_M). Note the difference in current scales for the data with and without zinc.

B Dose-response curves for the current produced by glutamate, in the presence (squares) and absence (circles) of 8μM free zinc, as shown in A. The data are normalized to the value recorded at 300μM glutamate in the absence of zinc. Each point represents the mean±SEM of the data from 6 cells. They are fitted with Michaelis-Menten curves (see inset), with the parameters shown by each curve.

Solutions - The external solution contained (mM) NaCl 75, choline-Cl 30, $CaCl_2$ 3, $MgCl_2$ 0.5, $BaCl_2$ 6, HEPES 5 and glucose 15. The pH was adjusted to 7.3 using NMDG.

The internal solution contained (mM) KCl 95, $(NMDG)_2EGTA$ 5, NaCl 5, Na_2ATP 5, $CaCl_2$ 1, $MgCl_2$ 7 and HEPES 5. The pH was adjusted to 7.0 using NMDG.

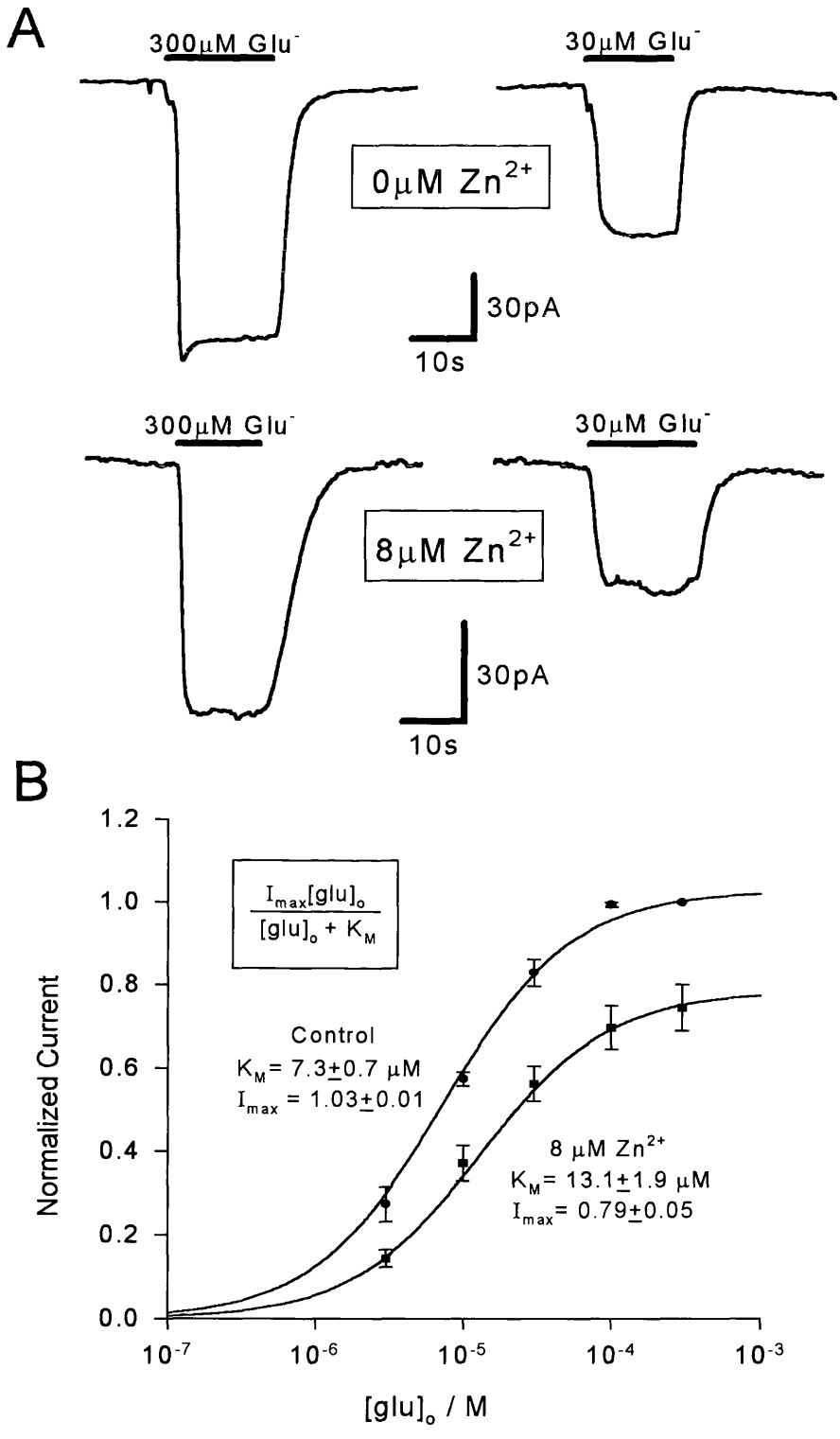
A
300μM Glu⁻
30μM Glu⁻
0μM Zn2+
30pA
10s
300μM Glu⁻
30μM Glu⁻
8μM Zn2+
30pA
10s
B
Normalized Current
1.2
1.0
0.8
0.6
0.4
0.2
0.0
Imax[glu]o / [glu]o + KM
Control
KM= 7.3±0.7 μM
Imax = 1.03±0.01
8 μM Zn2+
KM= 13.1±1.9 μM
Imax= 0.79±0.05
10-7
10-6
10-5
10-4
10-3
[glu]o / M

p value of 0.017 (two-tailed t-test). However the maximal rate of uptake was also suppressed. The normalized I_{max} was reduced from 1.03±0.01 to 0.79±0.05 (mean±SEM of data from 6 cells). This 23% reduction in the I_{max} ($p<0.001$, two-tailed t-test) indicates that the action of zinc is not by simple competitive inhibition at the glutamate binding site.

6.6 Zinc is not a competitive inhibitor of sodium binding

To test if the inhibitory action of zinc on the glutamate transporter is mediated by competitive inhibition at the sodium-binding site, the sodium-dependence of the glutamate evoked current was studied in the presence and absence of external zinc (figure 6.5A). The dependence of the forward uptake current on external sodium could be fitted by the square of a Michaelis-Menten curve (figure 6.5B, see also section 3.6) both in the presence and absence of 8μM free external zinc. Zinc increased the apparent affinity for sodium; the K_M (the value at which the current is a quarter of its value at a saturating sodium concentration) was reduced from 19.3±1.0mM to 13.9±1.2mM (mean±SEM of data from 6 and 5 cells respectively. $p=0.007$, two-tailed t-test). In addition, the predicted current in the presence of a saturating sodium concentration was reduced, from a normalized value of 1.40±0.02 to 0.79±0.04 ($p<0.0001$, two-tailed t-test). These results indicate that the mechanism of action of the inhibition of zinc is not one of competition at the sodium-binding site.

6.7 Zinc is not a competitive inhibitor of potassium binding

Since potassium is also a transported cation on glutamate transporters (Kanner and Sharon, 1978; Barbour *et al.*, 1988; Amato *et al.*, 1994), there is a possibility that zinc's inhibitory action is mediated via the potassium-binding site. This hypothesis was tested by examining the effects of external zinc on the ability

Figure 6.5 - Effect of external zinc on the sodium-dependence of the glutamate uptake current

A Specimen data from one cell showing the effects of external zinc on the current evoked at -60mV by 200μM glutamate (black bars), in high and low external sodium solutions.

B Dependence of the glutamate-evoked current on the external sodium concentration, in the presence (squares) and absence (circles) of 8μM free zinc. The data are normalized to the response in solution containing 110mM Na^+ and no zinc. Each point represents the mean±SEM of the data from 5 cells. They are fitted by the square of a Michaelis-Menten equation (see inset).

Solutions - The external solution contained (mM) NaCl 105, $CaCl_2$ 3, $MgCl_2$ 0.5, $BaCl_2$ 6, HEPES 5 and glucose 15. The pH was adjusted to 7.3 using NMDG. To reduce the sodium concentration, NaCl was replaced by choline-Cl.

The internal solution contained (mM) KCl 95, $(NMDG)_2EGTA$ 5, NaCl 5, Na_2ATP 5, $CaCl_2$ 1, $MgCl_2$ 7 and HEPES 5. The pH was adjusted to 7.0 using NMDG.

A

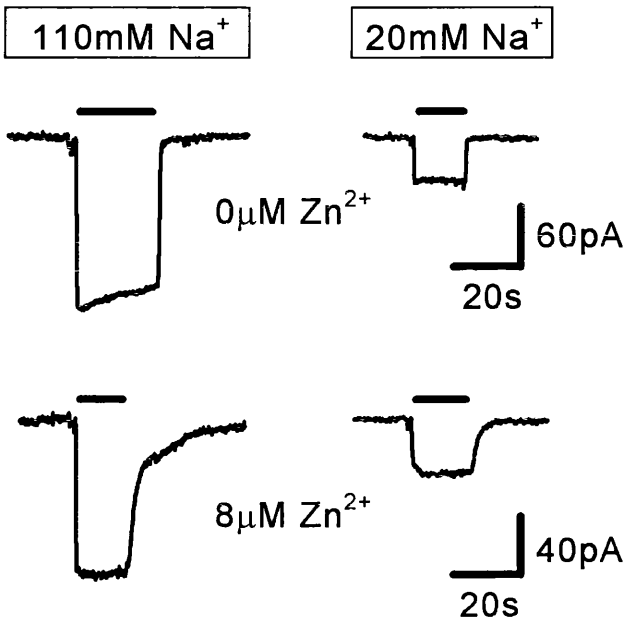
110mM Na+
20mM Na+
0μM Zn2+
60pA
20s
8μM Zn2+
40pA
20s

B

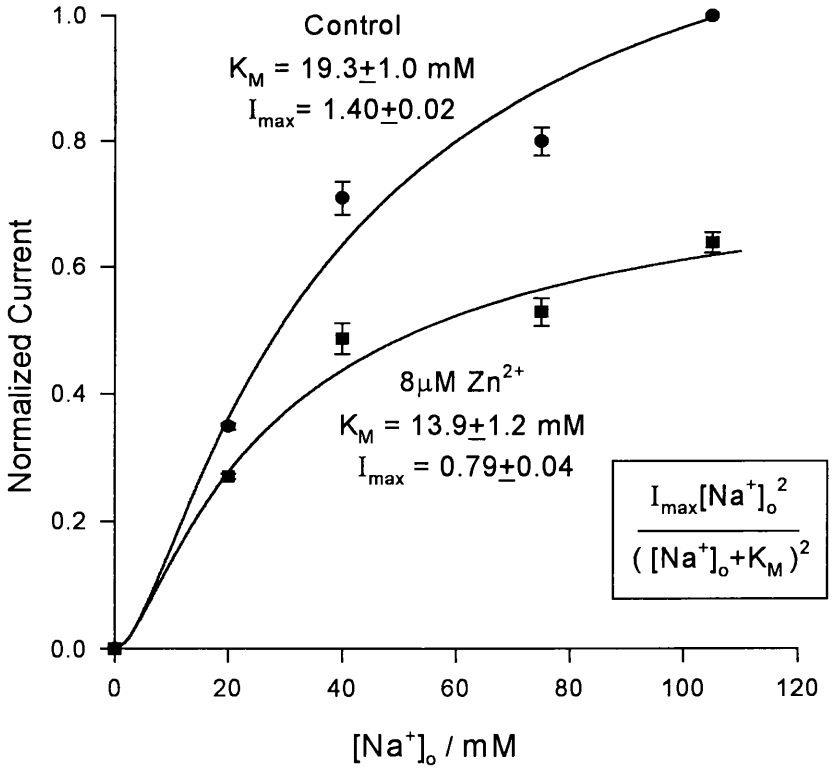
Control
K_M = 19.3±1.0 mM
I_max = 1.40±0.02
8μM Zn2+
K_M = 13.9±1.2 mM
I_max = 0.79±0.04
I_max[Na+]_o^2 / ([Na+]_o+K_M)^2
Normalized Current
[Na+]_o / mM
0.0
0.2
0.4
0.6
0.8
1.0
0
20
40
60
80
100
120

of potassium to stimulate reversed uptake (Szatkowski *et al.*, 1990). This approach allowed the effects of zinc to be tested in a single cell, rather than comparing different cells with and without zinc, as would have been necessary for looking at the effect of internal zinc on the activation of forward uptake by intracellular potassium. When 30μM free zinc was included in the external solution (a saturating dose for inhibiting reversed uptake) the reversed uptake current was inhibited by a similar fraction at all potassium concentrations (figure 6.6A). Michaelis-Menten fits to the dependence of the reversed uptake current on external potassium concentration (figure 6.6B) revealed that the apparent affinity for potassium was unchanged by the presence of external zinc. The K_M for potassium binding in the presence or absence of zinc was 13.5±1.3mM and 11.7±3.6mM respectively (mean±SEM of data from 7 cells). This represents no significant change ($p=0.65$, two-tailed t-test). However, the current at a saturating potassium concentration was reduced from a normalized value of 1.39±0.12 to 0.69±0.12 by the presence of external zinc ($p=0.001$, two-tailed t-test). Thus, zinc is not a competitive inhibitor acting at the potassium-binding site.

6.8 Zinc can only act from the outer membrane surface

One possible explanation of the 7-fold difference in the K_M values for zinc inhibition of forward and reversed uptake could be that zinc can only inhibit transport when binding to the same side of the carrier as the sodium and glutamate (i.e. the outside for forward uptake, and the inside for reversed uptake). The lower apparent affinity for the inhibition of reversed uptake would then be due to the zinc having to somehow enter the cell and act from the inside. To test this hypothesis, the effects of internal zinc on glutamate transport were studied (figure 6.7). The glutamate-evoked forward uptake current was unaffected by the addition of 100μM free zinc to the pipette solution. The average current (normalized by cell

Figure 6.6 - Effect of zinc on the external potassium-dependence of the reversed uptake current

A Specimen data from one cell showing the effect of 30μM free external zinc on currents evoked at +20mV by raising the external potassium concentration from 0 to 30mM (black bars, left-had traces) and from 0 to 8mM (black bars, right-hand traces).

B Potassium-dependence of the reversed uptake current in the presence (squares) and absence (circles) of external zinc. The data are normalized to the current produced by 30mM K^+ in the absence of zinc. Each point represents the mean±SEM of the data from 7 cells. They are fitted with Michaelis-Menten curves (see inset), with the parameters shown by each curve.

Solutions - The external solution contained (mM) NaCl 75, choline-Cl 30, $CaCl_2$ 3, $MgCl_2$ 0.5, $BaCl_2$ 6, HEPES 5, glucose 15 and ouabain 0.1. The pH was adjusted to 7.3 using NMDG. To stimulate reversed uptake the choline-Cl was replaced by KCl.

The internal solution contained (mM) choline-Cl 85, $(NMDG)_2EGTA$ 5, NaCl 5, Na_2ATP 5, $CaCl_2$ 1, $MgCl_2$ 7, HEPES 5 and Na-glutamate 10. The pH was adjusted to 7.0 using NMDG.

A

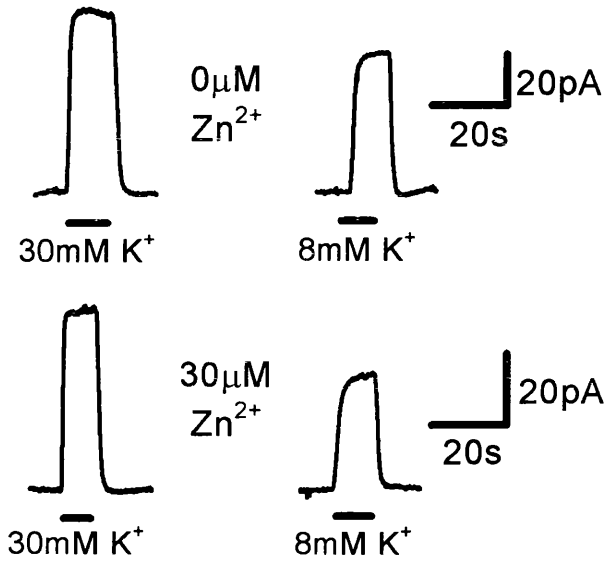
0μM
Zn2+
20pA
20s
30mM K+
8mM K+
30μM
Zn2+
20pA
20s
30mM K+
8mM K+

B

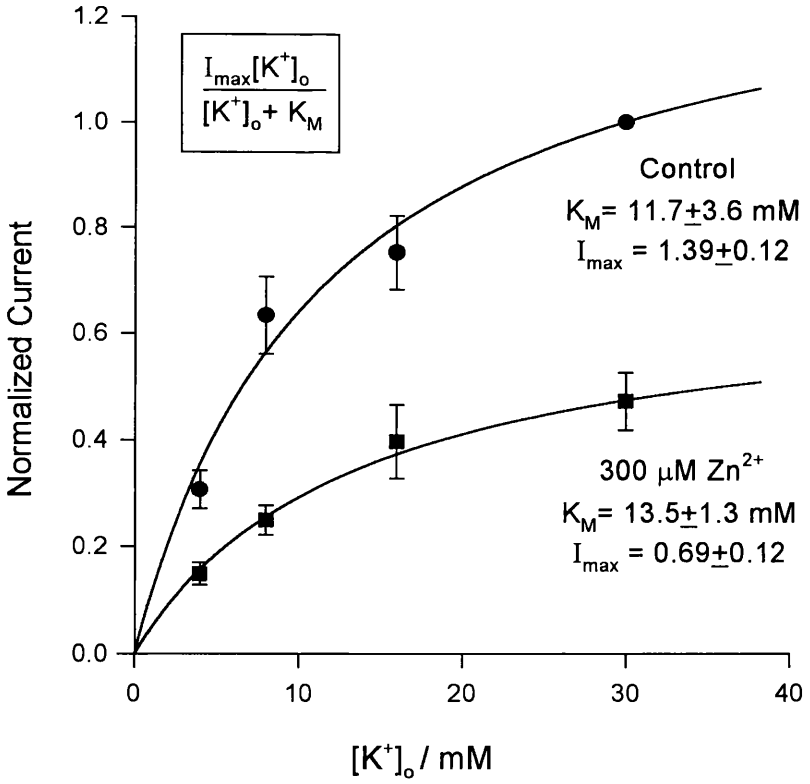
Imax[K+]o
[K+]o+ KM
Control
KM= 11.7±3.6 mM
Imax = 1.39±0.12
300 μM Zn2+
KM= 13.5±1.3 mM
Imax = 0.69±0.12
Normalized Current
[K+]o / mM
0.0
0.2
0.4
0.6
0.8
1.0
1.2
0
10
20
30
40

Figure 6.7 - Effect of internal zinc on the glutamate-dependence of the forward uptake current

A Specimen data recorded from one cell with no internal zinc and one cell with 100μM free internal zinc, showing forward uptake currents recorded at -60mV, evoked by different concentrations of external glutamate (black bars).

B Dose-response curves for the current produced by glutamate in the presence (squares and dashed line) and absence (circles and solid line) of internal zinc. The data are normalized by cell capacitance to compensate for variations in cell size (Barbour *et al.*, 1991). Each data point represents the mean±SEM of the data from 5 cells. They are fitted by Michaelis-Menten curves with the parameters listed in the inset.

Solutions - The external solution contained (mM) NaCl 75, choline-Cl 30, $CaCl_2$ 3, $MgCl_2$ 0.5, $BaCl_2$ 6, HEPES 5 and glucose 15. The pH was adjusted to 7.3 using NMDG.

The internal solution contained (mM) KCl 104, NaCl 5, $MgCl_2$ 2 and HEPES 5. The pH was adjusted to 7.0 using NMDG. 100μM $ZnCl_2$ was added to the solution used to record from the zinc containing cells. EGTA (and hence calcium) and ATP were omitted from the solutions because of their high affinity for zinc ions.

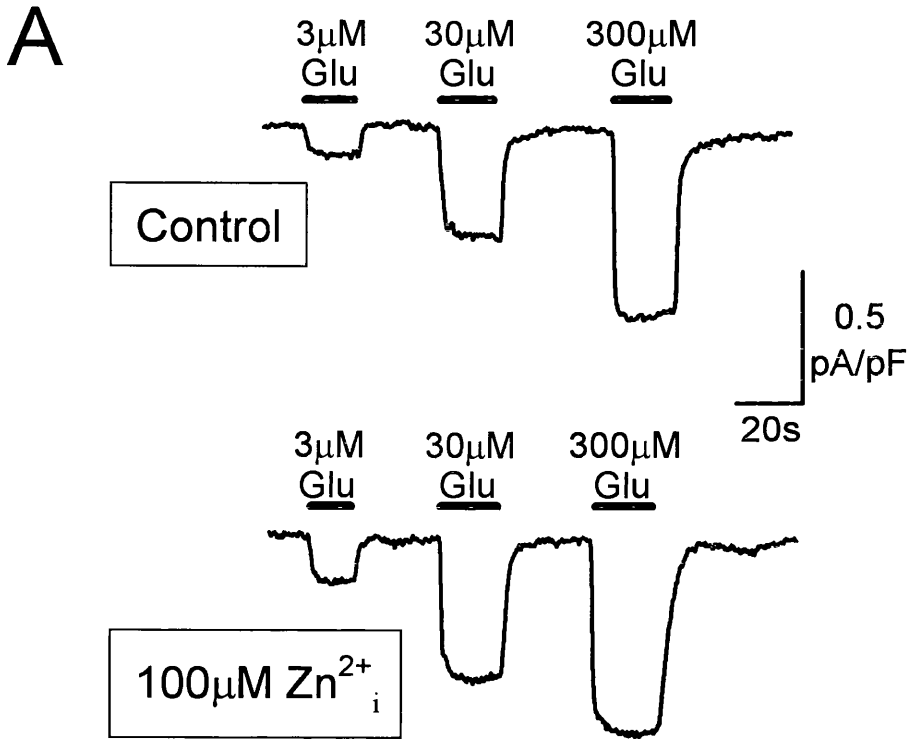
A
3μM Glu
30μM Glu
300μM Glu
Control
0.5 pA/pF
20s
3μM Glu
30μM Glu
300μM Glu
100μM Zn2+i

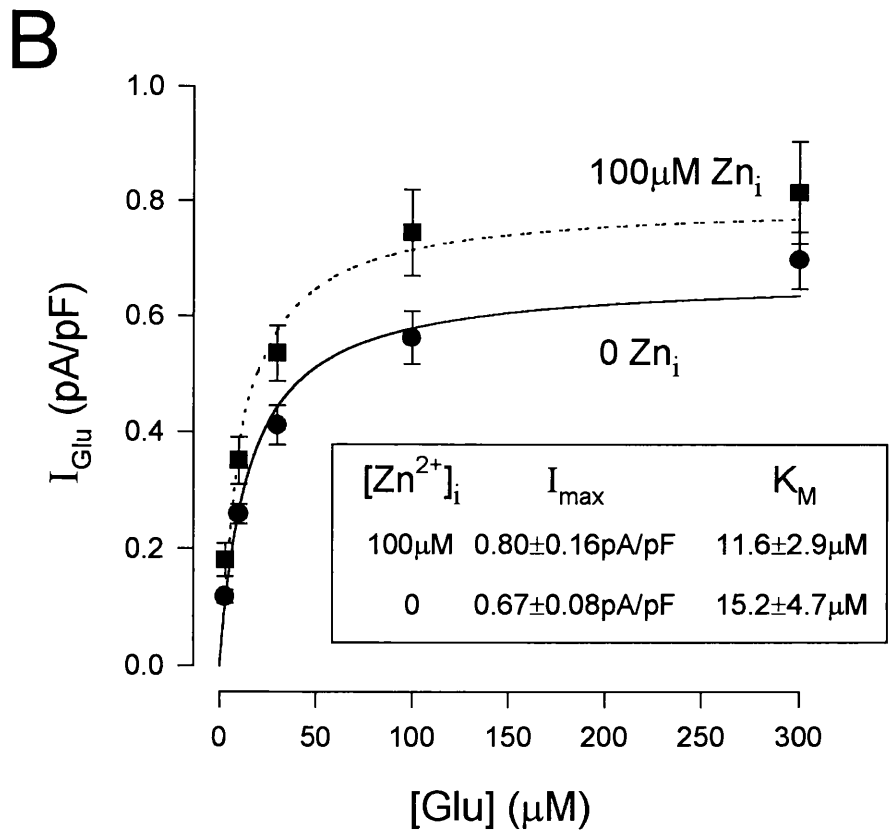
B
1.0
0.8
0.6
0.4
0.2
0.0
IGlu (pA/pF)
100μM Zni
0 Zni
[Zn2+]i Imax KM
100μM 0.80±0.16pA/pF 11.6±2.9μM
0 0.67±0.08pA/pF 15.2±4.7μM
0 50 100 150 200 250 300
[Glu] (μM)

capacitance to reduced variations in current due to the cells' size - Barbour *at al.*, 1991) was 0.67±0.08pA/pF (mean±SEM of data from 5 cells) for cells containing no internal zinc, compared to 0.80±0.16pA/pF (mean±SEM of data from 5 cells) for cells containing 100μM zinc. This represents no significant change in the magnitude of the current ($p=0.49$, two-tailed t-test). Thus, internal zinc does not inhibit forward glutamate uptake. Further experiments done by Mona Spiridon have shown that addition of 100μM free zinc to the internal solution does not affect the magnitude of the potassium-evoked reversed uptake current observed in the presence of internal sodium and glutamate. Thus, internal zinc does not inhibit either forward or reversed glutamate transport, and the inhibition of glutamate transport by extracellular zinc is probably mediated by zinc binding to the external carrier surface.

6.9 The voltage-dependence of the action of zinc

If zinc acts from the outside of the membrane, but has to reach a site within the membrane field to inhibit glutamate uptake, it might be expected that zinc would have a greater inhibitory effect at a more negative membrane potential due to the greater electrical attractive force pulling the cationic zinc into the membrane. To determine how far across the membrane field the zinc ion binds, the voltage-dependence of the zinc block of glutamate uptake was studied.

Although at negative potentials the proportion of glutamate-evoked current mediated by movement of chloride through the carrier's anion conductance is small, at positive membrane potentials when the current associated with glutamate transport is inhibited, the anion channel current is a significant proportion of the total glutamate-evoked current. To eliminate effects of zinc on the anion conductance (see below), and just study its effects on the transport component of the current, experiments were performed in the absence of chloride. Internal and

external chloride were replaced by gluconate. Under these conditions, the suppressive effect of 80μM zinc on forward uptake was greatest at negative membrane potentials (figure 6.8).

6.10 Discussion

6.10.1 Zinc inhibits glutamate uptake

The data presented above indicate that external zinc reversibly modulates the glutamate uptake carrier. Both forward and reversed glutamate uptake are inhibited, with maximal inhibitions of 33% and 41% respectively. Zinc is not simply a competitive inhibitor at the glutamate, sodium or potassium binding sites, but acts at the outer surface of the carrier

If the uptake of glutamate is accompanied by the cotransport of a proton (see section 5.11.4), the possibility that zinc inhibits glutamate uptake by competing with protons at a proton binding site remains open. If this were the case, the inhibition of forward uptake by an alkali external pH (see section 3.4) would be expected to be increased by the presence of external zinc. This possibility is currently under investigation.

6.10.2 Zinc binding within the membrane electrical field

The voltage-dependence of the inhibition by zinc of forward uptake (see figure 6.8) provides information about how far across the membrane electrical field zinc binds. If zinc binds to a site at a fractional distance α across the membrane field, with a Michaelis-Menten constant K when there is no potential across the membrane, then the fractional reduction in current might be given by:

$$\frac{R}{R_{max}} = \frac{[Zn^{2+}]}{[Zn^{2+}] + K} \qquad [6.8]$$

where $[Zn^{2+}]$ is the concentration of zinc at the binding site, R is the fractional

Figure 6.8 - Voltage-dependence of the block of forward uptake by external zinc

A Specimen I-V data from one cell showing the voltage dependence of the inhibition of the forward glutamate uptake current by 80μM external zinc. The solid symbols are the control currents, in the absence of external zinc, recorded before (solid circles) and after (solid squares) the application of zinc. The open symbols are the glutamate-evoked currents in the presence of 80μM zinc.

B The fractional reduction caused by external zinc of the glutamate-evoked current plotted as a function of membrane voltage. The data points represent the mean±SEM of the data from 5 cells. They are fitted by a second-order spline curve.

Solutions - The external solution contained (mM) Na-gluconate 105, $Ca(gluconate)_2$ 3, $Mg(gluconate)_2$ 0.5, $Ba(OH)_2$ 6, gluconic acid 12, HEPES 5 and glucose 15. The pH was adjusted to 7.3 using NMDG.

The internal solution contained (mM) K-gluconate 104, Na-gluconate 5, $Mg(gluconate)_2$ 2 and HEPES 5. The pH was adjusted to 7.0 using NMDG.

Chloride-free solutions were used to eliminate any contamination of the current from the carrier's anion conductance (see text).

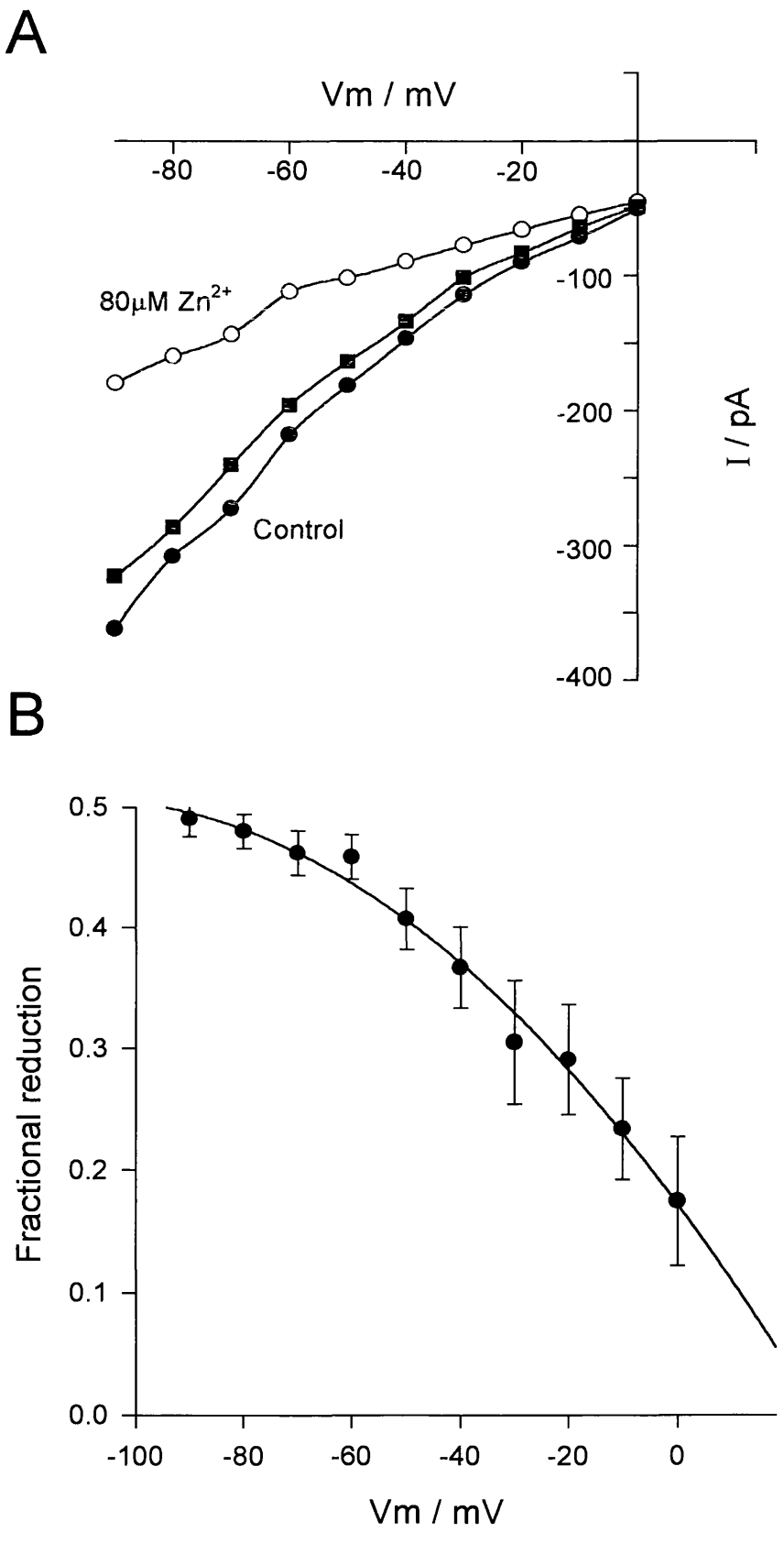
A
Vm / mV
-80
-60
-40
-20
80μM Zn2+
Control
-100
-200
-300
-400
I / pA
B
Fractional reduction
0.5
0.4
0.3
0.2
0.1
0.0
-100
-80
-60
-40
-20
0
Vm / mV

reduction in glutamate-evoked current at a particular zinc concentration and R_{max} is the maximum fractional reduction caused by a saturating zinc concentration. When there is a membrane potential V, the concentration of zinc at position α will be raised by a factor $e^{-2\alpha FV/RT}$ relative to the zinc concentration in the bulk solution, $[Zn^{2+}]_{bulk}$, where F is the Faraday constant, R is the gas constant and T is the absolute temperature. Thus, in general the inhibition produced at a membrane potential V will be given by:

$$\frac{R}{R_{max}} = \frac{[Zn^{2+}]_{bulk} \cdot e^{-2\alpha\frac{FV}{RT}}}{\left([Zn^{2+}]_{bulk} \cdot e^{-2\alpha\frac{FV}{RT}}\right) + K} \qquad [6.9a]$$

or

$$\frac{R}{R_{max}} = \frac{[Zn^{2+}]_{bulk}}{[Zn^{2+}]_{bulk} + Ke^{2\alpha\frac{FV}{RT}}} \qquad [6.9b]$$

where $[Zn^{2+}]_{bulk}$ is the free zinc concentration in the external solution and $Ke^{2\alpha FV/RT}$ is the apparent binding constant for inhibition by zinc at voltage V. equation 6.9b can be transformed to give:

$$\log_e\left\{\left(\frac{R_{max}}{R}\right) - 1\right\} = \log_e\left(\frac{K}{[Zn^{2+}]_{bulk}}\right) + 2\alpha\frac{FV}{RT} \qquad [6.10]$$

The data in figure 6.8 could be reasonably well fitted to this equation using the values R_{max}=0.53, α=0.48 and K=153μM (figure 6.9). Equation 6.9 predicts a Michaelis-Menten constant for the dependence of inhibition on $[Zn^{2+}]_{bulk}$ of $Ke^{2\alpha FV/RT}$ = 16μM at -60mV.

This value is two orders of magnitude above the K_M value obtained from figure 6.2A. This discrepancy could arise because the greater inhibition by zinc at a more negative membrane potential may not, contrary to the assumptions made above, be due to zinc binding to a portion of the carrier protein inside the membrane's electrical field. For example zinc might bind outside the membrane's electrical field with high affinity ($K_M \approx$140nM from figure 6.2), and then inhibit

Figure 6.9 - Fractional distance across membrane of zinc binding

A Linear transform of the data in figure 6.8 (from equation 6.10). The data are best-fitted by linear regression with values for the gradient and y-axis intercept at V=0mV of 0.0378/mV and 0.631 respectively.

B The fractional reduction caused by external zinc of the glutamate-evoked current plotted as a function of membrane voltage (see figure 6.8). The curve is a plot of equation 6.9, with Rmax=0.525, α=0.478 and K=153μM.

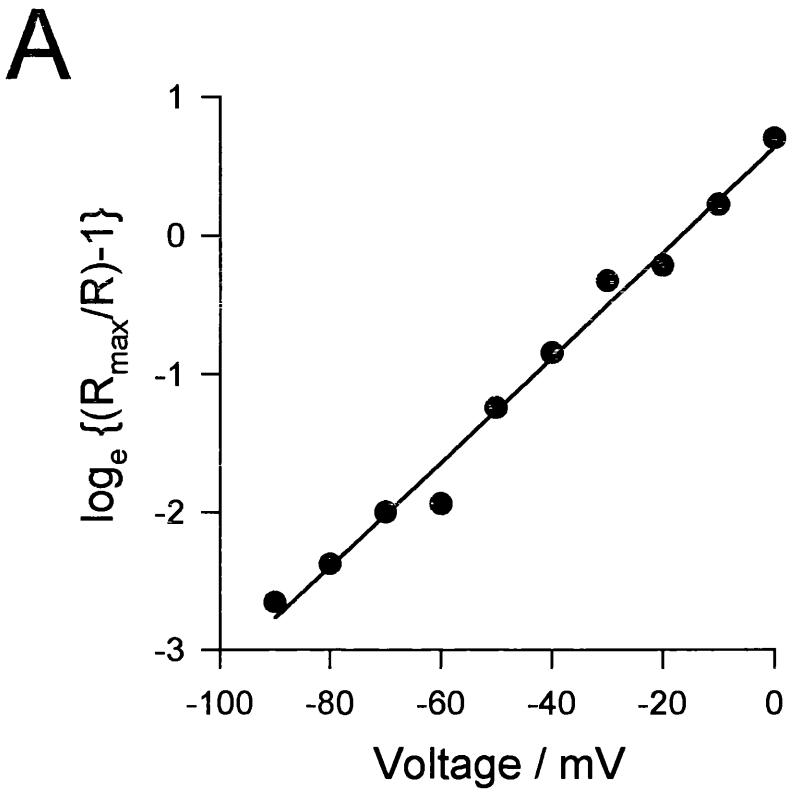
A
1
0
-1
-2
-3
$\log_e \{(R_{max}/R)-1\}$
-100
-80
-60
-40
-20
0
Voltage / mV

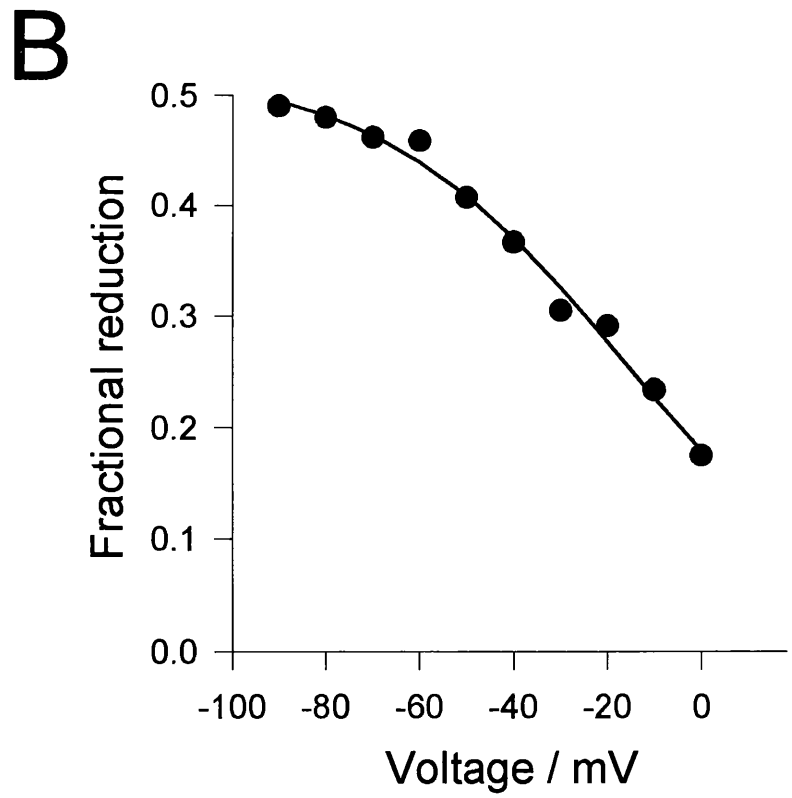
B
0.5
0.4
0.3
0.2
0.1
0.0
Fractional reduction
-100
-80
-60
-40
-20
0
Voltage / mV

transport to a degree which is set by the membrane potential, perhaps having more of an effect at negative membrane potentials because the carrier is then cycling more rapidly. To test this idea it is necessary to measure the dose-response curve for zinc inhibiting uptake at a depolarized potential: for the model just outlined (zinc binds outside the membrane field) the K_M would be the same as at -60mV in figure 6.2A but the maximum inhibition would be less, while if zinc bound inside the membrane field the K_M would be greater but the maximum inhibition the same as at -60mV.

6.10.3 The extracellular zinc concentration

The free zinc concentration in the extracellular space of the CNS has been estimated to be 10nM (Wensink *et al.*, 1988). This concentration is well below the affinity for zinc of the uptake carrier and thus will have little tonic effect. Assaf and Chung (1984) estimated the extracellular zinc concentration during electrical activity to be as high as 300μM. This figure was calculated by measuring the rise in zinc concentration in the superfusate from a stimulated hippocampal slice, and correcting the value for the dilution of the extracellular fluid. This value may be inaccurate since the calculations assumed that all of the zinc was released simultaneously during the 12 minutes that the superfusate was collected. A more accurate estimate can be made by scaling up the superfusate concentration of 186nM by the ratio of the superfusate volume (3.98ml) to the volume of the extracellular space in the slice (15% of the 45mg wet weight), i.e. by about 3.98/(0.15x0.045) = 590, giving a concentration of 110μM. This value assumes spatial uniformity in the release of zinc, however any non-uniformity (such as the zinc only being released from the stimulated mossy fibres) would further increase this estimate. These estimations of extracellular zinc concentration during neuronal activity indicate that the zinc concentration rises to a level which is far

above that which will block both forward and reversed uptake.

Although zinc has been shown to be present in retinal photoreceptors (Wu *et al.*, 1993), no evidence has been presented that it can be released during neuronal activity. It is not known, therefore, how high the extracellular zinc concentration can rise in the retina. The role of the modulation of Müller cell glutamate uptake by zinc in retinal information processing therefore remains, at present, unclear.

6.10.4 Physiological and pathophysiological consequences of zinc modulating glutamate transport

Inhibition of glutamate uptake by zinc released during normal synaptic activity will tend to raise the background level of glutamate and thus decrease the amplitude of synaptic currents by desensitizing postsynaptic glutamate receptors. It may also slow the removal of glutamate from the synaptic cleft and thus prolong the synaptic current. Both these effects are seen when glutamate uptake blockers are applied to glutamatergic synapses onto cerebellar Purkinje cells (Barbour *et al.*, 1994; Takahashi *et al.*, 1995). Thus, the net result may be little change in the charge transfer produced by a postsynaptic current, but a prolongation of the time over which it occurs, promoting temporal integration of input signals by neurons.

During brain ischaemia, zinc release may accompany the massive depolarization of neurons which occurs (Koh *et al.*, 1996). This will inhibit the release of glutamate which occurs by reversed glutamate uptake (Szatkowski and Attwell, 1994). The 41% slowing of reversed uptake which a high zinc concentration produces will not prevent the extracellular glutamate concentration rising to a neurotoxic level if sustained, but will prolong the time needed for the glutamate to rise. If ischaemia is only transient, this prolongation could be neuroprotective, as discussed for the inhibitory effect of an acid pH on reversed

uptake (see section 4.9.3).

Excessive levels of extracellular zinc in the CNS could be expected to inhibit uptake and thus cause neuronal degeneration, as occurs when glutamate transporter expression is prevented (Rothstein *et al.*, 1996). Interestingly, there is a form of amyotrophic lateral sclerosis associated with eating flour contaminated with zinc (Duncan *et al.*, 1992).

Chapter 7

Conclusion

The individual results chapters in this thesis each contain separate discussions of the results presented. In this chapter I will summarize the main conclusions presented and discuss points of interest which would require further investigation.

7.1 Summary of results

The most important conclusions drawn from the results presented in this thesis are as follows:

7.1.1 Forward glutamate uptake is inhibited by an acid or alkali pH (chapter 3)

The forward glutamate uptake current is inhibited by an alkali external pH, with a half maximal inhibition at pH 7.8 (figure 3.4). This is consistent with glutamate uptake transporting either a hydroxide ion out or a proton in with each glutamate ion (Bouvier *et al.*, 1992). A reduction in external proton concentration (or increase in hydroxide ion concentration) would be expected to inhibit carrier cycling.

The forward glutamate uptake current is also inhibited by an acid external pH, with a half maximal inhibition at pH 5.7 (figure 3.4). This is contrary to what is expected from the altered concentration of substrate OH^-/H^+, and is apparently due to protons competing with sodium for binding to the carrier's sodium-binding site and decreasing the carrier's affinity for external sodium (figure 3.7).

7.1.2 Reversed glutamate uptake is inhibited by an acid external pH (chapter 4)

The reversed glutamate uptake current was shown to be inhibited by an acid external pH (figure 4.1), consistent with the notion that a hydroxide ion is transported in (or a proton out) during reversed uptake (Szatkowski *et al.*, 1990). Since reversed glutamate uptake is thought to be responsible for the neurotoxic rise in external glutamate concentration seen in ischaemia (Szatkowski and Attwell, 1994), this inhibition may have important implications for events during this pathological condition. The intra- and extracellular acidification observed in ischaemia will inhibit reversed glutamate uptake approximately 14 fold (figures 4.1 and 4.12), and will slow the rise in external glutamate concentration long enough to be neuroprotective during a transient attack of ischaemia (figure 4.14). As described in section 1.3.3, the external potassium concentration rises to 60mM two minutes after the start of ischaemia, and reversed uptake increases the external glutamate concentration to a neurotoxic level: this rise of external glutamate concentration would take 3.7 seconds if the pH did not change, but is prolonged to 50.5 seconds as a result of the acid pH shift occurring in ischaemia.

7.1.3 Detecting glutamate release using glutamate-sensitive neurons (chapter 4)

Suggestion of an electroneutral mode of glutamate release (Schwartz and Tachibana, 1990), and uncoupled charge movements through the anion conductance of the glutamate uptake carrier (Fairman *et al.*, 1995; Wadiche *et al.*, 1995), bring into doubt the validity of conclusions based solely on measuring the charge movements associated with the carrier. In addition to measuring the effect of pH changes on the reversed glutamate uptake current, direct measurements of the release of glutamate using a glutamate sensitive neuron as a glutamate detector were therefore performed (section 4.4). Using this technique it was demonstrated that glutamate release was entirely potassium dependent and electrogenic (figures

4.8 and 4.11). The acid pH expected in ischaemia inhibited the release of glutamate approximately 14-fold (figure 4.12), confirming the results obtained by examining the reversed uptake current, and reinforcing the importance of the inhibition of reversed uptake during ischaemia.

7.1.4 The glutamate uptake carrier gates an anion channel (chapter 5)

The glutamate uptake carrier in Müller cells was shown to gate an anion conductance which has a permeability sequence $SCN^- > ClO_4^- > NO_3^- > Cl^-$. Current through the anion conductance is a relatively small proportion of the total glutamate-evoked current (15% at -100mV, figure 5.2) under normal conditions, with chloride as the main anion present..

The channel is activated when either forward or reversed glutamate uptake are stimulated (section 5.6), and can even be activated in the absence of net glutamate transport providing sodium and glutamate are present both inside and outside the cell (figures 5.12 and 5.16). Movement of anions through the channel is uncoupled to the movement of glutamate (section 5.7), and the pH changes which are associated with glutamate uptake are not due to hydroxide ions permeating through the channel (figure 5.19).

The ability of the channel to be activated in the absence of glutamate transport, and the lack of any pH-dependence to activation (figure 5.18), suggests a certain amount of autonomy between these two functions of the molecule. Based on these results a kinetic scheme was proposed for how channel activation is linked to carrier cycling (figure 5.20).

7.1.5 Zinc inhibits forward and reversed glutamate uptake (chapter 6)

Both forward and reversed glutamate uptake were shown to be reversibly inhibited by extracellular zinc, with K_M values of 0.14 and 1μM respectively

(figures 6.2 and 6.3). The mechanism of inhibition remains unclear, but it is not one of competitive inhibition at the glutamate, sodium or potassium binding sites (figures 6.4, 6.5 and 6.6). The extracellular zinc concentration in the CNS has been estimated to be around 10nM at rest (Wensink *et al.*, 1988) and rise to >100μM during synaptic activity (Assaf and Chung, 1984), i.e. within the range which would modulate glutamate uptake.

During normal synaptic transmission, inhibition of forward glutamate uptake by zinc may result in a prolongation of the synaptic current (Barbour *et al.*, 1994; Takahashi *et al.*, 1995), or may raise the external glutamate concentration and thus reduce the size of synaptic currents due to increased desensitization of post-synaptic glutamate receptors.

During brain ischaemia zinc release has been proposed to be partially responsible for the death of neurons (Koh *et al.*, 1996). However the rise in external zinc concentration will inhibit reversed glutamate uptake, and thus will slow the rise in external glutamate concentration due to glutamate release by reversed uptake. This may be neuroprotective during transient ischaemic attacks.

7.2 Points of further interest

7.2.1 Carriers which contain channels

In addition to the glutamate uptake carrier, uptake carriers for other neurotransmitters have also been demonstrated to contain uncoupled ion leaks and ligand-gated ion channels. Like the glutamate uptake carrier (Vandenberg *et al.*, 1995), the transporters of GABA (Cammack *et al.*, 1994), noradrenaline (Galli *et al.*, 1995) and serotonin (Mager *et al.*, 1994) also contain cation leaks. The ability of the glutamate uptake carrier to gate an ion conductance (Fairman *et al.*, 1995; Wadiche *et al.*, 1995) has also been demonstrated for the GABA (Cammack and Schwartz, 1996) and noradrenaline transporters (Galli *et al.*, 1996). The

sodium/glucose transporter also contains an ion leak (Panayotova-Heiermann *et al.*, 1995) and gates a water channel (Zampighi *et al.*, 1995).

Further studies into the mechanism of ion channel gating by substrate transport may give an important insight into the mechanics of transporter or channel operation, and will be relevant to a wide range of molecules.

The contribution of anion channel current to the total glutamate-evoked current in Müller cells is relatively small. However in retinal cones (Sarantis *et al.*, 1988) and in the EAAT4 cloned human carrier (Fairman *et al.*, 1995), which is expressed in cerebellar Purkinje cell bodies, the contribution of the anion channel current is much more significant. Further study into the differences between these carriers may provide clues about the mechanism of channel gating. There may be some kind of second messenger activation which is responsible for regulating the gating of the channel, and this could be investigated.

The independence of the carrier and channel functions of the molecule (chapter 5) opens the possibility of the discovery of a pharmacological agent which selectively modulate the anion channel. This would provide a valuable opportunity to investigate its physiological relevance. Any role of the anion channel during epilepsy, ischaemia or normal synaptic transmission could be unmasked by the ability to modulate the channel independently of the glutamate transport capabilities of the carrier. The therapeutic possibilities of such a compound could be considerable: the ability to selectively block the anion channel may promote neuronal survival during brain ischaemia by preventing cell swelling, whereas enhancing the anion channel's activation may inhibit epilepsy by reducing neuronal excitability.

7.2.2 Detecting glutamate release with glutamate sensitive neurons

Glutamate release by reversed uptake can be detected using glutamate-

gated ion channels on neurons. This technique has also been employed to study the GABA transporter (Schwartz, 1987), and could in principle be applied to other neurotransmitter transporters. Study of electroneutral transporters, those with ion leaks and those which gate ion channels would be greatly facilitated by using this technique, since it does not assume a fixed amount of charge movement per neurotransmitter molecule.

Detecting glutamate release with glutamate-gated ion channels in an outside-out membrane patch would be an improvement over using whole cells, as it would provide better spatial resolution. A source of membrane with a density of glutamate receptors high enough to enable detection of small concentrations of glutamate would be needed. Accurate quantification of the glutamate concentration would be difficult because of the large spatial gradients close to the glutamate releasing site. However, useful qualitative data could be obtained. This would enable experiments such as determining how the rise in external glutamate concentration in different areas varies when a brain slice is made anoxic.

REFERENCES

Amara S. G. and Kuhar M. J. (1993) Neurotransmitter transporters: recent progress. *Annu. Rev. Neurosci.* **16**, 73-93.

Amato A., Barbour B., Szatkowski M., and Attwell D. (1994) Counter-transport of potassium by the glutamate uptake carrier in glial cells isolated from the tiger salamander retina. *J. Physiol. Lond.* **479**, 371-380.

Arriza J. L., Kavanaugh M. P., Fairman W. A., Wu Y. N., Murdoch G. H., North R. A., and Amara S. G. (1993) Cloning and expression of a human neutral amino acid transporter with structural similarity to the glutamate transporter gene family. *J. Biol. Chem.* **268**, 15329-15332.

Arriza J. L., Fairman W. A., Wadiche J. I., Murdoch G. H., Kavanaugh M. P., and Amara S. G. (1994) Functional comparisons of three glutamate transporter subtypes cloned from human motor cortex. *J. Neurosci.* **14**, 5559-5569.

Assaf S. Y. and Chung S. H. (1984) Release of endogenous Zn^{2+} from brain tissue during activity. *Nature.* **308**, 734-736.

Attwell D., Barbour B., and Szatkowski M. (1993) Nonvesicular release of neurotransmitter. *Neuron.* **11**, 401-407.

Baetge E. E., Bulloch K., and Stallcup W. B. (1979) A comparison of glutamate

transport in cloned cell lines from the central nervous system. *Brain. Res.* **167**, 210-214.

Ballanyi K., Grafe P., and ten-Bruggencate G. (1987) Ion activities and potassium uptake mechanisms of glial cells in guinea-pig olfactory cortex slices. *J. Physiol. Lond.* **382**, 159-174.

Barbour B., Brew H., and Attwell D. (1988) Electrogenic glutamate uptake in glial cells is activated by intracellular potassium. *Nature.* **335**, 433-435.

Barbour B., Brew H., and Attwell D. (1991) Electrogenic uptake of glutamate and aspartate into glial cells isolated from the salamander (Ambystoma) retina. *J. Physiol. Lond.* **436**, 169-193.

Barbour B., Keller B. U., Llano I., and Marty A. (1994) Prolonged presence of glutamate during excitatory synaptic transmission to cerebellar Purkinje cells. *Neuron.* **12**, 1331-1343.

Bouvier M., Szatkowski M., Amato A., and Attwell D. (1992) The glial cell glutamate uptake carrier countertransports pH-changing anions. *Nature.* **360**, 471-474.

Brew H. and Attwell D. (1987) Electrogenic glutamate uptake is a major current carrier in the membrane of axolotl retinal glial cells. *Nature.* **327**, 707-709.

Brew H., Gray P. T., Mobbs P., and Attwell D. (1986) Endfeet of retinal glial cells have higher densities of ion channels that mediate K^+ buffering. *Nature.* **324**, 466-468.

Bridges R. J., Stanley M. S., Anderson M. W., Cotman C. W., and Chamberlin A. R. (1991) Conformationally defined neurotransmitter analogues. Selective inhibition of glutamate uptake by one pyrrolidine-2,4-dicarboxylate diastereomer. *J. Med. Chem.* **34**, 717-725.

Buhl E. H., Otis T. S., and Mody I. (1996) Zinc-induced collapse of augmented inhibition by GABA in a temporal lobe epilepsy model. *Science.* **271**, 369-373.

Burckhardt G., Kinne R., Stange G., and Murer H. (1980) The effects of potassium and membrane potential on sodium-dependent glutamic acid uptake. *Biochim. Biophys. Acta.* **599**, 191-201.

Busselberg D., Michael D., Evans M. L., Carpenter D. O., and Haas H. L. (1992) Zinc (Zn^{2+}) blocks voltage gated calcium channels in cultured rat dorsal root ganglion cells. *Brain. Res.* **593**, 77-81.

Cammack J. N. and Schwartz E. A. (1996) Channel behavior in a gamma-aminobutyrate transporter. *Proc. Natl. Acad. Sci. U. S. A.* **93**, 723-727.

Cammack J. N., Rakhilin S. V., and Schwartz E. A. (1994) A GABA transporter operates asymmetrically and with variable stoichiometry. *Neuron.* **13**, 949-960.

Chaillet J. R. and Boron W. F. (1985) Intracellular calibration of a pH-sensitive dye in isolated, perfused salamander proximal tubules. *J. Gen. Physiol.* **86**, 765-794.

Charton G., Rovira C., Ben-Ari Y., and Leviel V. (1985) Spontaneous and evoked

release of endogenous Zn^{2+} in the hippocampal mossy fiber zone of the rat in situ. *Exp. Brain. Res.* **58**, 202-205.

Chaudhry F. A., Lehre K. P., van-Lookeren-Campagne M., Ottersen O. P., Danbolt N. C., and Storm-Mathisen J. (1995) Glutamate transporters in glial plasma membranes: highly differentiated localizations revealed by quantitative ultrastructural immunocytochemistry. *Neuron.* **15**, 711-720.

Choi D. W. (1987) Ionic dependence of glutamate neurotoxicity. *J. Neurosci.* **7**, 369-379.

Choi D. W. and Rothman S. M. (1990) The role of glutamate neurotoxicity in hypoxic-ischemic neuronal death. *Annu. Rev. Neurosci.* **13**, 171-182.

Choi D. W., Maulucci-Gedde M., and Kriegstein A. R. (1987) Glutamate neurotoxicity in cortical cell culture. *J. Neurosci.* **7**, 357-368.

Collingridge G. L. and Bliss T. V. (1995) Memories of NMDA receptors and LTP. *Trends. Neurosci.* **18**, 54-56.

Dawson R. M. C., Elliot D. C., Elliot W. H., and Jones K. M. (1986) *Data for Biochemical Research*, 3rd ed. Oxford University Press, .

Derouiche A. and Rauen T. (1995) Coincidence of L-glutamate/L-aspartate transporter (GLAST) and glutamine synthetase (GS) immunoreactions in retinal glia: evidence for coupling of GLAST and GS in transmitter clearance. *J. Neurosci. Res.* **42**, 131-143.

Donaldson J., St.-Pierre T., Minnich J., and Barbeau A. (1971) Seizures in rats associated with divalent cation inhibition of Na^+-K^+-ATP'ase. *Can. J. Biochem.* **49**, 1217-1224.

Dowling J. E. (1987) *The retina: an approachable part of the brain.* Belknap Press of Harvard University Press, Cambridge, Massachusetts.

Drejer J. and Honore T. (1988) New quinoxalinediones show potent antagonism of quisqualate responses in cultured mouse cortical neurons. *Neurosci. Lett.* **87**, 104-108.

Drejer J., Benveniste H., Diemer N. H., and Schousboe A. (1985) Cellular origin of ischemia-induced glutamate release from brain tissue *in vivo* and *in vitro*. *J. Neurochem.* **45**, 145-151.

Duncan M. W., Marini A. M., Watters R., Kopin I. J., and Markey S. P. (1992) Zinc, a neurotoxin to cultured neurons, contaminates cycad flour prepared by traditional guamanian methods. *J. Neurosci.* **12**, 1523-1537.

Eliasof S. and Jahr C. E. (1996) Retinal glial cell glutamate transporter is coupled to an anionic conductance. *Proc. Natl. Acad. Sci. U. S. A* **93**, 4153-4158.

Eliasof S. and Werblin F. (1993) Characterization of the glutamate transporter in retinal cones of the tiger salamander. *J. Neurosci.* **13**, 402-411.

Erecinska M. (1987) The neurotransmitter amino acid transport systems. A fresh outlook on an old problem. *Biochem. Pharmacol.* **36**, 3547-3555.

Erecinska M., Wantorsky D., and Wilson D. F. (1983) Aspartate transport in synaptosomes from rat brain. *J. Biol. Chem.* **258**, 9069-9077.

Fairman W. A., Vandenberg R. J., Arriza J. L., Kavanaugh M. P., and Amara S. G. (1995) An excitatory amino-acid transporter with properties of a ligand-gated chloride channel. *Nature.* **375**, 599-603.

Fenwick E. M., Marty A., and Neher E. (1982) A patch-clamp study of bovine chromaffin cells and of their sensitivity to acetylcholine. *J. Physiol. Lond.* **331**, 577-597.

Friedman J. E. and Haddad G. G. (1994) Anoxia induces an increase in intracellular sodium in rat central neurons *in vitro*. *Brain. Res.* **663**, 329-334.

Gabrielsson B., Robson T., Norris D., and Chung S. H. (1986) Effects of divalent metal ions on the uptake of glutamate and GABA from synaptosomal fractions. *Brain. Res.* **384**, 218-223.

Galli A., DeFelice L. J., Duke B. J., Moore K. R., and Blakely R. D. (1995) Sodium-dependent norepinephrine-induced currents in norepinephrine-transporter-transfected HEK-293 cells blocked by cocaine and antidepressants. *J. Exp. Biol.* **198**, 2197-2212.

Galli A., Blakely R. D., and DeFelice L. J. (1996) Norepinephrine transporters have channel modes of conduction. *PNAS* **93**, 8671-8676.

Gill R., Foster A. C., and Woodruff G. N. (1988) MK-801 is neuroprotective in

gerbils when administered during the post-ischaemic period. *Neuroscience.* **25**, 847-855.

Goldberg M. P. and Choi D. W. (1993) Combined oxygen and glucose deprivation in cortical cell culture: calcium-dependent and calcium-independent mechanisms of neuronal injury. *J. Neurosci.* **13**, 3510-3524.

Grant G. B. and Dowling J. E. (1995) A glutamate-activated chloride current in cone-driven ON bipolar cells of the white perch retina. *J. Neurosci.* **15**, 3852-3862.

Hagberg H., Lehmann A., Sandberg M., Nystrom B., Jacobson I., and Hamberger A. (1985) Ischemia-induced shift of inhibitory and excitatory amino acids from intra- to extracellular compartments. *J. Cereb. Blood. Flow. Metab.* **5**, 413-419.

Hamill O. P., Marty A., Neher E., Sakmann B., and Sigworth F. J. (1981) Improved patch-clamp techniques for high-resolution current recording from cells and cell-free membrane patches. *Pflugers. Arch.* **391**, 85-100.

Hartley D. M. and Choi D. W. (1989) Delayed rescue of N-methyl-D-aspartate receptor-mediated neuronal injury in cortical culture. *J. Pharmacol. Exp. Ther.* **250**, 752-758.

Hertz L. (1979) Functional interactions between neurons and astrocytes I. Turnover and metabolism of putative amino acid transmitters. *Prog. Neurobiol.* **13**, 277-323.

Hexum T. D. (1974) Studies on the reaction catalyzed by transport (Na, K) adenosine

triphosphatase. I. Effects of divalent metals. *Biochem. Pharmacol.* **23**, 3441-3447.

Hollmann M. and Heinemann S. (1994) Cloned glutamate receptors. *Annu. Rev. Neurosci.* **17**, 31-108.

Hollmann M., Hartley M., and Heinemann S. (1991) Ca^{2+} permeability of KA-AMPA-gated glutamate receptor channels depends on subunit composition. *Science.* **252**, 851-853.

Honore T. and Drejer J. (1988) Chaotropic ions affect the conformation of quisqualate receptors in rat cortical membranes. *J. Neurochem.* **51**, 457-461.

Howell G. A., Welch M. G., and Frederickson C. J. (1984) Stimulation-induced uptake and release of zinc in hippocampal slices. *Nature.* **308**, 736-738.

Ikeda M., Nakazawa T., Abe K., Kaneko T., and Yamatsu K. (1989) Extracellular accumulation of glutamate in the hippocampus induced by ischemia is not calcium dependent--in vitro and in vivo evidence. *Neurosci. Lett.* **96**, 202-206.

Johnson J. W. and Ascher P. (1987) Glycine potentiates the NMDA response in cultured mouse brain neurons. *Nature.* **325**, 529-531.

Jonas P. and Sakmann B. (1992) Glutamate receptor channels in isolated patches from CA1 and CA3 pyramidal cells of rat hippocampal slices. *J. Physiol. Lond.* **455**, 143-171.

Kanai Y. and Hediger M. A. (1992) Primary structure and functional characterization of a high-affinity glutamate transporter. *Nature.* **360**, 467-471.

Kanai Y., Smith C. P., and Hediger M. A. (1993) A new family of neurotransmitter transporters: The high-affinity glutamate transporters. *FASEB Journal* 7, 1450-1459.

Kanai Y., Nussberger S., Romero M. F., Boron W. F., Hebert S. C., and Hediger M. A. (1995) Electrogenic properties of the epithelial and neuronal high affinity glutamate transporter. *Journal of Biological Chemistry* **270**, 16561-16568.

Kanner B. I. and Bendahan A. (1982) Binding order of substrates to the sodium and potassium ion coupled L-glutamic acid transporter from rat brain. *Biochemistry.* **21**, 6327-6330.

Kanner B. I. and Sharon I. (1978) Active transport of L-glutamate by membrane vesicles isolated from rat brain. *Biochemistry.* **17**, 3949-3953.

Kataoka Y. and Ohmori H. (1994) Activation of glutamate receptors in response to membrane depolarization of hair cells isolated from chick cochlea. *J. Physiol. Lond.* **477**, 403-414.

Katayama Y., Kawamata T., Tamura T., Hovda D. A., Becker D. P., and Tsubokawa T. (1991) Calcium-dependent glutamate release concomitant with massive potassium flux during cerebral ischemia in vivo. *Brain. Res.* **558**, 136-140.

Kauppinen R. A., McMahon H. T., and Nicholls D. G. (1988) Ca^{2+}-dependent and

Ca^{2+}-independent glutamate release, energy status and cytosolic free Ca^{2+} concentration in isolated nerve terminals following metabolic inhibition: possible relevance to hypoglycaemia and anoxia. *Neuroscience.* **27**, 175-182.

Kemp J. A. and Leeson P. D. (1993) The glycine site of the NMDA receptor-five years on. *Trends. Pharmacol. Sci.* **14**, 20-25.

Kimelberg H. K., Goderie S. K., Higman S., Pang S., and Waniewski R. A. (1990) Swelling-induced release of glutamate, aspartate, and taurine from astrocyte cultures. *J. Neurosci.* **10**, 1583-1591.

Koh J. Y., Suh S. W., Gwag B. J., He Y. Y., Hsu C. Y., and Choi D. W. (1996) The role of zinc in selective neuronal death after transient global cerebral ischemia. *Science.* **272**, 1013-1016.

Kutsuwada T., Kashiwabuchi N., Mori H., Sakimura K., Kushiya E., Araki K., Meguro H., Masaki H., Kumanishi T., Arakawa M. and Mishina, M. (1992) Molecular diversity of the NMDA receptor channel. *Nature.* **358**, 36-41.

Linser P. and Moscona A. A. (1979) Induction of glutamine synthetase in embryonic neural retina: localization in Muller fibers and dependence on cell interactions. *Proc. Natl. Acad. Sci. U. S. A.* **76**, 6476-6480.

Lobner D. and Lipton P. (1990) Sigma-ligands and non-competitive NMDA antagonists inhibit glutamate release during cerebral ischemia. *Neurosci. Lett.* **117**, 169-174.

Longuemare M. C. and Swanson R. A. (1995) Excitatory amino acid release from astrocytes during energy failure by reversal of sodium-dependent uptake. *J. Neurosci. Res.* **40**, 379-386.

Lord R. S. (1990) Transient monocular blindness. *Aust. N. Z. J. Ophthalmol.* **18**, 299-305.

MacDonald J. F. and Nowak L. M. (1990) Mechanisms of blockade of excitatory amino acid receptor channels. *Trends. Pharmacol. Sci.* **11**, 167-172.

Mager S., Min C., Henry D. J., Chavkin C., Hoffman B. J., Davidson N., and Lester H. A. (1994) Conducting states of a mammalian serotonin transporter. *Neuron.* **12**, 845-859.

Mayer M. L., Westbrook G. L., and Guthrie P. B. (1984) Voltage-dependent block by Mg^{2+} of NMDA responses in spinal cord neurones. *Nature.* **309**, 261-263.

Mayer M. L., MacDermott A. B., Westbrook G. L., Smith S. J., and Barker J. L. (1987) Agonist- and voltage-gated calcium entry in cultured mouse spinal cord neurons under voltage clamp measured using arsenazo III. *J. Neurosci.* 7, 3230-3244.

Meguro H., Mori H., Araki K., Kushiya E., Kutsuwada T., Yamazaki M., Kumanishi T., Arakawa M., Sakimura K., and Mishina M. (1992) Functional characterization of a heteromeric NMDA receptor channel expressed from cloned cDNAs. *Nature.* **357**, 70-74.

Mobbs P., Brew H., and Attwell D. (1988) A quantitative analysis of glial cell coupling in the retina of the axolotl (Ambystoma mexicanum). *Brain. Res.* **460**, 235-245.

Monaghan D. T., Bridges R. J., and Cotman C. W. (1989) The excitatory amino acid receptors: their classes, pharmacology, and distinct properties in the function of the central nervous system. *Annu. Rev. Pharmacol. Toxicol.* **29**, 365-402.

Mustafa M. G., Cross C. E., Munn R. J., and Hardie J. A. (1971) Effects of divalent metal ions on alveolar macrophage membrane adenosine triphosphatase activity. *J. Lab. Clin. Med.* 77, 563-571.

Mutch W. A. and Hansen A. J. (1984) Extracellular pH changes during spreading depression and cerebral ischemia: mechanisms of brain pH regulation. *J. Cereb. Blood. Flow. Metab.* **4**, 17-27.

Nadeau S. E. (1994) Transient ischemic attacks: diagnosis, and medical and surgical management. *J. Fam. Pract.* **38**, 495-504.

Nakajima Y., Iwakabe H., Akazawa C., Nawa H., Shigemoto R., Mizuno N., and Nakanishi S. (1993) Molecular characterization of a novel retinal metabotropic glutamate receptor mGluR6 with a high agonist selectivity for L-2-amino-4-phosphonobutyrate. *J. Biol. Chem.* **268**, 11868-11873.

Naruse S., Horikawa Y., Tanaka C., Hirakawa K., Nishikawa H., and Watari H. (1984) In vivo measurement of energy metabolism and the concomitant monitoring of

electroencephalogram in experimental cerebral ischemia. *Brain. Res.* **296**, 370-372.

Nawy S. and Jahr C. E. (1990) Suppression by glutamate of cGMP-activated conductance in retinal bipolar cells. *Nature.* **346**, 269-271.

Nelson P. J., Dean G. E., Aronson P. S., and Rudnick G. (1983) Hydrogen ion cotransport by the renal brush border glutamate transporter. *Biochemistry.* **22**, 5459-5463.

Newman E. A. (1984) Regional specialization of retinal glial cell membrane. *Nature.* **309**, 155-157.

Newman E. A. (1985) Voltage-dependent calcium and potassium channels in retinal glial cells. *Nature.* **317**, 809-811.

Newman E. A. and Odette L. L. (1984) Model of electroretinogram b-wave generation: a test of the K^+ hypothesis. *J. Neurophysiol.* **51**, 164-182.

Newman E. A., Frambach D. A., and Odette L. L. (1984) Control of extracellular potassium levels by retinal glial cell K^+ siphoning. *Science.* **225**, 1174-1175.

Nowak L., Bregestovski P., Ascher P., Herbet A., and Prochiantz A. (1984) Magnesium gates glutamate-activated channels in mouse central neurones. *Nature.* **307**, 462-465.

Olney J. W. and Sharpe L. G. (1969) Brain lesions in an infant rhesus monkey treated

with monsodium glutamate. *Science.* **166**, 386-388.

Olney J. W., Price M. T., Samson L., and Labruyere J. (1986) The role of specific ions in glutamate neurotoxicity. *Neurosci. Lett.* **65**, 65-71.

Panayotova-Heiermann M., Loo D. D., and Wright E. M. (1995) Kinetics of steady-state currents and charge movements associated with the rat Na^+/glucose cotransporter. *J. Biol. Chem.* **270**, 27099-27105.

Patneau D. K. and Mayer M. L. (1990) Structure-activity relationships for amino acid transmitter candidates acting at N-methyl-D-aspartate and quisqualate receptors. *J. Neurosci.* **10**, 2385-2399.

Peng Y. W., Blackstone C. D., Huganir R. L., and Yau K. W. (1995) Distribution of glutamate receptor subtypes in the vertebrate retina. *Neuroscience.* **66**, 483-497.

Perez-Clausell J. and Danscher G. (1985) Intravesicular localization of zinc in rat telencephalic boutons. A histochemical study. *Brain. Res.* **337**, 91-98.

Perkel D. J., Hestrin S., Sah P., and Nicoll R. A. (1990) Excitatory synaptic currents in Purkinje cells. *Proc. R. Soc. Lond. B. Biol. Sci.* **241**, 116-121.

Picaud S. A., Larsson H. P., Grant G. B., Lecar H., and Werblin F. S. (1995) Glutamate-gated chloride channel with glutamate-transporter-like properties in cone photoreceptors of the tiger salamander. *Journal of Neurophysiology* **74**, 1760-1771.

Pin J. P. and Duvoisin R. (1995) The metabotropic glutamate receptors: structure and functions. *Neuropharmacology.* **34**, 1-26.

Pines G., Danbolt N. C., Bjoras M., Zhang Y., Bendahan A., Eide L., Koepsell H., Storm-Mathisen J., Seeberg E., and Kanner B. I. (1992) Cloning and expression of a rat brain L-glutamate transporter. *Nature.* **360**, 464-467.

Rauen T. and Kanner B. I. (1994) Localization of the glutamate transporter GLT-1 in rat and macaque monkey retinae. *Neurosci. Lett.* **169**, 137-140.

Renard A., Crepel F., and Audinat E. (1995) Evidence for two types of non-NMDA receptors in rat cerebellar Purkinje cells maintained in slice cultures. *Neuropharmacology.* **34**, 335-346.

Riepe R. E. and Norenburg M. D. (1977) Muller cell localisation of glutamine synthetase in rat retina. *Nature.* **268**, 654-655.

Rink T. J., Tsien R. Y., and Pozzan T. (1982) Cytoplasmic pH and free Mg^{2+} in lymphocytes. *J. Cell. Biol.* **95**, 189-196.

Robinson R. A. and Stokes R. H. (1959) *Electrolyte solutions.* Butterworths, Bath.

Rothman S. M. (1985) The neurotoxicity of excitatory amino acids is produced by passive chloride influx. *J. Neurosci.* **5**, 1483-1489.

Rothstein J. D., Martin L., Levey A. I., Dykes-Hoberg M., Jin L., Wu D., Nash N.,

and Kuncl R. W. (1994) Localization of neuronal and glial glutamate transporters. *Neuron.* **13**, 713-725.

Rothstein J. D., DykesHoberg M., Pardo C. A., Bristol L. A., Jin L., Kuncl R. W., Kanai Y., Hediger M. A., Wang Y., Schielke J. P., and Welty D. F. (1996) Knockout of glutamate transporters reveals a major role for astroglial transport in excitotoxicity and clearance of glutamate. *Neuron.* **16**, 675-686.

Sarantis M. and Attwell D. (1990) Glutamate uptake in mammalian retinal glia is voltage- and potassium-dependent. *Brain. Res.* **516**, 322-325.

Sarantis M., Everett K., and Attwell D. (1988) A presynaptic action of glutamate at the cone output synapse. *Nature.* **332**, 451-453.

Sarantis M., Ballerini L., Miller B., Silver R. A., Edwards M., and Attwell D. (1993) Glutamate uptake from the synaptic cleft does not shape the decay of the non-NMDA component of the synaptic current. *Neuron.* **11**, 541-549.

Schwartz E. A. (1987) Depolarization without calcium can release gamma-aminobutyric acid from a retinal neuron. *Science.* **238**, 350-355.

Schwartz E. A. and Tachibana M. (1990) Electrophysiology of glutamate and sodium co-transport in a glial cell of the salamander retina. *J. Physiol. Lond.* **426**, 43-80.

Shafqat S., Tamarappoo B. K., Kilberg M. S., Puranam R. S., McNamara J. O., Guadano-Ferraz A., and Fremeau R. T. Jr. (1993) Cloning and expression of a novel

Na^+-dependent neutral amino acid transporter structurally related to mammalian Na^+/glutamate cotransporters. *J. Biol. Chem.* **268**, 15351-15355.

Siesjo B. K. (1990) Calcium, excitotoxins, and brain damage. *NIPS* **5**, 120-125.

Silver I. A. and Erecinska M. (1992) Ion homeostasis in rat brain in vivo: intra- and extracellular [$Ca2^+$] and [H^+] in the hippocampus during recovery from short-term, transient ischemia. *J. Cereb. Blood. Flow. Metab.* **12**, 759-772.

Sim J. A. and Cherubini E. (1990) Submicromolar concentrations of zinc irreversibly reduce a calcium-dependent potassium current in rat hippocampal neurons in vitro. *Neuroscience.* **36**, 623-629.

Smart T. G., Xie X., and Krishek B. J. (1994) Modulation of inhibitory and excitatory amino acid receptor ion channels by zinc. *Prog. Neurobiol.* **42**, 393-441.

Smith M. L., von-Hanwehr R., and Siesjo B. K. (1986) Changes in extra- and intracellular pH in the brain during and following ischemia in hyperglycemic and in moderately hypoglycemic rats. *J. Cereb. Blood. Flow. Metab.* **6**, 574-583.

Sommer B., Keinanen K., Verdoorn T. A., Wisden W., Burnashev N., Herb A., Kohler M., Takagi T., Sakmann B., and Seeburg P. H. (1990) Flip and flop: a cell-specific functional switch in glutamate-operated channels of the CNS. *Science.* **249**, 1580-1585.

Stallcup W. B., Bulloch K., and Baetge E. E. (1979) Coupled transport of glutamate

and sodium in a cerebellar nerve cell line. *J. Neurochem.* **32**, 57-65.

Storck T., Schulte S., Hofmann K., and Stoffel W. (1992) Structure, expression, and functional analysis of a Na^+-dependent glutamate/aspartate transporter from rat brain. *Proc. Natl. Acad. Sci. U. S. A.* **89**, 10955-10959.

Storm-Mathisen J., Danbolt N. C., Rothe F., Torp R., Zhang N., Aas J. E., Kanner B. I., Langmoen I., and Ottersen O. P. (1992) Ultrastructural immunocytochemical observations on the localization, metabolism and transport of glutamate in normal and ischemic brain tissue. *Prog. Brain. Res.* **94**, 225-241.

Szatkowski M. and Attwell D. (1994) Triggering and execution of neuronal death in brain ischaemia: two phases of glutamate release by different mechanisms. *Trends. Neurosci.* **17**, 359-365.

Szatkowski M., Barbour B., and Attwell D. (1990) Non-vesicular release of glutamate from glial cells by reversed electrogenic glutamate uptake. *Nature.* **348**, 443-446.

Szatkowski M., Barbour B., and Attwell D. (1991) The potassium-dependence of excitatory amino acid transport: resolution of a paradox. *Brain. Res.* **555**, 343-345.

Takahashi M., Kovalchuk Y., and Attwell D. (1995) Pre- and postsynaptic determinants of EPSC waveform at cerebellar climbing fiber and parallel fiber to Purkinje cell synapses. *J. Neurosci.* **15**, 5693-5702.

Takahashi M., Sarantis M., and Attwell D. (1996) Postsynaptic glutamate uptake in

rat cerebellar Purkinje cells. *J. Physiol. Lond.* In press.

Tang C. M., Dichter M., and Morad M. (1989) Quisqualate activates a rapidly inactivating high conductance ionic channel in hippocampal neurons. *Science.* **243**, 1474-1477.

Tessier-Lavigne M., Attwell D., Mobbs P., and Wilson M. (1988) Membrane currents in retinal bipolar cells of the axolotl. *J. Gen. Physiol.* **91**, 49-72.

Traynelis S. F. and Cull-Candy S. G. (1990) Proton inhibition of N-methyl-D-aspartate receptors in cerebellar neurons. *Nature.* **345**, 347-350.

Traynelis S. F. and Cull-Candy S. G. (1991) Pharmacological properties and H^+ sensitivity of excitatory amino acid receptor channels in rat cerebellar granule neurones. *J. Physiol. Lond.* **433**, 727-763.

van den Berg C. J. and Garfinkel D. (1971) A stimulation study of brain compartments. Metabolism of glutamate and related substances in mouse brain. *Biochem. J.* **123**, 211-218.

Vandenberg R. J., Arriza J. L., Amara S. G., and Kavanaugh M. P. (1995) Constitutive ion fluxes and substrate binding domains of human glutamate transporters. *Journal of Biological Chemistry* **270**, 17668-17671.

Verdoorn T. A., Burnashev N., Monyer H., Seeburg P. H., and Sakmann B. (1991) Structural determinants of ion flow through recombinant glutamate receptor channels.

Science. **252**, 1715-1718.

Wadiche J. I., Amara S. G., and Kavanaugh M. P. (1995) Ion fluxes associated with excitatory amino acid transport. *Neuron.* **15**, 721-728.

Wakakura M. and Yamamoto N. (1994) Cytosolic calcium transient increase through the AMPA/kainate receptor in cultured Muller cells. *Vision. Res.* **34**, 1105-1109.

Walz W., Klimaszewski A., and Paterson I. A. (1993) Glial swelling in ischemia: a hypothesis. *Dev. Neurosci.* **15**, 216-225.

Watson T. A. and Beamish F. W. (1981) The effects of zinc on branchial adenosine triphosphatase enzymes in vitro from rainbow trout, Salmo Gairdneri. *Comp. Biochem. Physiol. C.* **68C**, 167-173.

Wensink J., Molenaar A. J., Woroniecka U. D., and Van-den-Hamer C. J. (1988) Zinc uptake into synaptosomes. *J. Neurochem.* **50**, 782-789.

Wright E. M. and Diamond J. M. (1977) Anion selectivity in biological systems. *Physiol. Rev.* **57**, 109-156.

Wu S. M., Qiao X., Noebels J. L., and Yang X. L. (1993) Localization and modulatory actions of zinc in vertebrate retina. *Vision. Res.* **33**, 2611-2616.

Yamada K. A. and Tang C. M. (1993) Benzothiadiazides inhibit rapid glutamate receptor desensitization and enhance glutamatergic synaptic currents. *J. Neurosci.* **13**,

3904-3915.

Zampighi G. A., Kreman M., Boorer K. J., Loo D. D., Bezanilla F., Chandy G., Hall J. E., and Wright E. M. (1995) A method for determining the unitary functional capacity of cloned channels and transporters expressed in Xenopus laevis oocytes. *J. Membr. Biol.* **148**, 65-78.

Zerangue N. and Kavanaugh M. P. (1996) Flux coupling in a neuronal glutamate transporter. *Nature.* **383**, 634-637.

Zhao H. and Eide D. (1996) The yeast ZRT1 gene encodes the zinc transporter protein of a high-affinity uptake system induced by zinc limitation. *Proc. Natl. Acad. Sci. U. S. A.* **93**, 2454-2458.